

# Exploring the CXCR3 Chemokine Receptor with Small-Molecule Antagonists and Agonists

Maikel Wijtmans, Danny Scholten, Wouter Mooij, Martine J. Smit, Iwan J.P. de Esch, Chris de Graaf, and Rob Leurs

**Abstract** CXCR3 is a CXC chemokine receptor that, together with its three major ligands, CXCL9 (MIG), CXCL10 (IP-10), and CXCL11 (I-TAC), is involved in inflammatory responses, mediated mainly by T cells. In several immune-related diseases, including chronic obstructive pulmonary disease (COPD), inflammatory bowel disease (IBD), rheumatoid arthritis, multiple sclerosis, and atherosclerosis, CXCR3 and/or its ligands are found to be overexpressed, potentially indicating a role for this receptor in these diseases. Animal models have confirmed the therapeutic potential of targeting CXCR3 in the treatment of such diseases. Several peptidic, peptidomimetic, and small non-peptidomimetic CXCR3 ligands have been disclosed in the past 10 years. These ligands have served as chemical tools for the investigation of CXCR3 activation, blocking, and signaling, and some of these ligand series have been developed as potential therapeutic agents against inflammation. Computational modeling studies, facilitated by the recent developments in GPCR structural biology, together with mutagenesis and pharmacological studies, have aided in understanding how these ligands interact with CXCR3.

This chapter will give an overview on how the combination of these chemical, computational, and pharmacological tools and techniques has increased our understanding of the molecular mechanisms by which small-molecule antagonists and agonists bind to CXCR3 compared to the relatively large chemokines. A detailed overview of CXCR3 ligand structure-activity relationships and structure-function relationships will be presented. This comparative analysis reveals that the full spectrum of antagonist and agonist effects on CXCR3 is now within reach by appropriate scaffolds and chemical modifications. Many of these ligands display behavior deviating from simple competition and do not interact with the chemokine

---

M. Wijtmans (✉), D. Scholten, W. Mooij, M.J. Smit, I.J.P. de Esch, C. de Graaf, and R. Leurs  
Division of Medicinal Chemistry, Faculty of Sciences, Amsterdam Institute for Molecules  
Medicines and Systems, VU University, Amsterdam, De Boelelaan 1083, 1081 HV  
Amsterdam, The Netherlands  
e-mail: [m.wijtmans@vu.nl](mailto:m.wijtmans@vu.nl)

binding site, providing evidence for an allosteric mode of action. Moreover, the computer-assisted molecular modeling of CXCR3 receptor-ligand interactions is discussed in view of GPCR crystal structures and mutagenesis studies of CXCR3 and other chemokine receptors. Improved insights in the interplay between CXCR3-ligand interactions and CXCR3-mediated signaling pathways potentially open up novel therapeutic opportunities in the area of inflammation.

**Keywords** Allosteric modulation, C–X–C chemokine receptor type 3, G protein-coupled receptor, GPCR crystal structure, Homology modeling, Mutagenesis studies, Receptor–ligand interactions, Small-molecule agonist, Small-molecule antagonist, Structure–activity relationship, Structure–function relationship

## Contents

1	Introduction .....	120
1.1	CXCR3 .....	120
1.2	Small-Molecule Binding .....	124
1.3	Aim .....	126
2	Antagonists .....	127
2.1	(Aza)quinazolinones and Later-Generation Analogues .....	127
2.2	1-Aryl-3-Piperidin-4-yl-Ureas and Later-Generation Analogues .....	137
2.3	Piperazinyl-Piperidines .....	142
2.4	Ergolines .....	147
2.5	Iminobenzimidazoles .....	149
2.6	VUA Compounds: Targeting a Hypothesized Polycycloaliphatic Pocket .....	150
2.7	Miscellaneous .....	154
3	Agonists .....	160
3.1	Agonists Emerging from the Pharmacopeia Screen .....	160
3.2	Biaryl Ammonium Salt Agonists .....	164
4	CXCR3-Ligand Binding: From GPCR X-Rays to Presumed CXCR3 Binding Modes ..	166
4.1	GPCR Crystal Structures and Chemokine Receptor-Ligand Interaction Modeling .....	166
4.2	In Silico-Guided CXCR3 Mutation Studies to Elucidate CXCR3-Ligand Binding Modes .....	169
4.3	Perspectives for (Structure-Based) Virtual Screening for CXCR3 Ligands .....	172
5	Conclusion .....	173
	References .....	174

## 1 Introduction

### 1.1 CXCR3

#### 1.1.1 History and Pharmacological Aspects

Loetscher and colleagues first cloned the human C-X-C chemokine receptor type 3 (CXCR3) receptor in 1996 from a cDNA library derived from CD4<sup>+</sup> T cells. The receptor cDNA sequence encodes for a protein of 368 amino acid in length [1]. CXCR3 is predominantly expressed on activated Th1 cells but also on a

proportion of circulating blood T cells and B cells and is expressed on natural killer cells [1–3]. Furthermore, the chemokines CXCL9 (Mig), CXCL10 (IP-10), and CXCL11 (I-TAC) were found to be the endogenous agonists for this receptor, governing the migration of CXCR3-expressing leukocytes to sites of inflammation or infection [1, 4–8]. The expression of CXCR3 chemokines is induced under inflammatory conditions, mainly mediated by interferon  $\gamma$  [1, 2]. In addition, CXCL4 and CXCL13 chemokines were also reported to bind and activate CXCR3 at high concentrations [9, 10]. CXCL4 was also shown to bind a splice variant of CXCR3 with an extended N-terminus, called CXCR3B [11].

CXCR3 signaling occurs mainly through activation of the pertussis toxin-sensitive  $G\alpha_{i/o}$  class of G proteins, and receptor stimulation is associated with various downstream signaling pathways, including chemotaxis, activation of p44/42 and Akt kinases, mobilization of  $Ca^{2+}$  from intracellular stores, and lowering of cyclic AMP levels [1, 12–14]. After receptor activation, the receptor is rapidly desensitized, internalized, and degraded [15–17]. In general, after agonist exposure, a GPCR is phosphorylated at C-terminal serine/threonine residues by G protein-coupled receptor kinases (GRKs), a process also known as desensitization. Subsequently, these phosphorylated residues serve as recognition sites for  $\beta$ -arrestin proteins, generally involved in internalization of GPCRs [18]. Although, it has been shown that  $\beta$ -arrestin is involved in CXCR3 internalization to some extent, it is not the sole determinant in directing CXCR3 receptors away from the cell surface [12, 17]. Also caveolae, another route for receptor internalization, do not seem to be involved in the case of CXCR3. Taken together, the exact mechanism of CXCR3 internalization is still unclear [17]. Nevertheless, CXCR3 is able to efficiently recruit  $\beta$ -arrestin1 and –2 proteins after agonist stimulation [14]. However, its functional implications remain to be explored.

Although GPCRs generally are able to function as monomers, increasing evidence points towards assembly of multiple GPCRs in homo- and/or heteromeric complexes [19]. Chemokine receptors have been found to dimerize or oligomerize with other chemokine receptors [20]. To date, evidence suggests that CXCR3 dimerizes with viral chemokine receptor BILF1 (Epstein-Barr virus) in HEK293T cells [21]. The *in vivo* consequences are yet unclear, but it might be envisioned that such viruses modulate the host immune defense by altering chemokine receptor signaling, e.g., through dimerization, facilitating its survival [21]. Furthermore, a recent study reported on the formation of heteromeric complexes of CXCR3 and CXCR4 receptors in HEK293T cells [22]. It was found that CXCL10 could be displaced from CXCR3 by CXCR4 chemokine CXCL12 and vice versa. Moreover, CXCR3 agonists were able to increase the dissociation rate of CXCL12 from CXCR4 receptors, both suggesting negative cooperativity through a heteromer interface.

### 1.1.2 Functional Selectivity in CXCR3 Pharmacology

The ligands for CXCR3 have different efficacies and potencies when compared in different *in vitro* functional assays. CXCL11 seems to be the dominant ligand, as it has the highest affinity, potency, and efficacy in most assays [1, 5–8, 14, 23]. The

question why a receptor like CXCR3 would need three different ligands is intriguing, as it suggests redundancy in the chemokine system. However, multiple lines of evidence point at unique nonredundant roles for these ligands *in vivo*. First of all, CXCL9, CXCL10, and CXCL11 seem to interact with the receptor in a distinct mode, as they need different parts of the receptor for their binding and signaling activities [12, 24]. Next to that, CXCL10 and CXCL11 seem to bind different CXCR3 populations [14, 23], also suggesting distinct functions for these chemokines. This is furthermore supported by recent findings, where functional selectivity or biased signaling for the different CXCR3 chemokines was observed [25]. Whereas CXCL10- or CXCL11-mediated receptor activation both resulted in  $\beta$ -arrestin recruitment to the activated CXCR3 receptors, CXCL9 activation failed to do so, despite effective  $G_i$  protein activation [25]. Moreover, and in contrast to CXCL9 and CXCL10, CXCL11 was the only CXCR3 chemokine that provoked elevation of intracellular calcium in myofibroblasts [26]. Altogether, these data are in support of nonredundant functions for CXCR3 chemokines. Second, differential spatiotemporal patterns of expression for the different chemokines and chemokine receptors in our body indicate that these chemokines have distinct roles *in vivo* [27].

In general, chemokines are thought to activate their receptors according to a two-step model, where the core of the chemokine binds to the N-terminus and extracellular domains of the receptor (step 1) [20]. Subsequently, the N-terminus of CXCL9, CXCL10, or CXCL11 is positioned towards yet to be identified receptor domains, mediating receptor activation (step 2) [20, 24, 28]. This general hypothesis is substantiated by the observation that adding or deleting only a few N-terminal chemokine residues resulted in a change from agonist to antagonist behavior. Indeed, N-terminal truncation of CXCL11 (e.g., CXCL11 4–73) hardly influences binding affinity, yet results in a complete loss of agonism [29]. Similarly, deletion of residues 2–6 from the N-terminus of CXCL10 also resulted in a potent antagonist with high affinity for the receptor [30]. Interestingly, chemokines are also truncated *in vivo*, where they are processed by proteases to give chemokines with modified affinity and activity. Particularly, CXCL10 and CXCL11 are processed N-terminally by the dipeptidyl peptidase IV CD26, leading to a loss in their chemotactic and calcium signaling activity while retaining their ability to bind the receptor, albeit with reduced affinity [31, 32]. These processed chemokines act as antagonists, as they are able to antagonize activity of full-length CXCL10 and CXCL11 [32].

Altogether, these data indicate that expression and activity of chemokines is tightly regulated in a spatiotemporal manner, giving texture and robustness to the CXCR3 response *in vivo*, again refuting the notion of redundancy.

Hetero(di)merization might present another way by which selective fine-tuning of receptor signaling can be achieved in the chemokine system [20]. In the case of CCR5, heterodimerization with CXCR4 or CCR2 even led to a shift in coupling from  $G_i$ - to  $G_q$ -mediated signaling pathways [33]. Unfortunately, little is known about functional consequences of CXCR3 homo-/heteromerization. However, a recent report from our group has shown that  $\beta$ -arrestin can be specifically recruited to CXCR3 and CXCR4 heteromers, potentially leading to altered receptor desensitization and internalization [22].

### 1.1.3 The CXCR3 Receptor as Potential Drug Target

To date, two small-molecule antagonists targeting chemokine receptors have successfully reached the market. Maraviroc (CCR5, Selzentry<sup>®</sup>) and AMD-3100 (CXCR4, Mozobil<sup>®</sup>) are used for treatment of HIV-1 infection and non-Hodgkin lymphoma, respectively. However, they do not target chronic inflammation or autoimmune diseases, conditions that are most often associated with imbalanced expression and signaling within the chemokine system. The druggability of the chemokine system has been debated for quite some time now, mainly due to the high attrition rate of drug candidates in clinical trials [34]. The reason for this remains unclear, but it is often suggested that the complexity (“redundancy”) of the system is a key factor. As such, target validation of individual chemokines and/or receptors, linking them to specific diseases, is of vital importance to establish therapeutic potential. Fortunately, data pinpointing specific roles for chemokine receptors in disease models is emerging. In the case of CXCR3, the receptor and one or more of its ligands are found to be highly overexpressed in a variety of inflammatory disorders, including allograft rejection [35–37], atherosclerosis [38], and autoimmune diseases such as rheumatoid arthritis [2, 39], chronic obstructive pulmonary disease [40], multiple sclerosis [41], and systemic lupus erythematosus (SLE) [42]. In addition, the amounts of chemokine mRNA and number of infiltrating CXCR3-expressing leukocytes in tissues from transplant and SLE patients seem to correlate with the severity of disease [43–46]. Moreover, CXCR3 is suggested to play an important role in metastasis of melanoma and colon cancer cells to the lymph nodes and in metastasis of breast cancer cells to the lung [47–50].

Inhibition of CXCR3 by either antibodies or small-molecule antagonists significantly delays disease progression in various mouse models of disease, including atherosclerosis, transplant rejection, and cancer [37, 48, 51–55]. As such, antagonism has been the focus of CXCR3 drug discovery efforts.

Intriguingly, opposing data was reported on the role of CXCR3 in allograft rejection. Where some studies with CXCR3<sup>−/−</sup> mice reported delayed acute and chronic rejection of cardiac allografts [37] or pancreatic island allografts [56], others revealed that CXCR3 does not play an essential role in cardiac allograft rejection [57, 58]. Therefore, these studies challenge the potential of CXCR3 as a drug target in allograft rejection. Moreover, also contrasting evidence exists for the involvement of CXCR3 in cancer, as multiple lines of evidence point both at a protective and sustaining roles for CXCR3 in cancer. In some reports CXCR3 activation and expression is linked to proliferative signaling and metastasis of tumor cells to tissues with relatively high CXCL9-11 expression [47–49, 59–61], as CXCR3 antagonism is found to decrease tumor growth and metastasis [53, 60, 62–64]. On the other hand, others reported that the presence of CXCR3 or its ligands is associated with slower tumor growth and decreased metastasis [65, 66]. The latter might be explained by the recruitment of antitumor immune cells [67].

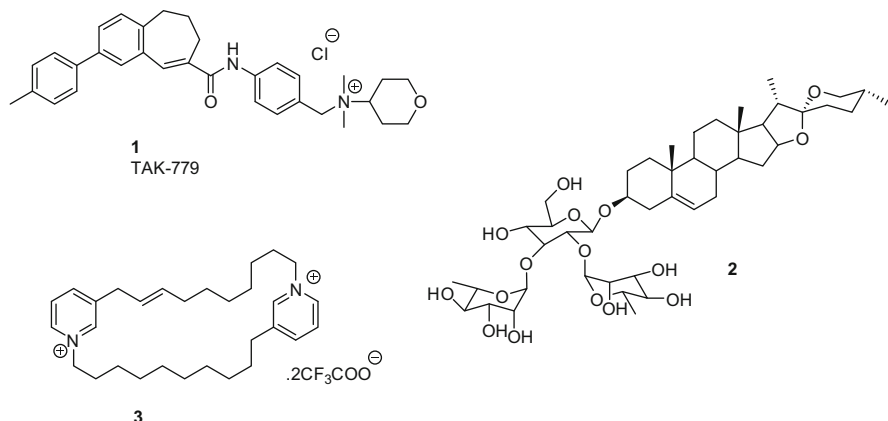
An alternative explanation that reconciles these apparent contradictory roles is the presence of different splice variants of CXCR3. Alternative splicing of the CXCR3 gene leads to expression of CXCR3A, CXCR3B (52 aa longer N-terminus compared to CXCR3A), and CXCR3-alt (loss of 3 TM domains as a result of skipping exon 2) [11, 68]. Unfortunately, little is known about the expression patterns and signaling properties of the alternative splice variants CXCR3B and especially CXCR3-alt. Nevertheless, accumulating evidence points at a tumorigenic role for CXCR3A [53, 63] and an angiostatic role for CXCR3B [69]. The angiostasis through CXCR3B might be the result of inhibition of the antiapoptotic protein heme-oxygenase-1 as shown by overexpression of CXCR3B in renal cancer cells [70]. Moreover, other evidence supporting this functional division of the two splice variants is provided by multiple reports that describe a trend for cancers with more invasive phenotypes generally exhibiting decreased CXCR3B mRNA expression compared to CXCR3A, as in the case of skin and prostate cancer [64, 71]. Consequently, the functional outcome would then depend on the relative expression of both splice variants in a given (diseased) tissue. Unfortunately, in the majority of CXCR3 target validation studies, no distinction is made between the different splice variants. In some cases, a distinction is made, yet almost exclusively by measurement of mRNA levels instead of actual protein levels. Altogether, in-depth characterization of the properties of CXCR3A, CXCR3B, and CXCR3-alt is needed, as it aids in the validation of CXCR3 as a therapeutic target.

The use of CXCR3<sup>-/-</sup> mice has also revealed other interesting effects. For example, CXCR3 plays a role in wound healing of the skin [72, 73]. Activation of CXCR3 on, e.g., fibroblasts seems to contribute to the healing of skin injuries, by recruitment of immune cells to the site of injury, leading to the migration of keratinocytes, and by affecting the reorganization of matrix components including collagen and fibrillin [74]. Absence of CXCR3 or its ligands leads to ineffective and slower healing and hypertrophic scarring [72, 73, 75]. These data suggest that CXCR3 agonism might also be a potential therapeutic avenue in some cases. The discovery and characterization of small-molecule CXCR3 agonists will be discussed in more detail in Sect. 3.1.

## 1.2 Small-Molecule Binding

Given the multifaceted role of CXCR3 in a variety of physiological processes, it is not surprising that many efforts have been devoted to the development of small-molecule CXCR3 modulators. As explained, CXCR3 blockade (rather than activation) has generally been regarded as the therapeutically more relevant approach. Thus, the huge majority of disclosures deal with CXCR3 antagonists from pharmaceutical companies and showcase the challenging balances researchers have to address when developing drug candidates [76–78]. From a molecular point of view, chemokines are relatively large compared to the small ligands ( $\pm 10\text{--}50$ -fold difference in molecular weight) that generally target this receptor family. Despite

the fact that low-molecular weight ligands engage in fewer receptor interactions than the chemokines, many of these small ligands have the ability to disrupt chemokine binding and function with nanomolar potencies [20]. Therefore, it seems likely that these ligands do not act via simple steric competition but rather through an allosteric mechanism (an allosteric site is referred to a binding location for a ligand that is distinct from that of the endogenous ligand). This notion is supported by the increasing number of reports revealing the allosteric nature of many of such compounds binding to chemokine receptors [20, 79]. Indeed, increasing evidence also suggests allosteric binding of small-molecule CXCR3 ligands to the receptor [80]. The first crystal structures of druggable GPCRs have been solved in the past few years [81, 82], including the chemokine CXCR4 [83] and CCR5 [84] chemokine receptors. These structures offer new insights into the molecular details of GPCR-ligand binding and suggest that small molecules can accommodate different (allosteric) binding modes in the relatively large chemokine receptor binding pocket [20]. Chemokine receptor crystal structures, chemokine receptor binding sites, and the elucidation of CXCR3-ligand binding modes by site-directed mutagenesis studies and computational modeling studies are discussed in more detail in Sect. 4.



TAK-779 (**1**,  $\text{IC}_{50}=369 \text{ nM}$ , [ $^{125}\text{I}$ ]-CXCL10) [51] and a few compounds emerging from a natural product screen, such as sugar-derivatized steroid **2** ( $\text{IC}_{50}=0.47 \mu\text{M}$ , [ $^{125}\text{I}$ ]-CXCL10) and dipyridinium salt **3** ( $\text{IC}_{50}=0.69 \mu\text{M}$ , [ $^{125}\text{I}$ ]-CXCL10) [85], can arguably be considered as the earliest disclosed examples of small-molecule binders of CXCR3. TAK-779 still finds some value as CXCR3 tool compound, but its moderate affinity and low selectivity over other chemokine receptors (notably CCR2 and CCR5) need to be borne in mind. As far as can be deduced from the literature, compounds **2** and **3** seem to have not been followed up upon.

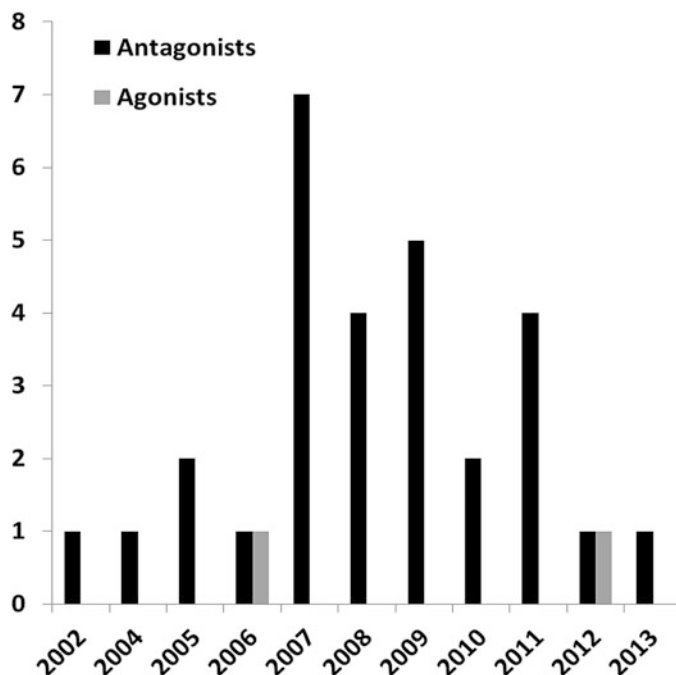


**Fig. 1** Number of medicinal chemistry-oriented publications on small-molecule CXCR3 ligands per year. The date of acceptance is used. A paper was included if it disclosed a new chemotype and/or SAR study on a known chemotype. A distinction is made between antagonists and agonists. All references can be found in the current review

### 1.3 Aim

The current manuscript aims to review small-molecule modulation of CXCR3 from a molecular point of view. That is, in contrast to our most recent review [78], we pay less attention to proven clinical relevance of published molecules (patents are not included) but instead describe all reported compound classes including ones that would best be classified as “tool compounds”. Considerable attention will be paid to articles which appeared after our 2008 review [77], and compact SAR tables are included to further illustrate SAR. In line with our aims, we will also pay special attention to CXCR3 agonists as well as to studies aimed at deciphering CXCR3-ligand binding modes by combining structural models (based on GPCR crystal structures) with ligand SAR and receptor site-directed mutagenesis studies. Collectively, our review aims to illustrate the many venues that have been followed in order to capitalize on small molecules to block or activate CXCR3.

Figure 1, which is an adapted continuation of a graph we published in our 2008 review [77], shows a visual depiction of the progress in CXCR3 ligand research. Two major trends are visible: (1) the publication rate on CXCR3 chemotypes seems

to have stalled in recent years, and (2) as expected, much less is published on agonists than on antagonists.

## 2 Antagonists

This paragraph deals with a detailed description of published small-molecule CXCR3 antagonists in order of number of papers on a particular scaffold. Chemotypes with multiple associated publications have been classified in separate subparagraphs. Clarity within a particular table provided, reported affinity/activity values are given in the units used in the corresponding papers.

### 2.1 (Aza)quinazolinones and Later-Generation Analogues

#### 2.1.1 (Aza)quinazolinones

The class of (aza)quinazolinones and the resulting offspring of sub-chemotypes is the most widely described collection of CXCR3 antagonists (Amgen) with patents appearing as early as 2001 [86].

The work started with compound **4** as an HTS hit [87]. Several early SAR approaches on hit **4** have been published, with reported affinity values slightly differing likely as a result of the exact assay conditions [87, 88]. Nevertheless, clear trends can be extracted from these reports (Table 1). Replacing the F atom by a cyano group yielded improved ligand VUF5834 (**5**), which could efficiently block CXCR3-mediated calcium release [88]. The decanoyl moiety in **4** could be replaced by a phenylacetyl moiety albeit that substitution with an electron-withdrawing group was required (compare **4** to **6** and **7**). The dimethylamino group could be exchanged for a 3-pyridyl moiety. This is exemplified by compound **8** and **9** (AMG1237845,  $IC_{50}=0.006\ \mu M$ ), the latter of which also showed good functional activity in a cell migration assay against all three chemokines [35]. Further SAR efforts maintained the OEt present in **9** as  $R^3$  for pharmacokinetic reasons while the  $CF_3$  was switched for an  $OCF_3$  group accompanied by insertion of an additional N-atom in the core bicyclic moiety. This afforded azaquinazolinone **10**, known as AMG487 ( $IC_{50}=0.008\ \mu M$ ) [87, 90]. The (*R*)-stereomer of AMG487 has the highest affinity [91]. A 4-F,3-CF<sub>3</sub> analogue (**11**, NBI-74330) from the same patent[90] was studied by others [89] and found to be more active ( $K_i=1.5\ nM$ ) than AMG487. Our lab also published on the SAR linking **5** to **10** and **11** [92].

A CXCR3 mutagenesis study to detail the binding of **11** has recently been described by our group [80] and highlighted the CXCR3 transmembrane (TM) region as interaction region for the molecule as opposed to N-terminus and extracellular loops which are mainly important for chemokine binding [24]. Particularly, **11** appears to bind mainly in transmembrane site 1 (TMS1) of the TM region, as mutations in this pocket affected affinity of **11** [80].

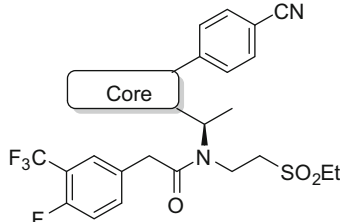
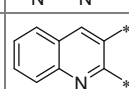
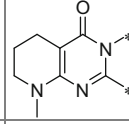
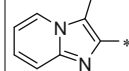
**Table 1** Optimization of quinazolinone derivatives by several research groups [87–89]

Compound	#	In ref.	R <sup>1</sup>	R <sup>2</sup>	R <sup>3</sup>
<b>4</b>	1 [87], 1c [88]	*	~~~~~	N <sup>+</sup> CH <sub>2</sub> CH <sub>2</sub> CH <sub>2</sub> *	F
<b>5</b>	1d [88]	*	~~~~~	N <sup>+</sup> CH <sub>2</sub> CH <sub>2</sub> CH <sub>2</sub> *	CN
<b>6</b>	16 [87]	*	~~~~~	N <sup>+</sup> CH <sub>2</sub> CH <sub>2</sub> CH <sub>2</sub> *	F
<b>7</b>	18 [87]	*	~~~~~	N <sup>+</sup> CH <sub>2</sub> CH <sub>2</sub> CH <sub>2</sub> *	F
<b>8</b>	28 [87]	*	~~~~~	CH <sub>2</sub> CH <sub>2</sub> *	F
<b>9</b>	34 [87]	*	~~~~~	CH <sub>2</sub> CH <sub>2</sub> *	OEt
<b>10</b>	47 [87]	*	~~~~~	CH <sub>2</sub> CH <sub>2</sub> *	OEt
<b>11</b>	NBI-74330 [89]	*	~~~~~	CH <sub>2</sub> CH <sub>2</sub> *	OEt

<sup>a</sup>Assay conditions vary. The reader is referred to the involved references for more details<sup>b</sup>Racemate

AMG487 is the only ligand, as far as can be deduced from available literature, to have advanced into the clinic. Results of a phase I trial on AMG487 were shared in 2003 [93]. AMG487 was evaluated for safety and pharmacokinetics in 30 healthy males in a randomized, double blind, placebo-controlled dose-escalation study. In general, the compound was well tolerated and adverse events were mild to moderate (25–1,100 mg doses) [93]. In a phase IIa trial, patients suffering from moderate to severe psoriasis received 50 or 200 mg of AMG487 or placebo orally once a day for 28 days. Yet no significant differences in Psoriasis Activity and Severity Index or Physician Global Assessment scores were seen when patient groups were

**Table 2** Optimization of quinazolinone derivatives by Li et al. [97]

Compound		Core	IC <sub>50</sub> (nM)	
#	In ref.		CXCL10 <sup>a</sup>	Migration <sup>b</sup>
<b>12</b>	1		11	115
<b>13</b>	5		0.80	72
<b>14</b>	16		4.0	88
<b>15</b>	28		3.0	72

<sup>a</sup>[<sup>125</sup>I]-labeled CXCL10 displacement assay to CXCR3 expressed on activated human PBMC in the absence of human plasma

<sup>b</sup>CXCL11-induced cellular migration assay of PBMC

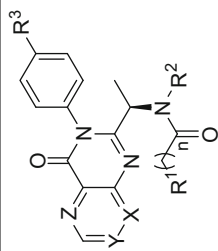
compared [94]. It was hypothesized that high variability in drug exposure may have caused the lack of clinical efficacy [94]. Two subsequent papers addressed the role of several AMG487 metabolites as possible players in the unexpected clinical pharmacokinetic parameters of AMG487 [95, 96]. Not surprisingly, several of the ensuing medicinal chemistry efforts by Amgen seem to have focused on chemically addressing these pharmacokinetic obstacles.

In one such effort, the 8-azaquinazolinone core was inspected for alternative bicyclic systems (Table 2). The 8-azaquinazolinone derivative **12** ( $IC_{50} = 11$  nM) exhibited similar affinities and potencies to those of AMG487, but did not induce the time-dependent inhibition of CYP3A4 resulting from *O*-deethylation of AMG487. Therefore, it was decided to explore the SAR of the core with **12** as template [97]. It should be borne in mind, though, that **12** and AMG487 differ in three respects in terms of the periphery of the molecules: –CN instead of –OEt, ethylsulfonyl moiety instead of a pyridine unit, and different substitution pattern of the fluorine-containing aryl moiety. Initially, a series of [6,6]-fused heterocyclic derivatives was synthesized to determine the influence of the carbonyl and the

nitrogen atom at the 3-position on the binding of the parental **12** to CXCR3 [97]. It was found that those functional groups are not essential for binding to the receptor. That is, quinoline analogue **13** ( $IC_{50}=0.80$  nM) displayed a more than tenfold increase in affinity for CXCR3 in buffer, although that increase was negligible when the assays were run in human plasma. A completely aromatic core was not necessary, given that **14** ( $IC_{50}=4.0$  nM) had similar affinity for CXCR3 as **12**. [6,5]-fused heterocycles were also investigated [97]. Most replacements gave compounds with good affinity for the receptor. Notably, the imidazopyridine-derived **15** ( $IC_{50}=3.0$  nM) afforded the highest affinity and showed improved blockade of CXCL11-induced lymphocyte migration compared to **12**. Given the many tolerated core structures, it was concluded by the authors that the main role of the heterocyclic core is to arrange the peripheral substituents in the appropriate orientation [97].

It had been disclosed that the progression of AMG487 in clinical trials proved to be complicated due to the formation of a major pyridine-N-oxide metabolite that was also active on CXCR3 [98]. Arguably as a result of this, the quinazolinone series was further optimized to reduce the risk of formation of a major active metabolite (Table 3) [98]. In these efforts, the quinazolinone core was initially revisited instead of the 8-azaquinazolinone core of AMG487, because quinazolinone derivatives were equally potent and readily available synthetically. First, the aromatic moiety of  $R^1$  of **16** ( $IC_{50}=0.006$   $\mu$ M) was altered with the trifluoromethyl group being conserved during the modifications, since it significantly improved potencies and microsomal stability [98]. Imidazole and pyridine moieties provided similar affinities as the phenyl derivative **16** (not shown). The phenyl unit was maintained, though, and the substituents on this phenyl ring and the linker ( $n$ ) were explored ( $R^1$ ). While a 4-methylsulfonyl group (and less so 4-CN) was not tolerated as a substituent, all other substitution patterns were well tolerated. This may indicate that the electron-withdrawing properties of the trifluoromethyl group cannot fully account for the increased affinity. Elongation of the chain ( $n=2$ ), however, was not accepted. Next, with the 3-trifluoromethyl-4-fluorophenylacetamide present, the azaquinazolinone core was reexamined [98]. As expected (vide supra), key 8-azaquinazolinone NBI-74330 (**11**) was equally potent to its quinazolinone analogue. However, regiosomeric azaquinazolinones **17** ( $IC_{50}=0.032$   $\mu$ M) and **18** ( $IC_{50}=0.11$   $\mu$ M) were less potent than **11**. This somewhat contrasts a previous paper, which indicated that many substitutions within the core ring system are tolerated [97]. The 8-azaquinazolinone core was chosen for further optimization, since it was more polar than the quinazolinone core, and the  $R^2$  was studied [98]. As previously reported [87], this area allowed several changes. Alkoxy-ethyl, amino-ethyl, and various heterocyclic moieties led to compounds with good affinity [98]. Notably, compounds such as **19** ( $IC_{50}=0.001$   $\mu$ M), **20** ( $IC_{50}=0.002$   $\mu$ M), and **21** ( $IC_{50}=0.001$   $\mu$ M) stand out. Taken together with previous SAR data (vide supra), it seems that polar groups are preferred in this area but that many types of polar groups are accepted. Compound **21** was taken as a further template, because it was found in in vitro studies that major metabolite formation was avoided for compounds with the ethylsulfonyl moiety [98]. Indeed,

**Table 3** Optimization of quinazolinone derivatives by Liu et al. [98]



Compound #	In ref.	R <sup>1</sup>	R <sup>2</sup>	R <sup>3</sup>	X	Y	Z	n	IC <sub>50</sub> (μM) CXCL10 <sup>a</sup>	Migration <sup>b</sup>
<b>11</b> (NBL-74330)	21	F <sub>3</sub> C C <sub>6</sub> H <sub>4</sub> F	*	pyridine C <sub>6</sub> H <sub>4</sub> *	OEt	N	CH	1	0.005	0.023
<b>16</b>	5	F <sub>3</sub> C C <sub>6</sub> H <sub>4</sub> F	*	pyridine C <sub>6</sub> H <sub>4</sub> *	OEt	CH	CH	1	0.006	0.35
<b>17</b>	22	F <sub>3</sub> C C <sub>6</sub> H <sub>4</sub> F	*	pyridine C <sub>6</sub> H <sub>4</sub> *	OEt	CH	N	CH	1	0.032
<b>18</b>	23	F <sub>3</sub> C C <sub>6</sub> H <sub>4</sub> F	*	pyridine C <sub>6</sub> H <sub>4</sub> *	OEt	CH	CH	N	1	0.11
<b>19</b>	30	F <sub>3</sub> C C <sub>6</sub> H <sub>4</sub> F	*	pyridine C <sub>6</sub> H <sub>4</sub> *	OEt	N	CH	1	0.001	0.005

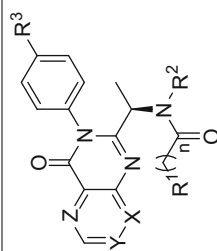
(continued)

**Table 3** (continued)

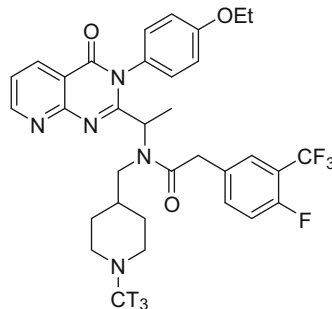
#	Compound	IC <sub>50</sub> (μM)				Migration <sup>b</sup>
		In ref.	R <sup>1</sup>	R <sup>2</sup>	R <sup>3</sup>	
<b>20</b>	29	F <sub>3</sub> C	—	*	OEt	N
			—	—	—	CH
			—	—	—	Z
<b>21</b>	33	F <sub>3</sub> C	—	*	OEt	N
			—	—	—	CH
			—	—	—	CH
<b>22</b>	34	F <sub>3</sub> C	—	*	OCH <sub>2</sub> CF <sub>3</sub>	N
			—	—	—	CH
			—	—	—	CH

<sup>a</sup>Displacement of [<sup>125</sup>I]-labeled CXCL10 from the CXCR3 receptor expressed on PMBC

<sup>b</sup>CXCL11-induced migration of PBMC in the presence of 100% human plasma



the ethylsulfonyl moiety was already present in previously discussed compounds (*vide supra*). In an attempt to reduce *O*-dealkylation, a 3,3,3-trifluoroethoxy moiety ( $R^3$ ) was introduced to give **22** ( $IC_{50} = 0.001 \mu M$ ). The PK profile of **22** was good across several species (including rat, dog, and cynomolgus monkeys), and **22** displayed increased affinity and potency in vitro and in vivo compared to AMG487.



**23** (RAMX3)

A racemic N-CT<sub>3</sub> analogue of **20** (i.e., **23** or RAMX3) has been disclosed for use as a CXCR3 radioligand. The paper was accompanied by a brief SAR on additional members of the 8-azaquinazolinone class [99]. This SAR, among others, showed the dramatic loss in potency when the ethoxyphenyl head is removed from AMG487. The radioligand **23** possesses high affinity for CXCR3 ( $K_d = 1 \text{ nM}$ ). Moreover, and in contrast to CXCL11, unlabelled **23** was not able to completely displace a fluorescently labeled isoform of CXCL11, suggesting an allosteric mechanism of binding for this compound [99].

Evaluation of AMG487 in phase I clinical trials had indicated that the drug accumulated when daily doses above 100 mg were administered [100]. It was hypothesized that a minor de-ethylated metabolite was responsible for the accumulation of the drug, since it was a time-dependent inhibitor of CYP3A4. New compounds were explored to address the potential formation of a similar phenol metabolite [100]. Not surprisingly, for reasons already discussed (N-oxide formation of pyridine), the peripheral ethylsulfonyl group was maintained during these explorations. It was hypothesized that core attachment of the 4-ethoxyphenyl ( $R^1$ ) through a carbon atom would give an oxidatively more stable ligand than attachment through a nitrogen atom. However, selected phenol analogues with a C-linkage were still time-dependent inhibitors of CYP3A4. Thus, it was suggested that the 4-ethoxyphenyl group had to be replaced. To that end, cyano derivatives of **21** were synthesized. Indeed, the general strategy of cyano replacements for the ethoxy group has already been explored previously (Table 2). Cyano-derivative **24** (Table 4) showed a promising potential, because it did not produce any metabolites with CYP3A4 time-dependent inhibitory activity. This compound did test positive in an in vitro chromosomal aberration assay, however. Likewise, most other tested cyano derivatives tested positive in the chromosomal aberration assay, with the

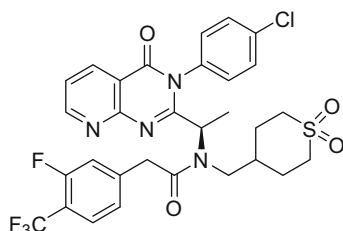
**Table 4** Optimization of quinazolinone derivatives by Chen et al. [100]

Compound		R <sup>1</sup>	R <sup>2</sup>	IC <sub>50</sub> (nM)	
#	In ref.			CXCL10 <sup>a</sup>	Migration <sup>b</sup>
<b>24</b>	15	CN	*CH <sub>2</sub> CH <sub>2</sub> SO <sub>2</sub> Et	11	n.s.
<b>25</b>	19	CN	*CH <sub>2</sub> CH <sub>2</sub> CyclohexylS(=O) <sub>2</sub>	12	39
<b>26</b>	25	Cl	*CH <sub>2</sub> CH <sub>2</sub> CyclohexylS(=O) <sub>2</sub>	6	45
<b>27</b>	28	F	*CH <sub>2</sub> CH <sub>2</sub> CyclohexylS(=O) <sub>2</sub>	7	72

<sup>a</sup>Displacement of [<sup>125</sup>I]-labeled CXCL10 from the CXCR3 receptor<sup>b</sup>CXCL11-mediated migration in the presence of 100% human serum

n.s. not shown in article

exception of, e.g., **25** ( $IC_{50}=12$  nM). When the cyano moiety as R<sup>1</sup> was replaced with a chlorine or a fluorine in certain members, as in **26** ( $IC_{50}=6$  nM), the chromosomal aberration assay activity was abolished. These findings suggest that the cyano group was responsible for the activity in the chromosomal aberration assay. The cyclic sulfone moiety (present in **26** and **27**,  $IC_{50}=7$  nM) generally gave higher potency compared to some ethylsulfone (R<sup>2</sup>) counterparts. Compounds **26** and **27** were selected for evaluation in multiple species. In general, **26** seemed to have the best PK profile, owing to a lower clearance and longer half-lives across the tested species (with the exception of dogs).

**28**

Interestingly, a paper on process chemistry aspects of the synthesis of **28** (the 4-CF<sub>3</sub>-3-F regioisomer of **26**) has been published, suggesting that **28** has also been of advanced interest for the Amgen CXCR3 research program. The paper contains valuable details for obtaining members of the (aza)quinazolinone class in enantiopure form [101].

### 2.1.2 Imidazole and Imidazopyrazine Derivatives

Since it was suggested that the core of the quinazolinone series tolerated many changes and served mainly to orient the peripheral groups correctly [97], a series of imidazole derivatives was explored (Table 5) [102]. It was hypothesized that the imidazole group would be a suitable replacement for the quinazolinone moiety, because both groups contain nitrogen atoms in a 1,3 relationship. However, **29** ( $IC_{50} = 1,800$  nM), the parent imidazole derivative, showed poor CXCR3 affinity. It was proposed that a lipophilic moiety mimicking the phenyl part of the quinazolinone core was necessary. Gratifyingly, appending a phenyl group on the 4-position increased the affinity (**30**,  $IC_{50} = 11$  nM). The *N*-alkyl moiety ( $R^2$ ) was then optimized [102]. The SAR for the (aza)quinazolinone series (vide supra) indicated that polar groups are preferred at this site [87, 98]. This trend held for the imidazole series. Similar to the (aza)quinazolinone SAR [98], ethylsulfonyl compounds like **31** ( $IC_{50} = 0.4$  nM) had the best affinity for the CXCR3 receptor. Amines, alkoxy groups, and several pyridyl moieties also displayed good affinity. With the aim to identify a more polar  $R^3$ -portion, the  $R^3$  part was tested for a variety of side chains, such as imidazole-phenyl, triazole-phenyl, and tetrazole-phenyl [102]. All tested side chains had less affinity for the receptor than **31**, although differences were not very dramatic.

As mentioned, metabolic studies of the 4-ethoxyphenyl-substituted analogues demonstrated the formation of phenolic metabolites that are time-dependent inhibitors of CYP3A4, a recurring problem with this class of compounds (vide supra). Thus, replacement of the ethoxy moiety ( $R^4$ ) was sought. The cyano analogue **32** displayed an  $IC_{50}$  value of 0.7 nM, and, thus, the cyano was considered a good replacement for the ethoxy moiety [102]. It is noted, however, that a later study by Chen et al. (vide supra) showed that the cyano moiety may cause activity in *in vitro* chromosomal aberration assays [100]. Exploration of the substitutions at the 4-position of the imidazole ring ( $R^1$ ) showed that replacement of the phenyl moiety by small alkyl groups, like **33** ( $IC_{50} = 6.6$  nM), or by pyridyl resulted in a loss of affinity compared to **32** [102]. However, evaluation of the PK properties indicated that **33** had better solubility and permeability than **32** and was cleared slower than **32**, justifying further inspection of the cyclopropyl class of compounds. Metabolic studies showed that a significant amount of glutathione (GSH) conjugates formed at the imidazole ring of **33** [102]. Consequently, it was tried to circumvent the GSH-conjugate formation by modification of  $R^5$ . Electron-withdrawing groups difluoromethyl (**34**,  $IC_{50} = 12$  nM) and chlorine (**35**,  $IC_{50} = 7.8$  nM) prevented

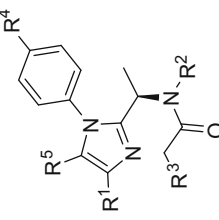
**Table 5** Optimization of imidazole derivatives by Du et al. [102]

Compound #	In ref.	R <sup>1</sup>	R <sup>2</sup>	R <sup>3</sup>	R <sup>4</sup>	R <sup>5</sup>	IC <sub>50</sub> (nM)		Migration <sup>b</sup>
							CXCL10 <sup>a</sup>	1,800	
<b>29</b>	2	H	*-C <sub>6</sub> H <sub>4</sub> -C <sub>6</sub> N	F <sub>3</sub> C-C <sub>6</sub> H <sub>4</sub> -*	OEt	H			n.s.
<b>30</b>	3		*-C <sub>6</sub> H <sub>4</sub> -C <sub>6</sub> N	F <sub>3</sub> C-C <sub>6</sub> H <sub>4</sub> -*	OEt	H	11		n.s.
<b>31</b>	16		*-C <sub>6</sub> H <sub>4</sub> -C <sub>6</sub> N	F <sub>3</sub> C-C <sub>6</sub> H <sub>4</sub> -*	OEt	H	0.4		n.s.
<b>32</b>	29		*-C <sub>6</sub> H <sub>4</sub> -C <sub>6</sub> N	F <sub>3</sub> C-C <sub>6</sub> H <sub>4</sub> -*	CN	H	0.7	10	
<b>33</b>	32		*-C <sub>6</sub> H <sub>4</sub> -C <sub>6</sub> N	F <sub>3</sub> C-C <sub>6</sub> H <sub>4</sub> -*	CN	H	6.6		53
<b>34</b>	40		*-C <sub>6</sub> H <sub>4</sub> -C <sub>6</sub> N	F <sub>3</sub> C-C <sub>6</sub> H <sub>4</sub> -*	CN	CHF <sub>2</sub>	12		20
<b>35</b>	43		*-C <sub>6</sub> H <sub>4</sub> -C <sub>6</sub> N	F <sub>3</sub> C-C <sub>6</sub> H <sub>4</sub> -*	CN	Cl	7.8		80

<sup>a</sup>[<sup>125</sup>I]-labeled CXCL10 displacement assay to CXCR3 expressed on IL-2 activated human PBMC in the absence of human plasma

<sup>b</sup>CXCL11-induced cellular migration assay of PBMC

n.s. not shown in article



the formation of such adducts while not compromising affinity. Compounds **34** and **35** have oral bioavailability and acceptable PK in rat.

Du et al. continued to improve the potency of the antagonists originating from the (aza)quinazolinone series [103]. Initial efforts on the 8-azaquinazolinone series focused on the C7-position (the CH adjacent to the pyridine unit of the bicyclic system), since a major metabolic pathway was found to be oxidation by aldehyde oxidase at C7. Although in vitro improvement was achieved with small substituents at C7, this did not translate to in vivo profiles. The efforts then turned to a series of imidazopyrimidines (Table 6), exemplified by initial compound **36** ( $IC_{50} = 10\text{ nM}$ ). However, neither the affinity of **36** nor the clearance rate of **36** was as good as desired. This prompted the researchers to shift the N by one atom in the core, giving imidazopyrazines. In accord with the affinity increase with small groups at C7 of 8-azaquinazolinone compounds, small groups (e.g., methyl, methoxy, ethyl, and chlorine) at the C8-position ( $R_2$ ) of the imidazopyrazine core significantly increased the affinity compared to  $R_2$  being H. Cyclopropyl-derivative **37** had 15-fold increased affinity for the receptor and was the most stable compound in rat microsomes. However, **37** gave significant pregnane X receptor (PXR) activation. PXR activation induces the formation of CYP3A4, which could potentially lead to drug-drug interactions. In order to solve the issue, a more rigid cyclic sulfone moiety was incorporated into the molecule ( $R^3$ ), and the substitution pattern at  $R^4$  was reevaluated for PXR activity. This led to compounds **38** and **39** which showed reduced PXR activity. Ligand **38** was more potent in a CXCL11 plasma migration assay and had in vivo efficacy in blocking bleomycin-induced leukocyte migration into the lung.

QSAR studies have been carried out on the early papers from Amgen [87, 102] collectively encompassing several different cores [104]. These studies indicated that highest occupied molecular orbital energy, principal moment of inertia, polar surface area, presence of triple bond, and Kier shape descriptors can be used to predict [ $^{125}\text{I}$ ]-CXCL10  $IC_{50}$  inhibition values [104].

## 2.2 *1-Aryl-3-Piperidin-4-yl-Ureas and Later-Generation Analogues*

An HTS campaign (UCB) using a FLIPR-based calcium flux assay delivered cyclooctenyl urea hit **40** ( $K_i = 110\text{ nM}$ ) [105]. An early scan of the aromatic moiety revealed fluorinated phenyl groups (e.g., **41**,  $K_i = 47\text{ nM}$ ) to be advantageous over the naphthyl group (Table 7). A SAR study at the cycloaliphatic right-hand side ( $R^2$ ), while maintaining the original naphthyl left-hand side, identified the (–) myrtenyl group as a reasonable substitute. With this group at hand, revisiting the aromatic left-hand side yielded a range of affinities with several fluorinated aromatic rings once again standing out. One of the most attractive compounds was **42** ( $K_i = 16\text{ nM}$ ) which, compared to hit **40**, had improved affinity, solubility, and

**Table 6** Optimization of imidazopyrazine derivatives by Du et al. [103]

Compound #	In ref.	R <sup>1</sup>	R <sup>2</sup>	R <sup>3</sup>	R <sup>4</sup>	IC <sub>50</sub> (nM)		Migration <sup>b</sup>
						CXCL10 <sup>a</sup>	Y	
<b>36</b>	3	H	—	*—SO <sub>2</sub> Et	F <sub>3</sub> C—*—F	N	10	643
<b>37</b>	18	—	△—*	*—SO <sub>2</sub> Et	F <sub>3</sub> C—*—F	C	0.9	17
<b>38</b>	21	—	△—*	*—Cyclohexane—S(=O) <sub>2</sub>	F <sub>3</sub> C—*—F	C	0.9	18.9
<b>39</b>	22	—	△—*	*—Cyclohexane—S(=O) <sub>2</sub>	F <sub>3</sub> CO—*—F	C	1.1	34

<sup>a</sup>[<sup>125</sup>I]-labeled CXCL10 displacement assay to CXCR3 expressed on IL-2 activated human PBMC in the absence of human plasma

<sup>b</sup>CXCL11-induced cellular migration assay of PBMC

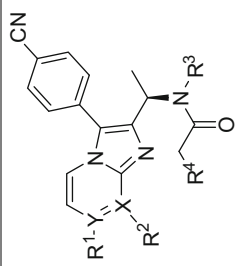


**Table 7** Optimization of 1-aryl-3-piperidin-4-yl-ureas and analogues by Allen et al. and Watson et al. [105, 106]

Compound		R <sup>1</sup>	R <sup>2</sup>	K <sub>i</sub> (nM)
#	In ref.			CXCL10/CXCL11 <sup>a</sup>
<b>40</b>	3 [105]			110
<b>41</b>	5g [105]			47
<b>42</b>	9t [105]			16
<b>43</b>	7a [106]			26
<b>44</b>	10d [106]			270

<sup>a</sup>CXCL10/CXCL11 stimulated [<sup>35</sup>S]-GTPγS assay using CXCR3 transfected CHO membranes

Log D. In a follow-up paper [106], the role of the urea portion was investigated further (Table 7). One of the approaches was to use a hydantoin constraint strategy, which afforded potent compounds (**43**, K<sub>i</sub> = 26 nM). Since the hydantoin series as a whole suffered from very high microsomal metabolism, replacements were sought. Although these did not match the potency of hydantoin **43**, arylazoles such as **44** (K<sub>i</sub> = 270 nM) did present advantages in terms of PK properties.

Efforts to further fine-tune the right-hand side of the original series were also initiated (Table 8) [107]. A previously [105] disclosed key myrtenyl analogue **45** (K<sub>i</sub> = 0.026 μM) was poorly soluble. In contrast, the cyclic sulfone analogue **46** (K<sub>i</sub> = 1.1 μM) and the piperidine analogue **47** (K<sub>i</sub> = 0.06 μM) showed good log D and improved solubility, but considerable affinity was lost especially in the case of **46**. It was hypothesized that the lost affinity could be regained by modification of the involved piperidine ring [107]. While methylated piperidine rings did not display an improved affinity, bridged piperidine derivatives like N-acetyl homotropene analogue **48** (IC<sub>50</sub> = 0.009 μM) gave good affinity. It was suggested

**Table 8** Optimization of piperidine urea derivatives by Watson et al. [107]

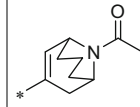
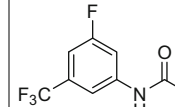
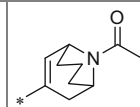
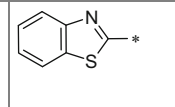
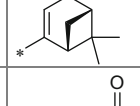
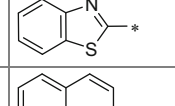
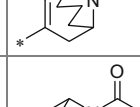
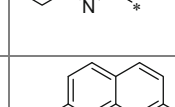
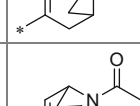
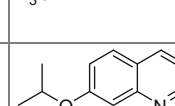
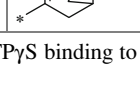
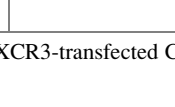
Compound		Core	R <sup>1</sup>	R <sup>2</sup>	$K_i$ ( $\mu\text{M}$ ) CXCL11 <sup>a</sup>
#	In ref.				
<b>45</b>	1b	A	*-CH <sub>2</sub> -C <sub>6</sub> H <sub>4</sub> -CH(CH <sub>3</sub> ) <sub>2</sub>	CF <sub>3</sub> F <sub>3</sub> C-C <sub>6</sub> H <sub>3</sub> -*	0.026
<b>46</b>	3a	A	*-CH <sub>2</sub> -CH <sub>2</sub> -C <sub>3</sub> H <sub>5</sub> S(=O)	CF <sub>3</sub> F <sub>3</sub> C-C <sub>6</sub> H <sub>3</sub> -*	1.1
<b>47</b>	3c	A	*-CH <sub>2</sub> -C <sub>6</sub> H <sub>11</sub> N(C <sub>2</sub> H <sub>5</sub> )C(=O)C <sub>2</sub> H <sub>5</sub>	CF <sub>3</sub> F <sub>3</sub> C-C <sub>6</sub> H <sub>3</sub> -*	0.06
<b>48</b>	9f	A	*-CH <sub>2</sub> -C <sub>6</sub> H <sub>4</sub> -C(=O)N <sub>2</sub> C <sub>2</sub> H <sub>5</sub>	F F <sub>3</sub> C-C <sub>6</sub> H <sub>3</sub> -*	0.009
<b>49</b>	9j	A	*-CH <sub>2</sub> -C <sub>6</sub> H <sub>4</sub> -C(=O)OCH <sub>2</sub> CH <sub>3</sub>	F CH <sub>3</sub> O-C <sub>6</sub> H <sub>3</sub> -*	0.003
<b>50</b>	15	B	*-CH <sub>2</sub> -C <sub>6</sub> H <sub>4</sub> -C(=O)OCH <sub>2</sub> CH <sub>3</sub>	F F <sub>3</sub> C-C <sub>6</sub> H <sub>3</sub> -*	0.007

<sup>a</sup>CXCL11-activated [<sup>35</sup>S]-GTP $\gamma$ S binding to hCXCR3-transfected CHO cell membranes

that the bridged piperidine fills a similar volume as the myrtenyl group, whereas this is less the case for non-bridged acylpiperidines. Revisiting the left-hand side, it was found that the incorporation of some polar aromatic substituents was tolerated on R<sup>2</sup> [107]. The 3-fluoro-5-isopropoxy derivative **49** ( $K_i = 0.003 \mu\text{M}$ ) showed an improved affinity compared to **48**. Several sites of metabolic oxidation were identified around the central piperidine ring of **48** [107]. It was postulated that bridging this ring could lower metabolism and that an *exo*-tropanyl moiety was of interest in this respect. Indeed, **50** ( $K_i = 0.007 \mu\text{M}$ ) showed the desired metabolic stability while maintaining an affinity comparable to **48**.

Knight et al. continued the development of **48** and aimed to create a series of non-urea derivatives with similar affinity and properties [108]. Initial efforts

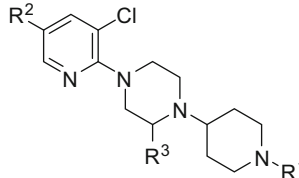
**Table 9** Optimization of piperidine urea derivatives by Knight et al. [108]

Compound		Core	R <sup>1</sup>	R <sup>2</sup>	R <sup>3</sup>	K <sub>i</sub> (nM)
#	In ref.					CXCL11 <sup>a</sup>
<b>48</b>	1b	A			H	9
<b>51</b>	6	A			Me	95
<b>52</b>	1c	A			Me	126
<b>53</b>	9a	A			H	135
<b>54</b>	14e	A			H	7
<b>55</b>	24d	B			H	5

<sup>a</sup>CXCL11-activated [<sup>35</sup>S]-GTPγS binding to hCXCR3-transfected CHO cell membranes

delivered azole analogue **51** ( $K_i = 95$  nM, Table 9) bearing a homotropene moiety similar to **48** and displaying similar affinity to myrtenyl-parent **52** ( $K_i = 126$  nM). However, **51** still had undesirable properties like high plasma protein binding. In order to improve the PK properties, it was decided to differentiate at the R<sup>2</sup> moiety [108]. Aminoquinoline analogue **53** ( $K_i = 135$  nM) showed good affinity and appropriate substitutions significantly increased the affinity further. For example, 7-trifluoromethyl derivative **54** showed good affinity and had a good clearance of 10 μL/min/mg. As previously discussed (vide supra) [107], replacement of the central piperidine ring for a tropane ring can have benefits in terms of affinities and metabolic stability. When applied here, the resulting compound **55** ( $K_i = 5$  nM) had a good affinity, log D of 2.9, and low intrinsic clearance [108].

**Table 10** Optimization of piperazinyl-piperidine derivatives by McGuinness et al. [109]

				
Compound #	In ref.	R <sup>1</sup>	R <sup>2</sup>	R <sup>3</sup>
<b>56</b>	1a	*-C <sub>6</sub> H <sub>4</sub> -C≡N	*-C <sub>6</sub> H <sub>4</sub> -O-CH <sub>2</sub> -NH-C(=O)-*	H
<b>57</b>	1f	*-C <sub>6</sub> H <sub>4</sub> -Cl	*-C <sub>6</sub> H <sub>4</sub> -O-CH <sub>2</sub> -NH-C(=O)-*	H
<b>58</b>	1q	*-C <sub>6</sub> H <sub>4</sub> -Cl	*-C <sub>6</sub> (Cl) <sub>2</sub> -CH <sub>2</sub> -NH-C(=O)-*	H
<b>59</b>	12a	*-C <sub>6</sub> H <sub>4</sub> -Cl	*-C <sub>6</sub> (Cl) <sub>2</sub> -CH <sub>2</sub> -NH-C(=O)-N-	H
<b>60</b>	36	*-C <sub>6</sub> H <sub>4</sub> -Cl	*-C <sub>6</sub> (Cl) <sub>2</sub> -CH <sub>2</sub> -NH-C(=O)-*	(S)-Me
<b>61</b>	37	*-C <sub>6</sub> H <sub>4</sub> -Cl	*-NH-C(=O)-*	(S)-Me

<sup>a</sup>Scintillation proximity binding assay using Ba/F3-CXCR3 membranes and [<sup>125</sup>I]-CXCL10 in buffer

### 2.3 Piperazinyl-Piperidines

McGuinness et al. (Merck) identified **56** ( $K_i = 110$  nM) as a high-throughput screening hit from an encoded combinatorial library [109]. Further exploration utilized a substantial amount of solid-phase synthesis to rapidly provide a collection of analogues (Table 10). Exploration of the R<sup>1</sup>-position indicated a preference for a *para*-substituted benzyl moiety given that, e.g., the unsubstituted benzyl analogue, the 3-cyanobenzyl analogue, and the 2-cyanobenzyl analogue all lost affinity. It was found that the 4-chlorobenzyl compound **57** ( $K_i = 70$  nM) represented an optimum. This SAR trend was noted to be similar to the benzetimide series described by Bongartz et al. (vide infra) [110]. The authors speculate that both classes may share a similar binding mode with the CXCR3 receptor. With the 4-chlorobenzyl at hand,

the left-hand nicotinyl amide was optimized [109]. It was mentioned that complete removal of the amide moiety led to a loss of affinity. Among amide substituents, electron-deficient benzyl rings were preferred (**58**,  $K_i = 35$  nM). Replacement of the amide moiety by, for example, a secondary amine, tertiary amine, or urea as well as inversion of the amide (**59**) reduced the affinity for CXCR3. Removal of the 5-chlorine on the pyridine ring or removal of the pyridine nitrogen likewise led to a drop in affinity. SAR was also strict on the piperidinyl-piperazine core [109]. Removal of a nitrogen atom was not tolerated, nor was relocation of nitrogen atoms or ring opening. However, (*S*)-methyl substitution of the piperazine ring increased affinity twofold (**60**,  $K_i = 16$  nM). Interestingly, affinity was only slightly reduced when the dichlorobenzyl moiety of  $R^2$  of **60** was changed to a methyl group (**61**,  $K_i = 32$  nM).

The SAR of the  $R^1$  unit was explored in more detail by Shao et al., largely using aromatic and heteroaromatic substitutions (Table 11) [111]. Replacement of the 4-chlorobenzyl moiety of **61** by heteroaromatics or a more polar substituent such as 4-(methanesulfonyl)benzyl resulted in a decrease of affinity, leading the authors to suggest an interaction with a lipophilic region of the receptor binding pocket. However, small lipophilic substituents such as 4-methyl and 4-trifluoromethyl led to a decrease in affinity too. On the other hand, 2,4-dihalo substitution (i.e., 2,4-dichloro analogue **62**,  $IC_{50} = 17$  nM) and methyl substitution of the benzylic methylene proved beneficial in increasing the affinity for the receptor (**63**,  $IC_{50} = 5$  nM, other diastereomer less active). As McGuinness et al. reported [109], (*S*)-methyl substitution at the 2'-position of the piperazine ring ( $R^2$ ) resulted in an improved affinity (see **60** and **61**). This triggered the examination of methyl substitutions throughout the core [111]. Substitution with (*S*)-methyl on the alternative 5'-position of the piperazine ring was tolerated, while an (*R*)-methyl resulted in a sixfold loss of affinity. Methylations of the 2'', 4'', and 5''-positions of the core piperidine ring were also tolerated, but did not improve the affinity for the receptor significantly. Since many of these methylations will add additional stereochemical complexity, the authors did not pursue these further. Both basic nitrogen atoms (i.e., trialkyl nitrogens) of the piperazinyl-piperidine ( $X=N$ ,  $Y=CH$ ) core were essential for CXCR3 affinity [111]. Since inverted piperidinyl-piperazine ( $X=CH$ ,  $Y=N$ ) analogues **64** ( $IC_{50} = 4,500$  nM) and **65** ( $IC_{50} = 280$  nM) gave reduced affinity, the hypothesis that both basic nitrogen atoms are crucial in a spatially defined way is further supported. The 5-pyridyl carboxamide ( $R^3$ ) could be reverted, leading to equal or better affinity compared to initial lead compound **61**, but (perhaps for toxicophore reasons) this series was not followed upon [111]. The primary amide **66** ( $IC_{50} = 39$  nM) displayed similar affinity as **61**, while an N-ethyl-amide (i.e., **67**,  $IC_{50} = 2.3$  nM) gave increased affinity. Having scanned most of the scaffold, the 2'-position substituent ( $R^2$ ) was re-optimized [111]. With the amide  $R^3$  being Me, the 2'(*S*)-ethyl analogue **68** ( $IC_{50} = 3$  nM) proved to have a tenfold better affinity than **61**. Larger substituents (**69**) or more polar substituents as  $R^2$  (**70**) led to a drop in affinity. A tenfold enhancement of affinity was achieved when  $R^3$  was substituted with an ethyl moiety (**71**,  $IC_{50} = 0.3$  nM; **72**,  $IC_{50} = 0.2$  nM) instead of a methyl moiety.

**Table 11** Optimization of piperazinyl-piperidine derivatives by Shao et al. [111]

Compound				R <sup>2</sup>	R <sup>3</sup>	X	Y	IC <sub>50</sub> (nM) <sup>a</sup>
#	In ref.	R <sup>1</sup>						
<b>62</b>	6i		(S)-Me	Me		N	CH	17
<b>63</b>	6k		(S)-Me	Me		N	CH	5
<b>64</b>	16a		H			CH	N	4,500
<b>65</b>	16d		(R,S)-Me	Me		CH	N	280
<b>66</b>	17f		(S)-Me	H		N	CH	39
<b>67</b>	17g		(S)-Me	Et		N	CH	2.3
<b>68</b>	18a		(S)-Et	Me		N	CH	3
<b>69</b>	18b		(S)-iBu	Me		N	CH	260
<b>70</b>	18e		(R,S)-CH <sub>2</sub> OH	Me		N	CH	910
<b>71</b>	18i		(S)-Et	Et		N	CH	0.3
<b>72</b>	18j		(S)-Et	Et		N	CH	0.2

<sup>a</sup>Details of assay conditions not given in reference

Compounds **71** and **72** represent the first reported sub-nanomolar CXCR3 antagonists. Indeed, at the time, compound **71** had already drawn our attention from the patent literature [112], and we used it in a hybrid-design strategy to probe a potential polycycloaliphatic pocket in CXCR3 (vide infra) [113]. Extensive mutation studies have been done by us on compound **71**, which we called VUF11211 [80]. The binding of **71** to CXCR3 was affected by mutations in the TM region of CXCR3, whereas CXCL11 affinity remained largely unchanged. A binding model was constructed based on homology modeling and the data from the mutagenesis study, revealing a cross-pocket binding mode for **71**, binding to both TMS1 and TMS2, and partially overlapping with the binding mode for **11** [80]. Since the CXCR3 chemokines are binding to the extracellular loops and N-terminus of the receptor, these small molecules probably bind in an allosteric manner (see Sect. 4) [20, 80].

Despite the extraordinary high in vitro affinity of **71**, work continued because **71** exhibited modest PK features in rat and had undesirable hERG affinity [114]. The pyridine ring of **71** was initially replaced by a pyrazine moiety (**73**), and the new core motif was optimized (Table 12), first of all by appending an NH<sub>2</sub> group onto the pyrazine (R<sup>3</sup>). First, the R<sup>1</sup>-substituent was modified maintaining a primary amide as R<sup>2</sup>, revealing that many analogues (like **74**) had reasonable affinity for CXCR3 if the R<sup>1</sup>-substituent was a benzylic group. With the 4-chlorobenzyl fixed, the SAR at the R<sup>2</sup>-position was probed. Polar substituents such as hydroxyalkyl moieties, sulfonamides, and lactone analogues showed good affinity (i.e., hydroxyalkyl analogue **75**, IC<sub>50</sub> = 0.3 nM). Unfortunately, many of those compounds also displayed affinity for the hERG channel. In an attempt to improve the hERG profile, polar substituents on R<sup>2</sup> in combination with polar groups as R<sup>1</sup> were investigated. The strategy worked as, e.g., sulfonamide analogues (R<sup>2</sup>) improved the hERG profile, while affinity was reasonably maintained. Likewise, the hERG affinity decreased for 6-amino-2-chloropyridine-5-carboxamide derivative **76** (IC<sub>50</sub> = 3.4 nM). Moreover, the exposure in rat was improved for **76**. Therefore, the 6-amino-2-chloropyridine-5-carboxamide moiety was fixed as R<sup>1</sup>, with SAR focusing on other parts of the scaffold. As the previous pyridine series proved good without a 6-amino moiety as R<sup>3</sup>, this amino group was removed and the R<sup>2</sup>-position was modified. Primary and secondary amides were both well tolerated, indicating that the 6-amino group was not essential for binding. Subsequently, a more stable replacement was sought for the 3-chloro moiety of the pyrazine, perhaps because it can act as an electrophile. Thus, replacements for R<sup>4</sup> were investigated, which showed that methyl and trifluoromethyl analogues were all acceptable. Exemplary cyclopropylamide **77** (IC<sub>50</sub> = 1.9 nM) possesses good affinity, little hERG affinity, and good PK in rat. Additional revisiting of the 4-chlorobenzamide as R<sup>1</sup> led to **78** (IC<sub>50</sub> = 1.1 nM), which showed a good combination of CXCR3 affinity and rat PK. The high percentage of hERG inhibition (74% at 10 μM) of **78** could be circumvented by introduction of an (R)-methyl moiety at R<sup>5</sup> (**79**, IC<sub>50</sub> = 1.3 nM, hERG inhibition of 7% at 10 μM).

Jenh et al. analyzed and reported the properties of **74**, also known as SCH 546738 [54]. The compound exhibited favorable pharmacokinetic properties in rodents and appeared effective as CXCR3 antagonist both in vitro and in vivo. For example, it inhibited the chemotaxis of isolated human T cells towards CXCL9,

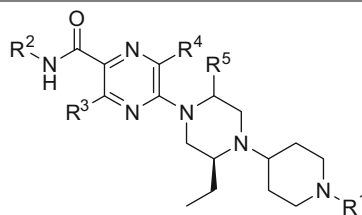
**Table 12** Optimization of piperazinyl-piperidine derivatives by Kim et al. [114]

Compound							IC <sub>50</sub> (nM)
#	In ref.	R <sup>1</sup>	R <sup>2</sup>	R <sup>3</sup>	R <sup>4</sup>	R <sup>5</sup>	CXCL10 <sup>a</sup>
73	2	*-Cl-C <sub>6</sub> H <sub>4</sub> -CH <sub>2</sub> -	Et	H	Cl	H	n.s.
74	8a	*-Cl-C <sub>6</sub> H <sub>4</sub> -CH <sub>2</sub> -	H	NH <sub>2</sub>	Cl	H	0.8
75	8i	*-Cl-C <sub>6</sub> H <sub>4</sub> -CH <sub>2</sub> -	HO-CH <sub>2</sub> -CH <sub>2</sub> -*	NH <sub>2</sub>	Cl	H	0.3
76	8r	*-Cl-C <sub>6</sub> H <sub>4</sub> -CH <sub>2</sub> -C(=O)-NH <sub>2</sub>	HO-CH <sub>2</sub> -CH <sub>2</sub> -*	NH <sub>2</sub>	Cl	H	3.4
77	15f	*-Cl-C <sub>6</sub> H <sub>4</sub> -CH <sub>2</sub> -C(=O)-NH <sub>2</sub>	1- <i>i</i> -propyl	H	Me	H	1.9
78	15j	*-Cl-C <sub>6</sub> H <sub>4</sub> -CH <sub>2</sub> -C(=O)-	1- <i>i</i> -propyl	H	Me	H	1.1
79	16e	*-Cl-C <sub>6</sub> H <sub>4</sub> -CH <sub>2</sub> -C(=O)-	1- <i>i</i> -propyl	H	Me	(R)-Me	1.3

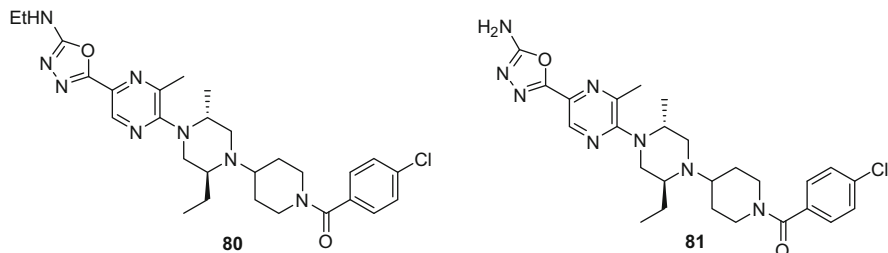
<sup>a</sup>[<sup>125</sup>I]-labeled CXCL10 displacement assay performed in Ba/F3 cells expressing human CXCR3  
n.s. not shown in article

CXCL10, and CXCL11 in a noncompetitive manner. In addition, **74** dose-dependently attenuated collagen-induced arthritis in a mouse model for rheumatoid arthritis. Similarly, it delayed disease onset and attenuated disease severity in murine experimental autoimmune encephalomyelitis, a model for human multiple sclerosis. Moreover, **74** significantly delayed graft rejection in a cardiac allograft model [54].

In the latest disclosed SAR work [115], efforts were directed towards improving PK, hERG, and metabolic parameters. The key approach involved replacing the amide functionality with heterocycles, among which oxadiazoles, imidazoles, and



triazoles were probed. Additional balancing involved revisiting other parts of the molecule. Exemplary resulting molecules are **80** ( $IC_{50}=2.8$  nM) and **81** ( $IC_{50}=6.4$  nM). Notably, both had significantly lower hERG affinities (25 and 0% in Rb efflux assay) than several predecessors while displaying good PK properties.



## 2.4 Ergolines

In 2009, Thoma et al. (Novartis) described the discovery of the lysergic acid-derived inhibitor **82**, a rather unusual type of CXCR3 binder [116]. GPCR selectivity was tested at an early stage, and unlike lysergic acid diethylamide (LSD) and its close derivative **83**, compound **82** did not significantly inhibit serotonin, adrenergic, and dopamine receptors. The selectivity may be explained by different electronic and steric properties of **82** compared to LSD and **83**. For example, **82** (lacking a highly basic N-atom) is neutral under physiological conditions, whereas LSD is protonated. Compound **82** was stable in rat and human microsomes and it had a similar metabolic pattern in all tested species. Preliminary SAR efforts indicated that relatively moderate changes of the core structure strongly affected the affinity [116]. Changes in the amide group ( $R^1$ ), such as removal of the carbonyl moiety, reduced the affinity, as did modification of the urea portion of the molecule ( $R^2$ ). Methylation or benzylation of the indole N ( $R^3$ ) were not of additional value either. In all, a preliminary strict SAR emerged.

In 2011, a more in-depth SAR of the ergoline series was described (also Table 13) [117]. In terms of amide N-substituents ( $R^1$ ), primary and secondary amide analogues lost affinity. Indeed, cyclic tertiary amides, such as **84** ( $IC_{50}=5$  nM), showed the best binding affinities. Various more polar aliphatic heterocycles, such as piperazines and sulfoxide derivatives, had lower affinity for the receptor. With the pyrrolidine amide at  $R^1$ , variation of  $R^2$  was explored [117]. In general, *meta*-substitution of the urea phenyl group was preferred over *ortho*- or *para*-substitution. Aliphatic cyclohexyl urea **85** ( $IC_{50}=24$  nM) and cycloheptyl urea **86** ( $IC_{50}=28$  nM) showed good affinities, while introduction of amides instead of ureas led to a decrease in affinity. In the end, the phenyl urea moiety (as in **84**) remained the best substituent. Unfortunately, **84** only modestly

**Table 13** Optimization of ergolines by Thoma et al. [116, 117]

Compound		R <sup>1</sup>	R <sup>2</sup>	R <sup>3</sup>	IC <sub>50</sub> (nM)	
#	In ref.				CXCL11 <sup>a</sup>	Ca <sup>2+</sup> <sup>b</sup>
	LSD		Me	H	n.s.	n.s.
82	1, [116] 1a [117]			H	51 [117]	18
83	2 [116]		H	H	>10,000	n.d.
84	1h [117]			H	5	4
85	8o [117]			H	24	11
86	8p [117]			H	28	14
87	1t [117]			H	14	5
88	11a [117]				2	2

<sup>a</sup>[<sup>125</sup>I]-labeled CXCL11 displacement assay performed in CHO cells expressing human CXCR3<sup>b</sup>CXCL11-induced Ca<sup>2+</sup>mobilization assessed in CXCR3-transfected L 1.2 cells

n.s. not shown in article, n.d. not determined

inhibited CXCL11 binding to CXCR3 in both rat ( $IC_{50} = 3,300$  nM) and human blood ( $IC_{50} = 700$  nM) [117]. Given that the more polar **87** ( $IC_{50} = 14$  nM) showed less reduced inhibition in human blood ( $IC_{50} = 200$  nM), polarity was postulated as a key factor. More polar groups were sought for at the nitrogen atom of the indole ( $R^3$ ), as polar groups in the amide portion and the urea portion had shown to lead to less potent derivatives. At  $R^3$ , an ethanol substituent or various basic amino functionalities (i.e., **88**,  $IC_{50} = 2$  nM) gave good affinity and potency which was,

gratifyingly, largely retained in rat blood ( $IC_{50} = 5 \text{ nM}$ ). Favorable features of **88** include the bioavailability (97%) and the half-life ( $t_{1/2} = 8.9 \text{ h}$ ).

A compound named NIBR2130 [118], assumed to be from the ergoline-type class, was recently shown to have only a limited impact on disease outcome in a diabetes type 1 mouse model [118] and on cardiac allograft rejection in mice and rats [57] while having favorable pharmacokinetics and nanomolar affinity for both human and murine CXCR3 (both  $IC_{50} = 2.2 \text{ nM}$ , [ $^{125}\text{I}$ ]-CXCL11) [57, 118].

## 2.5 *Iminobenzimidazoles*

An HTS of the Abbott corporate compound collection led to the discovery of **89**, a compound with moderate affinity for CXCR3 ( $IC_{50} = 3 \mu\text{M}$ ) [119]. The molecular weight and log P (2.7) of **89** were considered a suitable starting point for hit-to-lead (Table 14). In the acetophenone portion ( $R^1$ ) of the molecule, a cyano group instead of a nitro group was not tolerated, but the bromo and chloro analogues had affinities in the same range as **89**. Removal of the 4-substituent or replacement of the carbonyl moiety of the acetophenone portion with a sulfoxide or alcohol reduced the affinity. Substitution of the benzimidazole core was also explored ( $R^2$ ) [119]. While substitution with a 4-OMe (**90**,  $IC_{50} = 3 \mu\text{M}$ ) showed no change in affinity, substitution at the 5-position and 6-position resulted in compounds with only weak affinity. Because the 2-acyl analogues (collectively referred to as A) like **89** and **90** were poorly soluble in aqueous buffer, the 2-acyl was replaced for an imino group while an additional N-Me was appended as well (referred to as B) [119]. With the parent unsubstituted 2-imino compound **91** ( $IC_{50} = 0.8 \mu\text{M}$ ) at hand, the impact of substitution on the benzimidazole core ( $R^2$ ) and acetophenone moiety ( $R^1$ ) was reevaluated [119]. Notably, substitutions on the 4-position of the benzimidazole improved or maintained affinity compared to **91**, with 4-ethyl analogue **92** ( $IC_{50} = 0.03 \mu\text{M}$ ) displaying the best affinity. Larger substituents and more polar substituents did not perform as well, leading the authors to suggest that the binding subpocket for C4-groups is small and lipophilic. As in previous evaluations (vide supra), substitution on the 5- and 6-position did not improve the affinity.

The focus of Hayes et al. also turned to replacing the N-Me of the iminobenzimidazole core ( $R^1$  in Table 15) [120]. The beneficial ethyl moiety on the 4-position ( $R^2$ ) was removed in order to better examine the impact of N-modification. Thus, the N3-position of **91** was substituted with increasingly larger groups, which was generally tolerated. A notable improvement in functional antagonism (FLIPR assay) was found for amide analogue **93** ( $IC_{50} = 0.4 \mu\text{M}$ ). The reverse amide analogue **94** ( $IC_{50} = 0.4 \mu\text{M}$ ) was less potent in a functional assay, but was nevertheless used for further optimization. Introduction of a chlorine atom as  $R^2$  increased affinity, and with this substituent the optimal linker length between the iminobenzimidazole nitrogen atom and the amide nitrogen atom was found to be propylene. Several aryl, heteroaryl, and aliphatic amides were probed to identify a more optimal amide substituent. Amide analogue **95** ( $IC_{50} = 0.02 \mu\text{M}$ ) emerged

**Table 14** Optimization of benzimidazole derivatives by Hayes et al. [119]

Compound		Core	R <sup>1</sup>	R <sup>2</sup>	R <sup>3</sup>	IC <sub>50</sub> (μM)
#	In ref.					CXCL10 <sup>a</sup>
<b>89</b>	1	A	*-CH <sub>2</sub> -C(=O)-4-(NO <sub>2</sub> )C <sub>6</sub> H <sub>4</sub>	H	COMe	3
<b>90</b>	4e	A	*-CH <sub>2</sub> -C(=O)-4-(Br)C <sub>6</sub> H <sub>4</sub>	OMe	COMe	3
<b>91</b>	12d	B	*-CH <sub>2</sub> -C(=O)-4-(Cl)C <sub>6</sub> H <sub>4</sub>	H	H	0.8
<b>92</b>	12p	B	*-CH <sub>2</sub> -C(=O)-4-(Cl)C <sub>6</sub> H <sub>4</sub>	Et	H	0.03

<sup>a</sup>[<sup>125</sup>I]-labeled CXCL10 displacement assay performed in Chinese hamster ovary (CHO) cells expressing human CXCR3

from this, as it had good affinity for both human and murine CXCR3. However, the half-life of **95** in mouse liver microsomes was short due to *N*-demethylation as the main metabolic event *in vitro*. To prevent such *N*-demethylation, the *n*-propyl linker was constrained into a ring (**96**, IC<sub>50</sub> = 0.015 μM). Another compound with a ring-containing linker (2-pyrrolidine compound **97**, IC<sub>50</sub> = 0.008 μM) showed good potency across species, but was nonetheless rapidly metabolized (apparently not to the demethylated analogue) in mouse liver microsomes.

## 2.6 VUA Compounds: Targeting a Hypothesized Polycycloaliphatic Pocket

Our group has published multiple articles on tool compounds that make use of the recurring [105, 121] polycycloaliphatic motif in CXCR3 ligands. Several venues were followed.

**Table 15** Optimization of benzimidazole derivatives by Hayes et al. [120]

Compound		R <sup>1</sup>	R <sup>2</sup>	IC <sub>50</sub> (μM)
#	In ref.			CXCL10 <sup>a</sup>
<b>93</b>	11b	*-CH <sub>2</sub> -CH <sub>2</sub> -CONH-CH <sub>2</sub> -CH <sub>2</sub> -C <sub>6</sub> H <sub>5</sub>	H	0.4
<b>94</b>	14d	*-CH <sub>2</sub> -CH <sub>2</sub> -N(CH <sub>3</sub> ) <sub>2</sub> -CH <sub>2</sub> -C <sub>6</sub> H <sub>5</sub>	H	0.4
<b>95</b>	14n	*-CH <sub>2</sub> -CH <sub>2</sub> -N(CH <sub>3</sub> ) <sub>2</sub> -C <sub>6</sub> H <sub>4</sub> -2-pyridyl	Cl	0.02
<b>96</b>	14o	*-CH <sub>2</sub> -CH <sub>2</sub> -N(CH <sub>3</sub> ) <sub>2</sub> -C <sub>6</sub> H <sub>4</sub> -2-pyridyl	Cl	0.015
<b>97</b>	14r	*-CH <sub>2</sub> -CH <sub>2</sub> -N(CH <sub>3</sub> ) <sub>2</sub> -C <sub>6</sub> H <sub>4</sub> -2-pyridyl	Cl	0.008

<sup>a</sup>[<sup>125</sup>I]-labeled CXCL10 displacement assay performed in Chinese hamster ovary (CHO) cells expressing human CXCR3

In our earliest efforts, we decided to use the piperazinyl-piperidine series disclosed by Merck to explore the CXCR3 binding site and the receptor's apparent preference for polycycloaliphatic groups [113]. More specifically, **71** and **72** were selected as a starting point from the patent literature [112], because their picomolar affinities may allow the removal of a substantial portion of the molecule followed by the appending of a polycycloaliphatic group. In a first scan, the benzylaminopiperidine part of **71** was equipped with various (poly)cycloaliphatic groups (R<sup>1</sup>, Table 16) [113]. Neither introduction of monocyclic aliphatic rings, such as pyrrolidine and N-cyclohexyl rings, nor the introduction of bicyclic aliphatic rings, such as (-)-myrtenyl and tropine groups, resulted in an acceptable affinity. One exception is the 2-adamantane analogue **98** ( $pK_i = 6.8$ ). SAR around this 2-adamantane unit was very strict, with all further manipulations (shifting to the

**Table 16** Optimization of polycycloaliphatic aminopiperidines by Wijtmans et al. [113]

Compound		R <sup>1</sup>	R <sup>2</sup>	pK <sub>i</sub> CXCL10 <sup>a</sup>
#	In ref.			
<b>98</b>	19			6.8
<b>99</b>	28			5.1
<b>100</b>	37			<5
<b>101</b>	38			6.4

<sup>a</sup>[<sup>125</sup>I]-labeled CXCL10 displacement assay performed in HEK293 cells expressing human CXCR3

1-position, methylation, linker elongation, incorporation of an N-atom to give **99** ( $pK_i = 5.1$ ) leading to reduced affinity. SAR was also strict around the 4-aminopiperidine core [113]. Changes such as substitution on the benzylic methylene, methylene insertion, introduction of a (un)saturated ester, and incorporation of a urea group to give **100** ( $pK_i < 5$ ) all gave reduced affinity. For further efforts, another polycycloaliphatic group was sought to overcome the high crystallinity and poor solubility of many of the tested adamantane compounds. The (*R*)-isobornyl analogue **101** ( $pK_i = 6.4$ ) displayed a somewhat reduced affinity compared to **98**, but did have the desired reduced crystallinity and was therefore selected for in-depth SAR on the benzyl portion ( $R^2$ ). In general, the (*R*)-isobornyl series exhibited similar SAR trends as the adamantane series, but none of the tried substitutions matched the affinity of parent **101**. In contrast to the achiral 2-adamantane series, compounds with an isobornyl group as  $R^1$  could be used to probe the “polycycloaliphatic pocket” with stereochemical subtleties of the bornyl group. However, little effect of stereochemistry was observed.

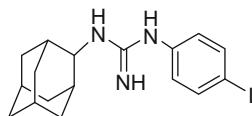
In second approach targeted at using the “polycycloaliphatic pocket”, we built on a medium-throughput screen of 3,360 pharmacologically active compounds performed in our labs [122]. The screen resulted in 90 hits that displace [<sup>125</sup>I]-CXCL10 for more than 50% at a concentration of 10 μM. One of those hits was IPAG (**102**), a sigma-receptor ligand. Although it had a moderate  $K_i$  of 4,000 nM

**Table 17** Optimization of polycycloaliphatic ammonium salts by Wijtmans et al. [122]

Compound		$\text{R}^1$	$\text{R}^2$	$\text{p}K_i$ CXCL10 <sup>a</sup>
#	In ref.			
<b>103</b>	8a			6.1
<b>104</b>	8f			6.6
<b>105</b>	9f			6.7
<b>106</b>	9j			6.5
<b>107</b>	10c			6.3
<b>108</b>	10q			6.9

<sup>a</sup>[<sup>125</sup>I]-labeled CXCL10 displacement assay performed in HEK293 cells expressing human CXCR3

for CXCR3, its adamantine substructure drew attention to the hypothesized “polycycloaliphatic pocket.” In order to simplify the generation of chemical diversity (Table 17), the guanidine unit was replaced with a tertiary amine or a quaternary ammonium cation. The distance between the aryl and adamantyl units was kept comparable to IPAG by the insertion of two methylene spacers.

**102** (IPAG)

The tertiary amine analogue of IPAG led to a reduced affinity, but insertion of a permanent cation by methylation of the nitrogen (i.e., **103**,  $\text{p}K_i = 6.1$ ) substantially

increased the affinity. It was hypothesized that the ability of the core to engage in electrostatic interactions plays a dominant role in this, so the permanent cation was maintained in subsequent SAR. During probing of the left-hand side portion ( $R^1$ ), the most notable observation was that introduction of a myrtenyl group resulted in an enhanced affinity (**104**,  $pK_i = 6.6$ ) compared to adamantane analogue **103**, which is opposite to what we discovered for the 4-aminopiperidine series (vide supra) [113]. This suggests that the IPAG derivatives bind in a different manner than the 4-aminopiperidine series. The aromatic right-hand side ( $R^2$ ) tolerated *para*-substitution with chlorine (**105**,  $pK_i = 6.7$ ), bromine, iodine but less so with fluorine. As a whole, the  $R^2$  SAR suggested that room for growth was available at the *para*-substitution of the benzyl substituent. Indeed, a biphenyl compound was found to have a good affinity for the receptor (**106**,  $pK_i = 6.5$ ) [122]. SAR at the biphenyl core itself was pretty strict, with, e.g., shifting of the phenyl ring, insertion of an oxygen atom, or constraint to give **107** ( $pK_i = 6.3$ ) not being of surplus value. The biphenyl moiety lends itself well to peripheral SAR, though. *Meta*-substitution was preferred, but protic polar *meta*-substitutions, such as hydroxyl and amino groups, reduced affinities. Indeed, substitution with the more lipophilic chlorine on the *meta*-position restored the affinity. In fact, *meta*-chloro analogue **108** was the compound with the best affinity of this series ( $pK_i = 6.9$ ).

This series served as a stepping stone for the discovery of a novel class of CXCR3 agonists (Sect. 3.2).

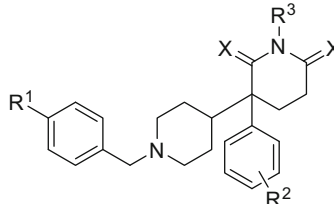
## 2.7 *Miscellaneous*

Several chemotypes have been the subject of one medicinal chemistry paper only. These have been collected in the current paragraph.

### 2.7.1 Benzetimide Derivatives

Bongartz et al. (Johnson & Johnson) screened a database of compounds for their inhibitory activity on cAMP in CXCL11-stimulated hCXCR3-transfected CHO cells [110]. Hit compound **109** inhibited [ $^{35}$ S]-GTP $\gamma$ S binding with an  $IC_{50}$  value of 0.78  $\mu$ M. Separation of the enantiomers showed that the (–) stereoisomer and the (+) stereoisomer had comparable CXCR3 antagonistic effects. Compound **109** resembles the muscarinic receptor antagonist benzetimide (where the Br is an H atom). For that reason, the anticholinergic activity of **109** was assayed as it may carry the risk of off-target effects. The (+) stereoisomer of **109** showed nanomolar affinity for the muscarinic receptors M1, M2, and M3, whereas the (–) stereoisomer of **109** showed only marginal affinity to M1. This is in accord with the notion that only the (+) stereoisomer of benzetimide (dexetimide) shows anticholinergic activity [110]. Acknowledging **109** as a good starting point for CXCR3 ligands, the N-substitution of the piperidine ring ( $R^1$ ) was explored (Table 18). Most substitution patterns for the benzyl ring were not of surplus value. Only a 3-fluoro-4-chloro

**Table 18** Optimization of benzetimide derivatives by Bongartz et al. [110]

							
Compound	In ref.	Stereochemistry	R <sup>1</sup>	R <sup>2</sup>	R <sup>3</sup>	IC <sub>50</sub> (μM)	
#					X	[ <sup>35</sup> S]-GTPγS <sup>a</sup>	
<b>109</b>	1	±	4-Br	H	H	O	0.78
<b>110</b>	12	–	3-F,4-Cl	H	H	O	0.34
<b>111</b>	18	±	4-Br	2,4-F	H	O	0.12
<b>112</b>	21	±	4-Br	2-OMe-5-SO <sub>3</sub> H	H	O	0.17
<b>113</b>	41a	–	4-Br	H	Acetyl	H, H	0.11
<b>114</b>	47b	+	4-Br	H	α-Acetamide	H, H	0.06
<b>115</b>	48a	–	4-Br	H	Phenylurea	H, H	0.03

<sup>a</sup>[<sup>35</sup>S]-GTPγS binding assay

substitution pattern, as in **110** ( $IC_{50} = 0.34 \mu M$ ), exhibited better affinity for the receptor than **109**. However, it was decided to continue with the original bromo-substituted moiety and the R<sup>2</sup>-substituted phenyl group was modified. Small *para*-substituents like fluorine were tolerated, as were various substituents on the *meta*-position, such as amine and carboxylic acid groups. The *ortho*-position was found to be a good additional anchor point, as suggested by the relatively high affinities of **111** ( $IC_{50} = 0.12 \mu M$ ) and **112** ( $IC_{50} = 0.17 \mu M$ ). When the glutarimide group was explored, retaining a carbonyl group (X=O) proved essential for affinity. The imide hydrogen (R<sup>3</sup>) was replaced by alkyl groups without improvement in affinity. Interestingly, testing of enantiopure acetyl (**113**,  $IC_{50} = 0.11 \mu M$ ), α-acetamide (**114**,  $IC_{50} = 0.06 \mu M$ ), or phenylurea derivatives (**115**,  $IC_{50} = 0.03 \mu M$ ) led to significantly enhanced activity even with the two glutarimide carbonyls (X) removed. In contrast to **113** and **115**, for **114** the (+) enantiomer proved most active. Compounds **113**, **114**, and **115** showed no antimuscarinic activity, and it was mentioned that those compounds had comparable affinity for mouse CXCR3.

### 2.7.2 N-Benzyl Benzenesulfonamides

Crosignani et al. (Merck Serono) reported on the screening of 90,000 compounds employing a high-throughput screening method [123]. As a result, compound **116**

**Table 19** Optimization of *N*-benzyl benzenesulfonamides by Crosignani et al. [123]

Compound		R <sup>1</sup>	R <sup>2</sup>	R <sup>3</sup>	R <sup>4</sup>	IC <sub>50</sub> (nM) Chemotaxis <sup>a</sup>
#	In ref.					
<b>116</b>	1	Cl			H	538
<b>117</b>	2	Cl			H	2,275
<b>118</b>	27	CN			H	13
<b>119</b>	13	Cl			H	192
<b>120</b>	14	Cl			H	238
<b>121</b>	28	Cl			H	2,940
<b>122</b>	47	CN			F	192

<sup>a</sup>Chemotaxis assay with CXCR3-overexpressing L1.2 cells and CXCL10 as chemoattractant

was discovered (Table 19). While the compound was selective against other tested GPCRs, it had low solubility, low permeability in the Caco-2 assay, high clearance in human and rat liver microsomes, and was unstable in acidic media. Some of those properties may be contributed to the acylhydrazone moiety present in **116**. Encouragingly, additional efforts delivered structure **117** indicating that the acylhydrazone moiety could be replaced. Assay values reported in this paper are mostly those of chemotaxis assays, strictly taken not binding values, but the authors show that the correlation with binding data is good. A first optimization was performed for R<sup>1</sup>, R<sup>2</sup>, and R<sup>3</sup>. SAR on R<sup>1</sup> was tight and it was mentioned that *ortho*- and *meta*-substitution

were not tolerated. A *para*-chlorine functioned well, but methoxy and cyano moieties were allowed too. The R<sup>2</sup>-position tolerated many (hetero)aromatic groups. Especially compounds containing a 2-pyridyl ring had good potencies (i.e., **118**, IC<sub>50</sub> = 13 nM). The authors state that an unsubstituted methylene linker should be present between the (hetero)aromatic ring and the core structure and that aliphatic or cycloaliphatic groups were not tolerated as R<sup>2</sup>. For the R<sup>3</sup> moiety, lipophilic groups could be used as exemplified by **118** and **119** (IC<sub>50</sub> = 192 nM). The thiophene analogue **119** had slightly better affinity than a 1-phenylcycloprop-1-yl analogue (**120**, IC<sub>50</sub> = 238 nM). The instability in liver microsomes of compounds in the series had to be addressed. Carboxylic acid analogue **121** (IC<sub>50</sub> = 2,940 nM) was found to be stable in human and rat liver microsomes, although the potency was reduced. This led the authors to believe log D was possibly involved in the metabolic stability. In order to boost potency, several carboxylic acid bioisosteres, such as tetrazole and oxadiazolone, were tested. Exploration of the SAR around these structures followed similar trends compared to the amide subseries. Yet the tetrazoles generally had higher microsomal stability than the amides. The compound with the best PK profile was **122** (chemotaxis IC<sub>50</sub> = 192 nM).

### 2.7.3 Camphor Sulfonamide Derivatives

A high-throughput screening described by Wang et al. (GlaxoSmithKline) led to the identification of **123** (pIC<sub>50</sub> = 6.6) [121]. The ligand bears a characteristic polycycloaliphatic moiety (camphor), a recurring motif in CXCR3 compounds [105, 113]. The left-hand aryl moiety (R<sup>1</sup>) was first explored (Table 20) [121]. Moving the trifluoromethyl substituent on the pyridine ring to other positions was not allowed. Replacement of the trifluoromethyl substituent by, for example, bromo, methyl, or cyano also led to a loss of affinity. Adding a second substituent could be beneficial, as evidenced by **124** (pIC<sub>50</sub> = 6.8). Several compounds with aromatic (phenyl) or heteroaromatic (i.e., pyridazinyl) rings as R<sup>1</sup> showed significantly reduced affinity, except for installing a pyrimidine, which gave only slightly reduced affinity (**125**, pIC<sub>50</sub> = 6.5). The piperazine core of the scaffold was subjected to an extensive SAR. Most manipulations (substituted piperazines, homopiperazine, other (a)cyclic diamines) gave reduced affinity. Noteworthy, though, (S)-methylation on the 3-position of the piperazine core (R<sup>3</sup>) resulted in a compound with a better affinity. Finally, the camphor portion of the molecule was probed (R<sup>2</sup>). The (S)-isomer **123** exhibited a better affinity than its (R)-isomer counterpart. Modification of the ketone of **123** was reasonably (but not fully) allowed. For example, while the alcohol **126** (pIC<sub>50</sub> = 6.8) showed better affinity than its ketone counterpart **123**, the amine **127** (pIC<sub>50</sub> = 6.1) displayed decreased affinity. Some of the best affinity-improving moieties in each region were combined to give, for example, **128** (pIC<sub>50</sub> = 7.1) and **129** (pIC<sub>50</sub> = 7.5).

**Table 20** Optimization of camphor sulfonamide derivatives by Wang et al. [121]

Compound					<i>pIC<sub>50</sub></i> CXCL10 <sup>a</sup>
#	In ref.	R <sup>1</sup>	R <sup>2</sup>	R <sup>3</sup>	
<b>123</b>	1a			H	6.6
<b>124</b>	5k			H	6.8
<b>125</b>	5q			H	6.5
<b>126</b>	8a			H	6.8
<b>127</b>	13a			H	6.1
<b>128</b>	18a			(S)-Me	7.1
<b>129</b>	18h			(S)-Me	7.5

<sup>a</sup>CXCL10 induced calcium mobilization assay performed on a CHO-K1 cell line expressing CXCR3 and Gα16

### 2.7.4 4-N-Aryl-[1,4]diazepane Ureas

Pharmacopeia researchers screened 90 libraries containing over 4 million compounds using Encoded Combinatorial Libraries on Polymeric Support (ECLiPS™) [124]. From this emerged the 4-N-aryl-[1,4]diazepane-urea chemotype on which SAR was carried out (Table 21). The R<sup>1</sup> group benefited from a 2,4-dichlorophenethyl moiety, as is evident from comparing, e.g., **130** ( $IC_{50} = 0.51 \mu M$ ) and **131** ( $IC_{50} = 0.06 \mu M$ ). On the R<sup>2</sup> side, several substituted phenyl groups as well as a few heteroaromatics were tolerated, with 3-Cl-Ph (as in

**Table 21** Optimization of 4-N-aryl-[1,4]diazepane-urea derivatives by Cole et al. [124]

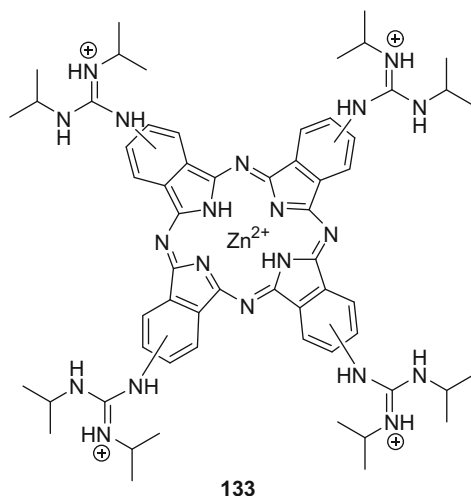
Compound		R <sup>1</sup>	R <sup>2</sup>	IC <sub>50</sub> (μM)
#	In ref.			CXCL11 <sup>a</sup>
<b>130</b>	6v			0.51
<b>131</b>	6c			0.06
<b>132</b>	6b			0.70

<sup>a</sup>Reduction in CXCL11-stimulated calcium release for a cell line (HEK293) overexpressing recombinant human CXCR3 and chimeric G protein Gqι5

**131**) and 3-F-Ph being optimal. Shifting the Cl atom by one position led to a drop in affinity (**132**, IC<sub>50</sub> = 0.70 μM). The ethylurea unit was probed with a selected set of groups, but this did not lead to significantly improved affinities. A decrease in diazepane ring size or its ring opening was not allowed. Compound **131** was used by the same research group in their investigation into small-molecule CXCR3 agonists [125]. A QSAR model has been constructed on this scaffold that consists of molecular descriptors that encode information about the structure, branching, electronic effects, chains, and rings and account for cooperative effects between functional groups [126].

### 2.7.5 Tetrakis-(Diisopropyl-Guanidino) Zinc Phthalocyanine

A metal complex (Zn-DIGP, **133**) has been claimed as a CXCR3 binder, albeit with low affinity ( $K_i = 29 \mu\text{M}$ , [<sup>125</sup>I]-CXCL10) [127]. The IC<sub>50</sub> of **133** for inhibition of CXCL10-CXCR3 activation amounted to 3.8 μM. The authors invoke this ability to interfere with CXCL10-CXCR3 signaling as a potential explanation for the antimetastatic activity of **133**.



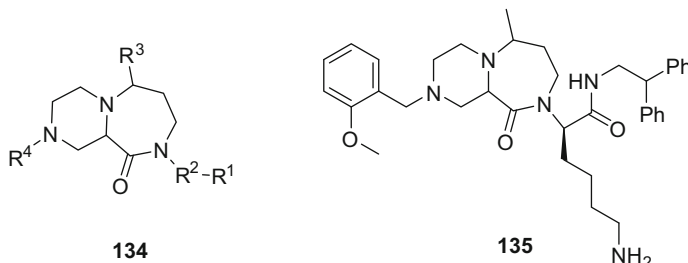
### 3 Agonists

As mentioned in the introduction of this chapter, the field of small-molecule CXCR3 agonists has been much less explored. Arguably, this is because relatively few therapeutic indications have been disclosed for CXCR3 agonists. Moreover, general trends seem to suggest that it is intrinsically complex to find small-molecule agonists for the chemokine receptor family [128]. In total, three distinct agonist small-molecule chemotypes for wild-type CXCR3 have been published (two of which in the same paper in 2006, the other in 2012), and these represent important tool compounds to interrogate the signaling events by CXCR3. Indeed, it will be shown how these agonists have attracted interest from researchers to facilitate fundamental CXCR3 research.

#### 3.1 *Agonists Emerging from the Pharmacopeia Screen*

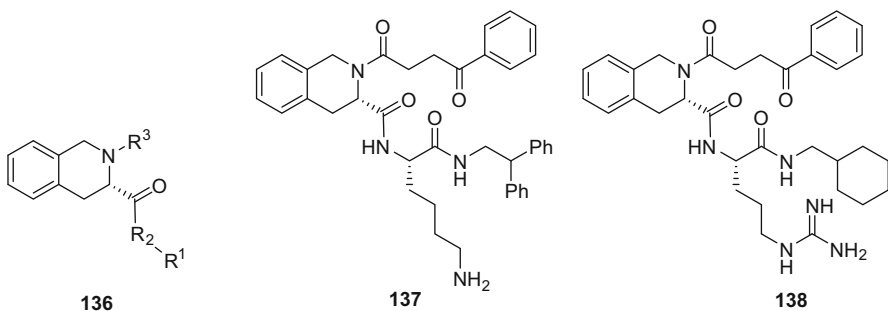
During what appears to be the same screen of 90 libraries [124] used for identification of the 4-N-aryl-[1,4]diazepane ureas, such as **131** (vide supra), Pharmacopeia researchers also picked up a few agonist chemotypes [125]. The paper only provides qualitative SAR and SFR statements, which will be recapped here. In general, it was noted that irrespective of the scaffold, an agonist chemotype preferably has a single basic amino acid (thus bearing some peptidomimetic character) and a hydrophobic peripheral group [125]. While three agonists are described in more

detail in the paper, they are best classified into two chemotypes: a fused piperidinyl diazepanone and two tetrahydroisoquinolines.



### 3.1.1 Fused Piperidinyl Diazepanone

One agonist chemotype is that of a fused piperidinyl diazepanone (general structure **134**). While this probed library contained ca. 80,000 members, CXCR3 agonists emerged only from a sublibrary containing an *ortho*-methoxybenzyl moiety as R<sup>4</sup>. Within this sublibrary of 1,575 compounds (which contained lysines as well as acidic and uncharged amino acids, presumably all on R<sup>2</sup>), only two compounds were identified as agonists, both bearing a (D)-Lys substituent. Thus, the structure-function relationship (SFR) around this fused piperidinyl diazepanone scaffold, as far as can be deduced, seems strict. The structure of one of the identified agonists was given: **135** ( $IC_{50} = 65$  nM, [<sup>125</sup>I]-CXCL10). In a calcium flux assay, **135** presented itself as an agonist with similar efficacy as CXCL11, albeit with lower potency ( $EC_{50} = 800$  nM,  $\alpha = 1$ ). Similarly, **135** provoked chemotaxis of human T cells with a maximum response around 1000 nM. Interestingly, the maximum effect in chemotaxis induced by **135** is  $\pm 50\%$  of that elicited by CXCL11 ( $\alpha = 0.5$ ). Pease et al. confirmed the agonistic properties of **135** in a murine L1.2 pre-B cell migration assay. Again, **135** showed lower efficacy and potency compared to CXCL11 [129]. In addition, *mutational* studies combined with ab initio modeling on **135** binding to CXCR3 suggested that residue D112<sup>2,63</sup> acts as the counterion for the positive charge of the arginine moiety in **135** [129]. This suggests that **135** binds to TMS1 of the TM region of CXCR3.



### 3.1.2 Tetrahydroisoquinolines

The second agonist chemotype emerging from the Pharmacopeia screen [125] is that of a tetrahydroisoquinoline (general structure **136**). This library, with ca. 30,000 members, only provided agonists when  $R^3$  was a 3-benzoyl-propionyl side chain. Even so, with that particular  $R^3$ , only 7 out of the 2520 embedded compounds gave CXCR3 agonism. All of these 7 compounds possessed a basic amino acid as  $R^2$  (arginine in 6 out of 7 cases, lysine 1 out of 7). Interestingly, both (L) and (D) amino acids were present in the original library, but the 7 hits all contained the (L) stereomers of the basic amino acid. In terms of  $R^1$ , it was qualitatively described how a SAR was visible and suggested a preference for a hydrophobic moiety as  $R^1$ . In all, also for this chemotype, the SFR seems strict. Of the found 7 agonists, the structures of two were disclosed: **137** ( $EC_{50} = 3.3 \mu M$ , calcium flux assay) and **138** ( $IC_{50} = 42 nM$ , [ $^{125}I$ ]-CXCL10;  $EC_{50} = 1.1 \mu M$ , calcium flux assay). They are very much alike but differ from each other in the exact nature of the hydrophobic and basic groups.

No synthesis for **137** and **138** was described in the paper. Therefore, our group developed a synthesis strategy for **137** [14]. During these efforts, we also made a handful of derivatives of **137** (Wijtmans et al., unpublished data) which are in line with the qualitative statements from the Pharmacopeia paper [125]. That is, when the  $R^3$  group of **137** was changed for an acetyl moiety and/or the  $R^2$  for a glycine, the affinity dropped by at least by 1.5 log unit (activity not tested).

The synthesis of **137** enabled detailed pharmacological and mutation studies [14]. Stroke and colleagues showed that both **137** and **138** acted as agonists in a calcium flux and chemotaxis assay. In later publications from our group and Pease et al., these molecules were described in more detail [14, 25, 129].

Our group reported a detailed pharmacological characterization of **137** (called VUF10661), which acts as agonist in different assays, including [ $^{35}S$ ]-GTP $\gamma$ S ( $EC_{50} = 0.6 \mu M$ ), cAMP ( $EC_{50} = 0.5 \mu M$ ),  $\beta$ -arrestin recruitment ( $EC_{50} = 1.0 \mu M$ ), and receptor internalization ( $EC_{50} \sim 3 \mu M$ ) [14]. **137** also produced PTX-sensitive impedance responses ( $EC_{50} = 0.8 \mu M$ ) in a label-free impedance assay, comparable to CXCR3 chemokines [25]. Interestingly, **137** showed differential behavior in

some assays compared to CXCL11, suggesting functional selectivity. For example, CXCR3 stimulation with **137** resulted in a maximum migration of L1.2 pre-B cells that was about 50% lower than when CXCL11 was used, while in a  $\beta$ -arrestin recruitment assay the efficacy of **137** was 167% compared to CXCL11 [14]. In G protein-dependent assays like [<sup>35</sup>S]-GTP $\gamma$ S and cAMP the efficacy of CXCL11 and **137** were identical. Moreover, **137** likely binds to specific subset of CXCR3 conformations (with distinct functional properties), as it was unable to completely displace [<sup>125</sup>I]-CXCL11, yet completely displaced [<sup>125</sup>I]-CXCL10 radioligand in a whole-cell binding assay. Moreover, in saturation binding experiments, **137** was able to decrease the  $B_{max}$  but left the affinity of both chemokine radioligands unchanged [14]. Preliminary mutagenesis studies highlight a binding site for **137** in the TM region of CXCR3 (Scholten et al., unpublished data). Altogether these data indicate that **137** operates in a noncompetitive, potential allosteric way at CXCR3.

In the L1.2 cell migration assay compound **138** also exhibited potency and efficacy comparable to **135** [129]. However, **138** was not able to fully displace [<sup>125</sup>I]-CXCL10 from the receptor, suggesting differential binding to CXCR3 (e.g., different receptor populations). Computational modeling revealed the possibility that **138** mimics residues 35–39 of the 30s loop of CXCL10 and might suggest a similar CXCR3 activation mechanism for this small-molecule agonist. In keeping with this, Pease et al. showed that CXCR3 activation by either CXCL10 or **138** was affected by the same mutations, which did not affect CXCL11 action [129]. Similar to **135**, D112<sup>2,63</sup> from TMS1 is suggested to act as the counterion for the positive charge in **138**.

O’Boyle has shown how these tool compounds can shed more light on the physiological role of CXCR3 [130]. Based on the molecular mass given [130], they used **138**, which they refer to as PS372424. They expanded on the signaling repertoire of this class of agonists, as by showing ERK phosphorylation induced by **138** comparable to CXCL11. Furthermore, the compound caused significant and sustained internalization of CXCR3 receptors from the cell surface. Again, the compound was able to direct cell migration of T cells over a bare filter (comparable to previous studies [14, 129]). Interestingly, and in contrast to CXCL11, **138** was not able to induce transendothelial migration, but instead antagonized the migration of T cells towards CXCL11 but also CXCL12 and CCL5. The latter two are ligands for CXCR4 and CCR5 receptors, respectively, also expressed on activated T cells [130]. The authors suggest that the inability of **138** to induce transendothelial migration is due to the lack of glycosaminoglycan (GAG) binding, which is probably needed for a ligand concentration gradient serving as a vectorial cue for the immune cells, also shown with a study on a non-GAG-binding mutant of CXCL12 [131]. However, it cannot be ruled out that these ligands are functionally selective agonists that are less efficacious in activating cell migration compared to chemokines. As **138** does not appear to bind to the murine CXCR3 receptor, human T cells were introduced in NOD.Cg-*Prkdc*<sup>scid</sup> Il2rgtm1<sup>Wjl/SzJ</sup> mice, as a model to mimic human arthritic inflammation [130]. In this model, migration of T cells was observed towards air pouches injected with solutions containing CXCL11 alone or

synovial fluid of rheumatoid arthritis patients (RASF), containing a broad spectrum of chemokines. Interestingly, **138** significantly antagonized migration towards both solutions, whereas selective CXCR3 antagonism by **11** (NBI-74330) or a CXCR3-blocking antibody was not able to block migration towards RASF. In the article, O’Boyle and colleagues show that next to CXCR3 desensitization, cross-desensitization of other chemokine receptors on the human T cells, including CCR5, is likely the mechanism of action for this small-molecule CXCR3 agonist that produces a functional antagonistic response *in vivo* [130]. The work by O’Boyle presents an interesting new avenue for the treatment of CXCR3-linked disease and potentially for immune diseases in general. Instead of pursuing selective chemokine receptor antagonists, selective small-molecule agonists might be developed that functionally antagonize the chemokine-induced responses by receptor (cross-)desensitization and internalization, without producing a migratory response themselves.

### 3.2 Biaryl Ammonium Salt Agonists

Our CXCR3 biaryl ammonium antagonist class [122] (*vide supra*) harbored a very subtle agonism trigger [132]. This represented a clear departure from the pioneer agonists **135**, **137** and **138** which were all peptidomimetic in nature and needed, e.g., the basic amino acid substructure. Our ammonium chemotype, in contrast, does not possess any peptidomimetic character. The trigger revealed itself when the *ortho*-position of the “outer” aryl ring was probed with a Cl-substituent (Table 22) [132]. The resulting compound **139** proved to be a partial agonist ( $pEC_{50} = 5.8$ ,  $\alpha = 0.73$ , [ $^{35}\text{S}$ ]-GTP $\gamma$ S assay). Since the analogous *meta*-compound **108** did not show any agonism, we investigated the SFR of the biaryl substructure using 26 compounds. The focus was on the *ortho*-position of the “outer” ring but also that of the “inner” ring was probed. Interestingly, though, regioisomeric compound **140** did not show agonism. Collectively, variation of R<sup>1</sup> led to the whole spectrum of efficacies, but only a large halogen atom on the *ortho*-position of the “outer” ring provided *full agonists* of CXCR3, as illustrated by **141** (VUF11222,  $pEC_{50} = 6.1$ ,  $\alpha = 0.95$ , [ $^{35}\text{S}$ ]-GTP $\gamma$ S assay) and **142** (VUF11418,  $pEC_{50} = 6.0$ ,  $\alpha = 0.99$ , [ $^{35}\text{S}$ ]-GTP $\gamma$ S assay). Once again, shifting this large halogen atom to the *meta*-position abolished all agonism while reasonably maintaining affinity (**143**). Stereochemical and regiochemical exploration of the myrtenyl moiety did not qualitatively change these results. All this clearly underscores the *ortho*-position of the “outer” ring as the activity switch. We have since confirmed this switch with a thiophene as “outer” ring as well (Wijtmans et al., unpublished results). Some efforts were directed towards elucidating the switch using a combination of QSAR, QM, and NOESY NMR techniques [132]. This analysis suggests key roles for a dihedral angle within the biaryl system of ca. 60° and for appropriate electrostatic potential of the biaryl rings.

Compounds **141** and **142** were investigated in more detail, mostly with the *meta*-chloro antagonist (**108**) as in-class reference. Both **141** and **142** showed agonist

**Table 22** Exploration of polycycloaliphatic ammonium salt agonists by Wijtmans et al. [132]

Compound		R <sup>1</sup>	R <sup>2</sup>	pK <sub>i</sub> CXCL10 <sup>a</sup>	pEC <sub>50</sub> <sup>b</sup>	α <sup>c</sup>
#	In ref.					
<b>139</b>	6		H	7.0	5.8	0.73
<b>108</b>	27		H	6.6	— <sup>d</sup>	0.05
<b>140</b>	31		Cl	6.2	— <sup>d</sup>	0.06
<b>141</b>	38		H	7.2	6.1	0.95
<b>142</b>	39		H	7.2	6.0	0.99
<b>143</b>	40		H	6.7	— <sup>d</sup>	0.08

<sup>a</sup>[<sup>125</sup>I]-labeled CXCL10 displacement assay performed in HEK293 cells expressing human CXCR3

<sup>b</sup>[<sup>35</sup>S]-GTPγS functional assay with membranes prepared from HEK293 cells stably expressing the CXCR3 receptor

<sup>c</sup>α represents the relative efficacy of a ligand compared to the endogenous agonist CXCL11 (which is set at α = 1.0)

<sup>d</sup>Could not be determined due to the too low functional assay window

responses in a second functional assay: a cAMP-dependent CRE-luciferase reporter gene assay, whereas **108** did not [132]. Selective CXCR3 antagonist **11** (NBI-74330) inhibited these agonist responses. Moreover, no effects were observed in a [<sup>35</sup>S]-GTPγS assay for these compounds on cells lacking CXCR3 expression. Altogether these data indicate that the induced responses are specifically mediated by the activation of CXCR3 receptors present on these cells. Preliminary mutagenesis studies indicate a potential binding mode for these compounds within the TM region of CXCR3 (Scholten et al., unpublished data).

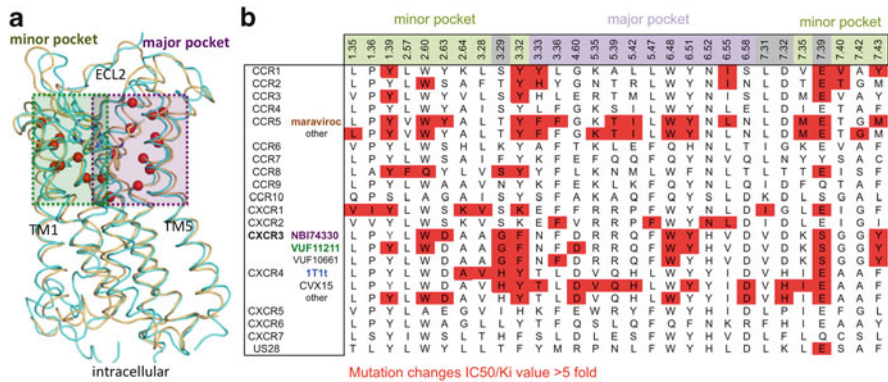


**Fig. 2** (a) Alignment of GPCR crystal structures, including structures of the CXCR4 (cyan) and CCR5 (orange) chemokine receptors [83, 84], highlighting the positions of amino acid residues (C $\alpha$  atoms depicted by red spheres) that play a role in ligand binding of chemokine receptors based on mutation studies [20, 80], as presented in more detail in panel. (b) Alignment of residues in the transmembrane binding pockets of chemokine receptors (enumerated according to the Ballesteros-Weinstein residue numbering scheme [133]). Residues lining the minor pocket (TMS1), major pocket (TMS2), and interface are marked green, purple, and gray, respectively. Residues are marked red per receptor when mutation of that particular residue is reported to affect affinity or antagonism of any ligand. CCR5 residues that interact with maraviroc and CXCR4 residues that interact with 1T1t and CVX15 in crystal structures are marked red on additional lines, while CXCR3 mutation effects are presented for **11** (NBI74330), **71** (VUF11211), and **137** (VUF10661) individually

## 4 CXCR3-Ligand Binding: From GPCR X-Rays to Presumed CXCR3 Binding Modes

### 4.1 GPCR Crystal Structures and Chemokine Receptor-Ligand Interaction Modeling

After the first GPCR crystal structure of bovine rhodopsin in 2000, the first crystal structures of druggable GPCRs have been solved only in the past 7 years [81, 82]. The three-dimensional structures of 25 different GPCRs have been determined, including the CXCR4 and CCR5 chemokine receptors [83, 84] (Figs. 2a and 3a, b), members of other class A GPCR subfamilies (opioid, aminergic, peptide, adenosine, and lipid receptors) [81, 82], and recently also the first crystal structures of class B [134], C [135], and F [136] GPCRs. These GPCR crystal structures give new opportunities to push the limits of structure-based rational ligand discovery and design and offer higher resolution templates for modeling the structures of GPCRs for which crystal structures have not yet been solved [137]. It should however be noted that modeling of GPCRs with low homology to the currently available GPCR crystal structures still remains a difficult task in which experimental data are of utmost importance to restrict the number of possible models. Several of the challenges of GPCR structural modeling have been demonstrated in

recent community-wide competitions to predict GPCR crystal structures (GPCR DOCK [138, 139], including modeling challenge to predict ligand-bound crystal structures of the CXCR4 chemokine receptor [139]), and GPCR structure modeling methods and applications have been described in recent reviews [79, 137].

CXCR4 crystal structures have been elucidated with a large cyclic peptide CVX15 and with the small-molecule antagonist IT1t [83] (Fig. 3a), while recently a crystal structure complex of CCR5 and the small-molecule HIV entry inhibitor maraviroc was solved (Fig. 3b) [84]. The CXCR4 crystal structures have been solved as parallel dimers that interact at the extracellular side of helices V and VI [83], in a similar way as observed in  $\mu$ -opioid receptor crystallized dimers [140]. Comparison of other dimer/tetramer GPCR crystal structures however suggests the existence of different dimer interfaces for different GPCR homodimers, and complementary biochemical and biophysical studies indicate that GPCR oligomerization interfaces may depend on receptor conformations that can be stabilized by specific ligands [19]. While the overall seven transmembrane helical fold is conserved between GPCRs, the CCR5 and CXCR4 chemokine receptor crystal structures show differences compared to other GPCRs, including a more outward orientated second extracellular loop (ECL2) and a different conformation of the top of transmembrane (TM) helix 2. Chemokine receptors (as well as opioid receptors) contain a S/T<sup>2.56</sup>XP<sup>2.58</sup> sequence motif that stabilizes a different helical kink in TM2 compared to other GPCR crystal structures and orients residues 2.60 and 2.63 (W94<sup>2.60</sup> and D97<sup>2.63</sup> in CXCR4 and W86<sup>2.60</sup> and Y89<sup>2.63</sup> in CCR5) towards the minor ligand binding site TMS1 [20]. These structural differences create a wider, more open ligand binding site between TM1, 2, 3, and 7 (TMS1 or “minor pocket”) [20] in chemokine receptors compared to most other class A GPCRs. While the ligands in most other class A GPCR co-crystal structures primarily occupy a “major pocket” surrounded by TM3, 4, 5, 6, and 7 (TMS2) [20], the CXCR4 and CCR5 crystal structures show that small chemokine receptor modulators can target TMS1 exclusively (CXCR4-IT1t, Fig. 3a) [83] or TMS1 and TMS2 simultaneously (CCR5-maraviroc, Fig. 3b) [84].

The GPCR DOCK 2010 competition demonstrated that the computational prediction of chemokine receptor-ligand interactions [139] is particularly challenging because of the existence of multiple potential binding sites and ligand binding modes in chemokine receptors [79, 141]. Furthermore the symmetry in both chemokine ligands and chemokine receptor binding sites [20, 79] makes it difficult to prioritize plausible ligand binding mode hypotheses, even when experimental ligand structure-activity relationship (SAR) and receptor mutagenesis data are available. The CXCR4 and CCR5 crystal structures (Fig. 3a, b) and site-directed mutagenesis studies (Fig. 2b) indicate that acidic residues (e.g., D/E<sup>2.63</sup>, D/E<sup>4.60</sup>, D/E<sup>6.58</sup>, E<sup>7.39</sup>) and aromatic residues (e.g., Y<sup>1.39</sup>, W<sup>2.60</sup>, Y/F<sup>3.32</sup>, W<sup>6.48</sup>, Y/F<sup>6.51</sup>, Y<sup>7.43</sup>) present in the TMS1 and/or TMS2 of many chemokine receptors play important role in binding the basic and aromatic/hydrophobic moieties of small-molecule ligands [20, 79]. Mutation of these acidic and/or aromatic residues has an effect on chemokine binding to and/or potency for some but not all receptors. This suggests that small ligands and chemokines bind overlapping yet differential

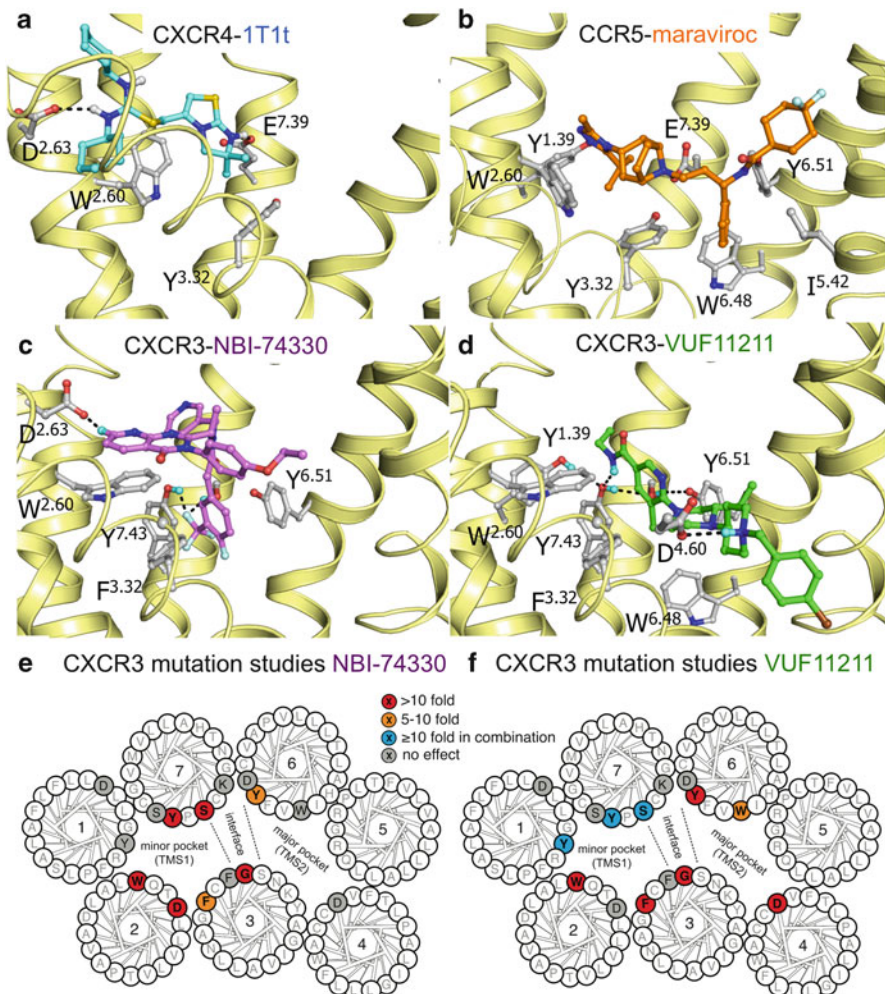


**Fig. 3** Comparison of binding modes of **145** (1 T1, cyan, a) in the CXCR4 crystal structure, maraviroc **144** (orange, b) in the CCR5 crystal structure, and **11** (NBI-74330, magenta, c) and **137** (VUF11211, green, d) bound CXCR3 homology models. TM helices around the TMS1 and TMS2 binding sites (see Fig. 2) are shown in yellow. Side chains of proposed interacting residues are shown in gray. Hydrogen bonds/polar interactions are shown as dashed blue lines. Helical wheel diagrams are shown for a top view of the TM domains of CXCR3 with effects of mutations highlighted for (e) **11** (NBI-74330) and (f) **137** (VUF11211). Residues that show a 10-fold or more decrease in affinity upon mutation are indicated in red, and mutations that result in a decrease in affinity between 5- and 10-fold are indicated in orange. Residues that give a significant decrease (10-fold or more) in affinity when mutated together are shown in blue. Other residues that were mutated but did not give a significant change in affinity are colored gray

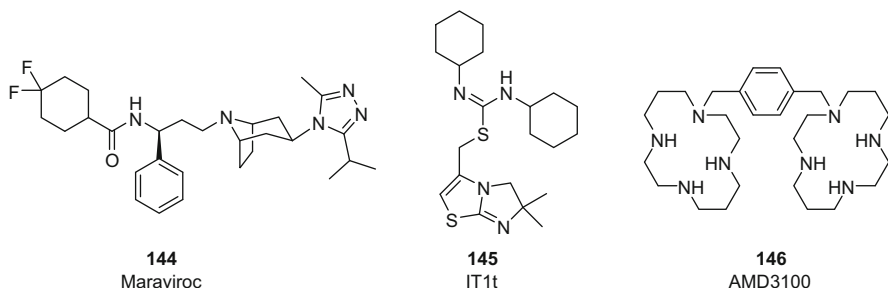
binding sites [20]. For example, while mutation of D97<sup>2.63</sup> and E288<sup>7.39</sup> affects CXCL12 binding to CXCR4 [142, 143], mutation of Y60<sup>1.39</sup>, W109<sup>2.60</sup>, D112<sup>2.63</sup>, F131<sup>3.32</sup>, D186<sup>4.60</sup>, W268<sup>6.48</sup>, Y271<sup>6.51</sup>, D278<sup>6.58</sup>, or Y308<sup>7.43</sup> does not affect CXCL11 binding to CXCR3 [80].

The following paragraphs show how the combination of CXCR3 mutagenesis studies, CXCR3 ligand SAR, and computational modeling studies can be used to map CXCR3-ligand binding sites and predict the three-dimensional structure of CXCR3-ligand complexes (Sect. 4.2), and give a perspective on the use of such structural models for CXCR3 (structure-based) virtual screening (Sect. 4.3).

## 4.2 *In Silico-Guided CXCR3 Mutation Studies to Elucidate CXCR3-Ligand Binding Modes*

### 4.2.1 Chemokine and Small Ligand Binding Regions in CXCR3

Chimera and point mutation studies have shown that multiple extracellular domains of CXCR3 are required for chemokine binding and/or receptor activation, including the N-terminus, and regions in the second and three extracellular loops (ECL1–3) [24, 144]. M1–V16 and sulfated Y27 and Y29 in the N-terminus and D282 in ECL3 are required for both CXCL10 and CXCL11 binding, while charged residues in the top of TM2 (D112<sup>2.63</sup>), ECL2 (D195, E196), the top of TM6 (D278<sup>6.58</sup>), ECL3 (E293), and the top of TM7 (D297<sup>7.32</sup>) are required only for CXCL10 binding, but not CXCL11 binding [24, 129, 144]. Recent mutagenesis studies guided by CXCR4 crystal structure-based CXCR3 homology models have shown that residues that play a role in binding of small ligands **11** (NBI-74330), **71** (VUF11211), and **137** (VUF10661) are primarily located in the TM binding site (Fig. 3c, d). Almost all mutations in TMS1 and TMS2 that affect binding of small ligands do not significantly affect CXCL11 affinity [80], suggesting that the TM domains do not play an important role in CXCL11 binding. It should be noted however that chemokines are considerably larger and that most of their binding affinity is determined by interactions with the N-terminus and ECLs of the receptor [20]. The N-terminus of the chemokine is thought to interact with the receptor TM bundle for receptor activation [20], and its binding site may overlap with the binding pockets of small molecules in TMS1 and TMS2. Moreover, alignment of the peptidomimetic CXCR3 agonists **135** and **138** with the CXCL10 chemokine and mutation studies suggest that these small molecules mimic the 30s loop of CXCL10 and target both ECL2 and TMS1 [129, 145]. In general, radiolabeled chemokines are used to investigate the effect of mutations on allosteric ligand affinity. However, the effect on allosteric ligand binding is most likely a combination of both ligand affinity and allosteric cooperativity towards the chemokine radioligand. This cooperativity might also change depending on the specific mutation, potentially resulting in under- or overestimated influences of the mutation on the binding affinity of small-molecule ligands.



#### 4.2.2 CXCR3 Ligand-Specific Anionic Interaction Sites

Maraviroc (**144**)-bound CCR5 and 1T1t (**145**)-bound CXCR4 crystal structures [83, 84] as well as CCR1, CCR2, CCR3, CCR5, CCR8, CXCR1, CXCR4, and US28 mutation studies [20] (Fig. 2b) show that E<sup>7,39</sup> acts as an important acidic ionic anchor for the basic moieties of small ligands in most chemokine receptors. Unlike other chemokine receptors, CXCR3 does not contain an acidic (glutamate) residue at position 7,39 in TM7, but a small polar S304<sup>7,39</sup> serine residue (Fig. 2b). Mutation of S304<sup>7,39</sup> into a glutamate residue (in combination with the K300<sup>7,35</sup>A mutation) results in a significant increase in affinity of the CXCR4 ligand AMD-3100 (**146**) for CXCR3, demonstrating its role in CXCR3/CXCR4 ligand selectivity [146]. In addition to several acidic residues in N-terminal region and extracellular loops ECL1, ECL2, and ECL3, there are four acidic residues in the TM helical binding site of CXCR3: D112<sup>2,63</sup> in TM2, D186<sup>4,60</sup> in TM4, D278<sup>6,58</sup> in TM6, and D297<sup>7,32</sup> in TM7. D112<sup>2,63</sup> is specific for CXCR3, CXCR4 (D97<sup>2,63</sup>), and CXCR5 (E308<sup>2,63</sup>) and forms an ionic interaction with 1T1t in one of the CXCR4 crystal structures (Fig. 3a). D186<sup>4,60</sup> and D278<sup>6,58</sup> are present in several chemokine receptors and form ionic interactions with basic moieties of the CVX15 peptide ligand in the other CXCR4 crystal structure [83].

The important role of basic nitrogen atoms in piperazinyl-piperidines (Sect. 2.3) in CXCR3 binding has been demonstrated in SAR studies [111] (e.g., **61** vs. **65**, Tables 10 and 11), and recent CXCR3 mutation studies guided by a CXCR4 crystal structure-based CXCR3 homology model [80] have identified D186<sup>4,60</sup> as an ionic interaction site of the piperidine moiety of **71** (VUF11211) (Fig. 3d, f). Piperidinyl diazepanone (Sect. 3.1.1) and tetrahydroisoquinoline (Sect. 3.1.2) peptidomimetic agonist ligands contain a basic amino acid that is required for CXCR3 binding [125], and mutation studies have indicated that E196 in ECL2 plays a role in CXCR3 binding of **135** [129] and **137** (VUF10661) [147]. Azaquinazolinone **11** (NBI-74330) does not possess a highly basic moiety, but SAR studies show (Sect. 2.1) that the 8-azaquinazolinone nitrogen atoms and associated positive partial charge on the 7-position are important for CXCR3 binding affinity (e.g., see **11** vs. **17** and **18**, Table 3) [87, 98]. CXCR3 homology model-guided mutation studies indicate that the negatively charged carboxylate group of

D112<sup>2,63</sup> plays an important role in **11** (NBI-74330) and suggest that an electro-positive aromatic –CH group of the ligand forms a weak hydrogen bond to this residue (Fig. 3c, e) [80]. Similar H-bonds between N-heteroaromatic –CH groups and oxygen atoms play, for example, an important role in intermolecular bonding of N-heteroaromatic ring systems [148] and kinase-ligand interactions (i.e., CH–O hydrogen bonds with hinge backbone carbonyl oxygen atoms) [149, 150]. D46N, D52<sup>1,31</sup> N, D195N, D278<sup>6,58</sup> N, E293<sup>7,28</sup>Q, and D297<sup>7,32</sup> N mutations do *not* significantly affect binding of any of the abovementioned small ligands [80]. The ligand-specific roles of different acidic residues in CXCR3 demonstrate the ligand binding mode diversity in chemokine receptors and make it challenging to predict the (main) anionic interaction sites of the basic moieties of other CXCR3 ligands, e.g., aryl-3-piperidin-4-yl-ureas (Sect. 2.2), ergolines (Sect. 2.4), iminobenzimidazoles (Sect. 2.5), polycycloaliphatic aminopiperidines (Sect. 2.6), benzetimides (Sect. 2.7.1), and polycycloaliphatic ammonium salts (Sects. 2.6 and 3.2).

#### 4.2.3 Overlapping, but Differential (Aromatic) Binding Pockets for Different CXCR3 Ligand Chemotypes

Several conserved aromatic residues line the minor (Y<sup>1,39</sup>, W<sup>2,60</sup>, Y/F<sup>3,32</sup>, Y<sup>7,43</sup>) and major (W<sup>6,48</sup>, Y/F<sup>6,51</sup>) subpockets of CXCR3 and other chemokine receptors (Figs. 2 and 3). Mutation studies indicate that the roles of these residues in CXCR3 binding are ligand dependent. W109<sup>2,60</sup>, F131<sup>3,32</sup>, and Y308<sup>7,43</sup> are important residues for binding all three CXCR3 ligands **11** (NBI-74330), **71** (VUF11211), and **137** (VUF10661). Mutation of Y271<sup>6,51</sup> on the other hand only affects CXCR3 binding affinity for **11** and **71** (but does not affect **137** affinity), while mutation of W268<sup>6,48</sup> only affects binding affinity for **71** (but does not affect **11** or **137** affinity), and point mutation of Y60<sup>1,39</sup> and F135<sup>3,36</sup> only affect binding affinity for **137** (but do not affect **11** or **71** affinity) [80, 147]. These and other (see Sect. 4.2.1) ligand-dependent mutational effects (Fig. 3e, f) and ligand SAR data (vide infra) suggest that these small CXCR3 ligands have overlapping but differential binding modes (Fig. 3c, d). While **11** (NBI-74330) primarily occupies the minor binding pocket and minor and major pocket interface between TM2, TM3, TM6, and TM7 (Fig. 3c, e), combined mutation and modeling studies suggest that **71** (VUF11211) occupies both minor and major pockets between TM1–7 (Fig. 3d, f). For both ligands, the G128<sup>3,29</sup> mutant diminishes CXCR3 binding affinity, suggesting that the binding site volume at the interface between major and minor pockets is restricted. This binding mode is in line with SAR studies that show that rigidification of the benzyl moiety of **71** either by ring closure or intramolecular hydrogen bonding could maintain ligand affinity, indicating the importance of directionality for the chlorobenzyl moiety [111, 114]. The tight fit of the rigid **71** ligand in the CXCR3 pocket (Fig. 3d) furthermore explains the steep SAR and preference for small apolar substituents over larger or polar substituents of the piperazine ring (e.g., **68** vs. **69–70**, Table 11) [111, 112] that are proposed to bind in a small subpocket between TM5 and TM6. SAR studies have also identified hydrophobic groups in

other ligand chemotypes that are important for CXCR3 binding, including the benzene substituent of imidazole **30** (vs. **29**, Table 5), the adamantyl group of polycyclic aliphatic aminopiperidine **98** (vs. **99**, Table 16), the cyclopropyl substituent of imidazopyrazine **37** (vs. **36**, Table 6), and the ethyl substituent of benzimidazole **92** (vs. **91**, Table 14), that may target similar hydrophobic subpockets in CXCR3 as **11** and/or **71**.

The recent CCR5 crystal structure shows that the hydroxyl groups of conserved tyrosine residues Y<sup>1,39</sup> and Y<sup>6,51</sup> can also form H-bond interactions with polar functional groups in the ligand (Fig. 3b). CXCR3 modeling studies in combination with CXCR3 mutation and ligand SAR studies suggest that these tyrosine aromatic residues may form a H-bond network with S304<sup>7,39</sup> and Y308<sup>7,43</sup> and can act as (alternative) H-bond interaction partners of polar functional groups in CXCR3 ligands **11** and **71** (Fig. 3c–f). SAR studies indicate that the (geometry of the) amide moiety of **71** (e.g., **58** vs. **59**, Table 10) and electron-withdrawing character of the trifluoromethyl group of **11** (e.g., **6** vs. **7**, Table 1) are important determinants for CXCR3 binding, and the CXCR3 models suggest that these functional groups may interact with this H-bond network in the CXCR3 binding site. Electron-withdrawing groups are also important determinants of CXCR3 binding by piperidine ureas (e.g., **54** vs. **53**, Table 9).

### 4.3 Perspectives for (Structure-Based) Virtual Screening for CXCR3 Ligands

As described in Sects. 4.1 and 4.2, refined chemokine receptor models have successfully been used to guide site-directed mutagenesis studies and design new compounds. Despite the challenges in chemokine receptor-ligand modeling [79, 139], customized chemokine homology models based on bRho and ADRB2 crystal structures as well as de novo receptor models have already been successfully used to identify new ligands for several chemokine receptors [79], including CCR3 [151], CCR4 [152], CCR5 [153], and CXCR4 [154]. *Retrospective* virtual screening experiments have been used to validate CXCR3 homology models and virtual screening methods to discriminate known receptor ligands from decoy molecules with similar physicochemical properties [155]; *prospective* virtual screening studies to discover new CXCR3 ligands have *not* yet been reported. The recent crystal structures of CXCR4 [83, 156] and CCR5 [84] have opened up new opportunities for structure-based discovery and design novel chemokine receptor ligands, as exemplified by successful structure-based virtual screening studies against the CXCR4 crystal structure [156, 157] and CXCR4 crystal structure-based homology models of CXCR7 [158]. It should be noted that hit rates (i.e., the percentage of experimentally confirmed ligands among all tested in silico hits) and binding affinity and/or potency of hits identified in structure-based virtual studies for chemokine receptors are somewhat lower than the hit rates reported for other GPCRs, like aminergic receptors

ADA1A [159], ADRB2 [160], DRD3 [161, 162], and H<sub>1</sub>R [163]. This can on one hand be explained by the challenges in computer-aided prediction of chemokine receptor-ligand interactions compared to aminergic GPCRs, for which more crystal structure templates are available and the protein-ligand interaction binding mode is generally more well defined (including a key ionic interaction with the conserved D<sup>3.32</sup> residue [164]). On the other hand the binding sites of aminergic GPCRs are considered more druggable than the binding sites of chemokine receptors. The TM binding pockets of aminergic receptors contain a combination of hydrophilic and hydrophobic regions that are compatible with the features of drug-like small molecule and favor water displacement upon ligand binding, whereas the open binding region of chemokine receptors (Fig. 3), with its limited number of energetically unfavorable (unhappy) water molecules, is more challenging from a drug design perspective [165]. In addition to the minor and major TM binding sites (Fig. 2), alternative binding sites in chemokine receptors may be targeted by small molecules, including dimer interfaces and intracellular G protein binding site region (as, e.g., proposed for CXCR2 [166–168]). The identification of (chemokine) receptor selective regions in such alternative, relatively shallow, binding pockets (compared to the more occluded TM binding sites) for efficient ligand design is also expected to be difficult. Despite these challenges, the availability of more homologous structural templates, successful virtual screening campaigns for several chemokine receptors, and increased understanding of CXCR3-ligand binding (Sect. 4.2), has made structure-based virtual discovery and design of small CXCR3 modulators more and more feasible.

## 5 Conclusion

This review has addressed, from a molecular point of view, all the progress made in discovery and development of small-molecule CXCR3 ligands. The present efforts have made the full spectrum of efficacies (from antagonists to full agonists) within reach for detailed biological probing of the role of CXCR3 and its ligands. Antagonist papers amount to 28 total and describe chemotypes that vary widely. Most of these papers have been published by the pharmaceutical industry aiming to utilize CXCR3 to address therapeutic needs. While no clinical successes can be reported here yet, the studies represent a valuable arsenal of tool compounds that can be used to study the CXCR3 receptor. Small-molecule CXCR3 agonists have been much less described (only three chemotypes, two of which peptidomimetic), while they too are useful tools especially for emerging concepts such as biased agonism. A unified pharmacophore model for CXCR3 ligands seems challenging to construct as recent combined mutagenesis and CXCR3-ligand modeling studies indicate that the binding modes of different ligand chemotypes are different and only partially overlapping. Gratifyingly, the progress in GPCR crystal structural biology (including CCR5 and CXCR4 chemokine receptor crystal structures) and emerging 3D CXCR3-ligand interaction models have improved our understanding of ligand-dependent molecular

determinants of CXCR3 binding. These new structural insights into CXCR3-ligand binding mode (diversity), in combination with (experimentally supported) virtual screening methods, can be used to guide future CXCR3 ligand discovery and design.

## References

1. Loetscher M, Gerber B, Loetscher P, Jones SA, Piali L, Clark-Lewis I, Baggiolini M, Moser B (1996) Chemokine receptor specific for IP10 and mig: structure, function, and expression in activated T-lymphocytes. *J Exp Med* 184(3):963–969. doi:[10.1084/jem.184.3.963](https://doi.org/10.1084/jem.184.3.963)
2. Qin S, Rottman JB, Myers P, Kassam N, Weinblatt M, Loetscher M, Koch AE, Moser B, Mackay CR (1998) The chemokine receptors CXCR3 and CCR5 mark subsets of T cells associated with certain inflammatory reactions. *J Clin Invest* 101(4):746–754. doi:[10.1172/JCI1422](https://doi.org/10.1172/JCI1422)
3. Bonecchi R, Bianchi G, Bordignon PP, D'Ambrosio D, Lang R, Borsatti A, Sozzani S, Allavena P, Gray PA, Mantovani A, Sinigaglia F (1998) Differential expression of chemokine receptors and chemotactic responsiveness of type 1 T helper cells (Th1s) and Th2s. *J Exp Med* 187(1):129–134. doi:[10.1084/jem.187.1.129](https://doi.org/10.1084/jem.187.1.129)
4. Liu L, Callahan MK, Huang D, Ransohoff RM (2005) Chemokine receptor CXCR3: an unexpected enigma. *Curr Top Dev Biol* 68:149–181. doi:[10.1016/S0070-2153\(05\)68006-4](https://doi.org/10.1016/S0070-2153(05)68006-4)
5. Cole KE, Strick CA, Paradis TJ, Ogborne KT, Loetscher M, Gladue RP, Lin W, Boyd JG, Moser B, Wood DE, Sahagan BG, Neote K (1998) Interferon-inducible T cell alpha chemoattractant (I-TAC): a novel non-ELR CXC chemokine with potent activity on activated T cells through selective high affinity binding to CXCR3. *J Exp Med* 187(12):2009–2021. doi:[10.1084/jem.187.12.2009](https://doi.org/10.1084/jem.187.12.2009)
6. Weng Y, Siciliano SJ, Waldburger KE, Sirotina-Meisher A, Staruch MJ, Daugherty BL, Gould SL, Springer MS, DeMartino JA (1998) Binding and functional properties of recombinant and endogenous CXCR3 chemokine receptors. *J Biol Chem* 273(29):18288–18291. doi:[10.1074/jbc.273.29.18288](https://doi.org/10.1074/jbc.273.29.18288)
7. Tensen CP, Flier J, Van Der Raaij-Helmer EM, Sampat-Sardjoepersad S, Van Der Schors RC, Leurs R, Scheper RJ, Boorsma DM, Willemze R (1999) Human IP-9: a keratinocyte-derived high affinity CXC-chemokine ligand for the IP-10/Mig receptor (CXCR3). *J Invest Dermatol* 112(5):716–722. doi:[10.1046/j.1523-1747.1999.00581.x](https://doi.org/10.1046/j.1523-1747.1999.00581.x)
8. Loetscher M, Loetscher P, Brass N, Meese E, Moser B (1998) Lymphocyte-specific chemokine receptor CXCR3: regulation, chemokine binding and gene localization. *Eur J Immunol* 28 (11):3696–3705. doi:[10.1002/\(SICI\)1521-4141\(199811\)28:11<3696::AID-IMMU3696>3.0.CO;2-W](https://doi.org/10.1002/(SICI)1521-4141(199811)28:11<3696::AID-IMMU3696>3.0.CO;2-W)
9. Jenh CH, Cox MA, Hipkin W, Lu T, Pugliese-Sivo C, Gonsiorek W, Chou CC, Narula SK, Zavodny PJ (2001) Human B cell-attracting chemokine 1 (BCA-1; CXCL13) is an agonist for the human CXCR3 receptor. *Cytokine* 15(3):113–121. doi:[10.1006/cyto.2001.0923](https://doi.org/10.1006/cyto.2001.0923)
10. Mueller A, Meiser A, McDonagh EM, Fox JM, Petit SJ, Xanthou G, Williams TJ, Pease JE (2008) CXCL4-induced migration of activated T lymphocytes is mediated by the chemokine receptor CXCR3. *J Leukocyte Biol* 83:875–882. doi: [10.1189/jlb.1006645](https://doi.org/10.1189/jlb.1006645)
11. Lasagni L, Francalanci M, Annunziato F, Lazzeri E, Giannini S, Cosmi L, Sagrinati C, Mazzinghi B, Orlando C, Maggi E, Marra F, Romagnani S, Serio M, Romagnani P (2003) An alternatively spliced variant of CXCR3 mediates the inhibition of endothelial cell growth induced by IP-10, Mig, and I-TAC, and acts as functional receptor for platelet factor 4. *J Exp Med* 197(11):1537–1549. doi: [10.1084/jem.20021897](https://doi.org/10.1084/jem.20021897)
12. Colvin RA, Campanella GSV, Sun JT, Luster AD (2004) Intracellular domains of CXCR3 that mediate CXCL9, CXCL10, and CXCL11 function. *J Biol Chem* 279(29):30219–30227

13. Smit MJ, Verdijk P, van der Raaij-Helmer EMH, Navis M, Hensbergen PJ, Leurs R, Tensen CP (2003) CXCR3-mediated chemotaxis of human T cells is regulated by a G(i)- and phospholipase C-dependent pathway and not via activation of MEK/p44/p42 MAPK nor Akt/PI-3 kinase. *Blood* 102(6):1959–1965. doi: [10.1182/blood-2002-12-3945](https://doi.org/10.1182/blood-2002-12-3945)
14. Scholten DJ, Canals M, Wijtmans M, de Munnik S, Nguyen P, Verzijl D, de Esch IJ, Vischer HF, Smit MJ, Leurs R (2012) Pharmacological characterization of a small-molecule agonist for the chemokine receptor CXCR3. *Br J Pharmacol* 166(3):898–911. doi: [10.1111/j.1476-5381.2011.01648.x](https://doi.org/10.1111/j.1476-5381.2011.01648.x)
15. Canals M, Scholten DJ, de Munnik S, Han MK, Smit MJ, Leurs R (2012) Ubiquitination of CXCR7 controls receptor trafficking. *PLoS One* 7(3):e34192. doi: [10.1371/journal.pone.0034192](https://doi.org/10.1371/journal.pone.0034192)
16. Dagan-Berger M, Feniger-Barish R, Avniel S, Wald H, Galun E, Grabovsky V, Alon R, Nagler A, Ben-Baruch A, Peled A (2006) Role of CXCR3 carboxyl terminus and third intracellular loop in receptor-mediated migration, adhesion and internalization in response to CXCL11. *Blood* 107(10):3821–3831. doi: [10.1182/blood-2004-01-0214](https://doi.org/10.1182/blood-2004-01-0214)
17. Meiser A, Mueller A, Wise EL, McDonagh EM, Petit SJ, Saran N, Clark PC, Williams TJ, Pease JE (2008) The chemokine receptor CXCR3 is degraded following internalization and is replenished at the cell surface by de novo synthesis of receptor. *J Immunol* 180(10):6713–6724
18. Luttrell LM, Gesty-Palmer D (2010) Beyond desensitization: physiological relevance of arrestin-dependent signaling. *Pharmacol Rev* 62(2):305–330. doi: [10.1124/pr.109.002436](https://doi.org/10.1124/pr.109.002436)
19. Ferre S, Casado V, Devi LA, Filizola M, Jockers R, Lohse MJ, Milligan G, Pin JP, Guitart X (2014) G protein-coupled receptor oligomerization revisited: functional and pharmacological perspectives. *Pharmacol Rev* 66(2):413–434. doi: [10.1124/pr.113.00805266/2/413](https://doi.org/10.1124/pr.113.00805266/2/413)
20. Scholten DJ, Canals M, Maussang D, Roumen L, Smit MJ, Wijtmans M, de Graaf C, Vischer HF, Leurs R (2012) Pharmacological modulation of chemokine receptor function. *Br J Pharmacol* 165(6):1617–1643. doi: [10.1111/j.1476-5381.2011.01551.x](https://doi.org/10.1111/j.1476-5381.2011.01551.x)
21. Vischer HF, Nijmeijer S, Smit MJ, Leurs R (2008) Viral hijacking of human receptors through heterodimerization. *Biochem Biophys Res Commun* 377 (1):93–97. doi: [10.1016/j.bbrc.2008.09.082](https://doi.org/10.1016/j.bbrc.2008.09.082)
22. Watts AO, van Lipzig MM, Jaeger WC, Seeber RM, van Zwam M, Vinet J, van der Lee MM, Siderius M, Zaman GJ, Boddeke HW, Smit MJ, Pfleger KD, Leurs R, Vischer HF (2013) Identification and profiling of CXCR3-CXCR4 chemokine receptor heteromer complexes. *Br J Pharmacol* 168(7):1662–1674. doi: [10.1111/bph.12064](https://doi.org/10.1111/bph.12064)
23. Cox MA, Jenh CH, Gonsiorek W, Fine J, Narula SK, Zavodny PJ, Hipkin RW (2001) Human interferon-inducible 10-kDa protein and human interferon-inducible T cell alpha chemoattractant are allotypic ligands for human CXCR3: differential binding to receptor states. *Mol Pharmacol* 59(4):707–715. doi: [10.1124/mol.59.4.707](https://doi.org/10.1124/mol.59.4.707)
24. Xanthou G, Williams TJ, Pease JE (2003) Molecular characterization of the chemokine receptor CXCR3: evidence for the involvement of distinct extracellular domains in a multi-step model of ligand binding and receptor activation. *Eur J Immunol* 33(10):2927–2936. doi: [10.1002/eji.200324235](https://doi.org/10.1002/eji.200324235)
25. Watts AO, Scholten DJ, Heitman LH, Vischer HF, Leurs R (2012) Label-free impedance responses of endogenous and synthetic chemokine receptor CXCR3 agonists correlate with Gi-protein pathway activation. *Biochem Biophys Res Commun* 419(2):412–418. doi: [10.1016/j.bbrc.2012.02.036](https://doi.org/10.1016/j.bbrc.2012.02.036)
26. Kouroumalis A, Nibbs RJ, Aptel H, Wright KL, Kolios G, Ward SG (2005) The chemokines CXCL9, CXCL10, and CXCL11 differentially stimulate G alpha i-independent signaling and actin responses in human intestinal myofibroblasts. *J Immunol* 175(8):5403–5411. doi: [10.4049/jimmunol.175.8.5403](https://doi.org/10.4049/jimmunol.175.8.5403)
27. Mantovani A (1999) The chemokine system: redundancy for robust outputs. *Immunol Today* 20(6):254–257. doi: [10.1016/S0167-5699\(99\)01469-3](https://doi.org/10.1016/S0167-5699(99)01469-3)

28. Allen SJ, Crown SE, Handel TM (2007) Chemokine: receptor structure, interactions, and antagonism. *Annu Rev Immunol* 25:787–820. doi:[10.1146/annurev.immunol.24.021605.090529](https://doi.org/10.1146/annurev.immunol.24.021605.090529)
29. Clark-Lewis I, Mattioli I, Gong JH, Loetscher P (2003) Structure-function relationship between the human chemokine receptor CXCR3 and its ligands. *J Biol Chem* 278(1): 289–295. doi:[10.1074/jbc.M209470200](https://doi.org/10.1074/jbc.M209470200)
30. Hasegawa H, Inoue A, Kohno M, Muraoka M, Miyazaki T, Terada M, Nakayama T, Yoshie O, Nose M, Yasukawa M (2006) Antagonist of interferon-inducible protein 10/CXCL10 ameliorates the progression of autoimmune sialadenitis in MRL/lpr mice. *Arthritis Rheumat* 54(4):1174–1183. doi: [10.1002/art.21745](https://doi.org/10.1002/art.21745)
31. Hensbergen PJ, van der Raaij-Helmer EMH, Dijkman R, van der Schors RC, Werner-Felmayer G, Boorsma DM, Schepers RJ, Willemze R, Tensen CP (2001) Processing of natural and recombinant CXCR3-targeting chemokines and implications for biological activity. *Eur J Biochem* 268(18):4992–4999. doi:[10.1046/j.0014-2956.2001.02433.x](https://doi.org/10.1046/j.0014-2956.2001.02433.x)
32. Proost P, Schutyser E, Menten P, Struyf S, Wuyts A, Opdenakker G, Detheux M, Parmentier M, Durinx C, Lambeir A-M, Neyts J, Liekens S, Maudgal PC, Billiau A, Van Damme J (2001) Amino-terminal truncation of CXCR3 agonists impairs receptor signaling and lymphocyte chemotaxis, while preserving antiangiogenic properties. *Blood* 98 (13):3554–3561. doi:[10.1182/blood.V98.13.3554](https://doi.org/10.1182/blood.V98.13.3554)
33. Mellado M, Rodriguez-Frade JM, Vila-Coro AJ, Fernandez S, Martin de Ana A, Jones DR, Toran JL, Martinez AC (2001) Chemokine receptor homo- or heterodimerization activates distinct signaling pathways. *EMBO J* 20(10):2497–2507. doi:[10.1093/emboj/20.10.2497](https://doi.org/10.1093/emboj/20.10.2497)
34. Schall TJ, Proudfoot AE (2011) Overcoming hurdles in developing successful drugs targeting chemokine receptors. *Nat Rev Immunol* 11(5):355–363. doi:[10.1038/nri2972](https://doi.org/10.1038/nri2972)
35. Rosenblum JM, Zhang Q-W, Siu G, Collins TL, Sullivan T, Dairaghi DJ, Medina JC, Fairchild RL (2009) CXCR3 antagonism impairs the development of donor-reactive, IFN- $\gamma$ -producing effectors and prolongs allograft survival. *Transplantation* 87(3):360–369. doi:[10.1097/TP.0b013e31819574e9](https://doi.org/10.1097/TP.0b013e31819574e9)
36. Romagnani P, Crescioli C (2012) CXCL10: a candidate biomarker in transplantation. *Clinica Chimica Acta* 413(17–18):1364–1373. doi:[10.1016/j.cca.2012.02.009](https://doi.org/10.1016/j.cca.2012.02.009)
37. Hancock WW, Lu B, Gao W, Csizmadia V, Faia K, King JA, Smiley ST, Ling M, Gerard NP, Gerard C (2000) Requirement of the chemokine receptor CXCR3 for acute allograft rejection. *J Exp Med* 192(10):1515–1520. doi:[10.1084/jem.192.10.1515](https://doi.org/10.1084/jem.192.10.1515)
38. Mach F, Sauty A, Iarossi AS, Sukhova GK, Neote K, Libby P, Luster AD (1999) Differential expression of three T lymphocyte-activating CXC chemokines by human atheroma-associated cells. *J Clin Invest* 104(8):1041–1050. doi:[10.1172/JCI6993](https://doi.org/10.1172/JCI6993)
39. Mohan K, Issekutz TB (2007) Blockade of chemokine receptor CXCR3 inhibits T cell recruitment to inflamed joints and decreases the severity of adjuvant arthritis. *J Immunol* 179(12):8463–8469. doi:[10.4049/jimmunol.179.12.8463](https://doi.org/10.4049/jimmunol.179.12.8463)
40. Saetta M, Mariani M, Panina-Bordignon P, Turato G, Buonsanti C, Baraldo S, Bellettato CM, Papi A, Corbetta L, Zuin R, Sinigaglia F, Fabbri LM (2002) Increased expression of the chemokine receptor CXCR3 and its ligand CXCL10 in peripheral airways of smokers with chronic obstructive pulmonary disease. *Am J Respir Crit Care Med* 165(10):1404–1409. doi:[10.1164/rccm.2107139](https://doi.org/10.1164/rccm.2107139)
41. Sorensen TL, Tani M, Jensen J, Pierce V, Lucchinetti C, Folcik VA, Qin S, Rottman J, Sellebjerg F, Strieter RM, Frederiksen JL, Ransohoff RM (1999) Expression of specific chemokines and chemokine receptors in the central nervous system of multiple sclerosis patients. *J Clin Invest* 103(6):807–815. doi: [10.1172/JCI5150](https://doi.org/10.1172/JCI5150)
42. Enghard P, Humrich JY, Rudolph B, Rosenberger S, Biesen R, Kuhn A, Manz R, Hiepe F, Radbruch A, Burmester GR, Riemekasten G (2009) CXCR3+CD4+ T cells are enriched in inflamed kidneys and urine and provide a new biomarker for acute nephritis flares in systemic lupus erythematosus patients. *Arthritis Rheumat* 60(1):199–206. doi:[10.1002/art.24136](https://doi.org/10.1002/art.24136)

43. Meltzer M, Exeni A, Reinders ME, Fang JC, McMahon G, Ganz P, Hancock WW, Briscoe DM (2001) Expression of the chemokine receptor CXCR3 and its ligand IP-10 during human cardiac allograft rejection. *Circulation* 104(21):2558–2564. doi:[10.1161/hc4601.098010](https://doi.org/10.1161/hc4601.098010)
44. Kao J, Kobashigawa J, Fishbein MC, MacLellan WR, Burdick MD, Belperio JA, Strieter RM (2003) Elevated serum levels of the CXCR3 chemokine ITAC are associated with the development of transplant coronary artery disease. *Circulation* 107(15):1958–1961. doi:[10.1161/01.CIR.0000069270.16498.75](https://doi.org/10.1161/01.CIR.0000069270.16498.75)
45. Bauer JW, Baechler EC, Petri M, Batliwalla FM, Crawford D, Ortmann WA, Espe KJ, Li W, Patel DD, Gregersen PK, Behrens TW (2006) Elevated serum levels of interferon-regulated chemokines are biomarkers for active human systemic lupus erythematosus. *PLoS Med* 3(12):e491. doi:[10.1371/journal.pmed.0030491](https://doi.org/10.1371/journal.pmed.0030491)
46. Lit LC, Wong CK, Tam LS, Li EK, Lam CW (2006) Raised plasma concentration and ex vivo production of inflammatory chemokines in patients with systemic lupus erythematosus. *Ann Rheumat Dis* 65(2):209–215. doi:[10.1136/ard.2005.038315](https://doi.org/10.1136/ard.2005.038315)
47. Kawada K, Sonoshita M, Sakashita H, Takabayashi A, Yamaoka Y, Manabe T, Inaba K, Minato N, Oshima M, Taketo MM (2004) Pivotal role of CXCR3 in melanoma cell metastasis to lymph nodes. *Cancer Res* 64(11):4010–4017. doi:[10.1158/0008-5472.CAN-03-1757](https://doi.org/10.1158/0008-5472.CAN-03-1757)
48. Walser TC, Rifat S, Ma XR, Kundu N, Ward C, Goloubtseva O, Johnson MG, Medina JC, Collins TL, Fulton AM (2006) Antagonism of CXCR3 inhibits lung metastasis in a murine model of metastatic breast cancer. *Cancer Res* 66(15):7701–7707. doi:[10.1158/0008-5472.CAN-06-0709](https://doi.org/10.1158/0008-5472.CAN-06-0709)
49. Kawada K, Hosogi H, Sonoshita M, Sakashita H, Manabe T, Shimahara Y, Sakai Y, Takabayashi A, Oshima M, Taketo MM (2007) Chemokine receptor CXCR3 promotes colon cancer metastasis to lymph nodes. *Oncogene* 26(32):4679–4688. doi:[10.1038/sj.onc.1210267](https://doi.org/10.1038/sj.onc.1210267)
50. Murakami T, Kawada K, Iwamoto M, Akagami M, Hida K, Nakanishi Y, Kanda K, Kawada M, Seno H, Taketo MM, Sakai Y (2013) The role of CXCR3 and CXCR4 in colorectal cancer metastasis. *Int J Cancer* 132(2):276–287. doi:[10.1002/ijc.27670](https://doi.org/10.1002/ijc.27670)
51. Gao P, Zhou XY, Yashiro-Ohtani Y, Yang YF, Sugimoto N, Ono S, Nakanishi T, Obika S, Imanishi T, Egawa T, Nagasawa T, Fujiwara H, Hamaoka T (2003) The unique target specificity of a nonpeptide chemokine receptor antagonist: selective blockade of two Th1 chemokine receptors CCR5 and CXCR3. *J Leukocyte Biol* 73(2):273–280. doi:[10.1189/jlb.0602269](https://doi.org/10.1189/jlb.0602269)
52. van Wanrooij EJ, De Jager SC, van Es T, de Vos P, Birch HL, Owen DA, Watson RJ, Biessen EA, Chapman GA, van Berkel TJ, Kuiper J (2008) CXCR3 antagonist NBI-74330 attenuates atherosclerotic plaque formation in LDL receptor-deficient mice. *Arterioscler Thromb Vasc Biol* 28:251–257. doi:[10.1161/ATVBAHA.107.147827](https://doi.org/10.1161/ATVBAHA.107.147827)
53. Liu C, Luo D, Reynolds BA, Meher G, Katritzky AR, Lu B, Gerard CJ, Bhadha CP, Harrison JK (2011) Chemokine receptor CXCR3 promotes growth of glioma. *Carcinogenesis* 32(2):129–137. doi:[10.1093/carcin/bgq224](https://doi.org/10.1093/carcin/bgq224)
54. Jenh CH, Cox MA, Cui L, Reich EP, Sullivan L, Chen SC, Kinsley D, Qian S, Kim SH, Rosenblum S, Kozlowski J, Fine JS, Zavodny PJ, Lundell D (2012) A selective and potent CXCR3 antagonist SCH 546738 attenuates the development of autoimmune diseases and delays graft rejection. *BMC Immunol* 13(1):2. doi: [10.1186/1471-2172-13-2](https://doi.org/10.1186/1471-2172-13-2)
55. Kakuta Y, Okumi M, Miyagawa S, Tsutahara K, Abe T, Yazawa K, Matsunami K, Otsuka H, Takahara S, Nonomura N (2012) Blocking of CCR5 and CXCR3 suppresses the infiltration of macrophages in acute renal allograft rejection. *Transplantation* 93(1):24–31. doi:[10.1097/TP.0b013e31823aa585](https://doi.org/10.1097/TP.0b013e31823aa585)
56. Baker MS, Chen X, Rotramel AR, Nelson JJ, Lu B, Gerard C, Kanwar Y, Kaufman DB (2003) Genetic deletion of chemokine receptor CXCR3 or antibody blockade of its ligand IP-10 modulates posttransplantation graft-site lymphocytic infiltrates and prolongs functional graft survival in pancreatic islet allograft recipients. *Surgery* 134(2):126–133. doi:[10.1067/msy.2003.213](https://doi.org/10.1067/msy.2003.213)

57. Zerwes HG, Li J, Kovarik J, Streiff M, Hofmann M, Roth L, Luyten M, Pally C, Loewe RP, Wieczorek G, Banteli R, Thoma G, Luckow B (2008) The chemokine receptor Cxcr3 is not essential for acute cardiac allograft rejection in mice and rats. *Am J Transplant* 8(8): 1604–1613. doi: [10.1111/j.1600-6143.2008.02309.x](https://doi.org/10.1111/j.1600-6143.2008.02309.x)
58. Kwun J, Hazinedaroglu SM, Schadde E, Kayaoglu HA, Fechner J, Hu HZ, Roenneburg D, Torrealba J, Shiao L, Hong X, Peng R, Szewczyk JW, Sullivan KA, DeMartino J, Knechtle SJ (2008) Unaltered graft survival and intragraft lymphocytes infiltration in the cardiac allograft of Cxcr3<sup>-/-</sup> mouse recipients. *Am J Transplant* 8(8):1593–1603. doi:[10.1111/j.1600-6143.2008.02250.x](https://doi.org/10.1111/j.1600-6143.2008.02250.x)
59. Pradelli E, Karimjee-Soilihi B, Michiels JF, Ricci JE, Millet MA, Vandenbos F, Sullivan TJ, Collins TL, Johnson MG, Medina JC, Kleinerman ES, Schmid-Alliana A, Schmid-Antomarchi H (2009) Antagonism of chemokine receptor CXCR3 inhibits osteosarcoma metastasis to lungs. *Int J Cancer* 125(11):2586–2594. doi:[10.1002/ijc.24665](https://doi.org/10.1002/ijc.24665)
60. Goldberg-Bittman L, Sagi-Assif O, Meshel T, Nevo I, Levy-Nissenbaum O, Yron I, Witz IP, Ben-Baruch A (2005) Cellular characteristics of neuroblastoma cells: regulation by the ELR–CXC chemokine CXCL10 and expression of a CXCR3-like receptor. *Cytokine* 29(3): 105–117. doi:[10.1016/j.cyto.2004.10.003](https://doi.org/10.1016/j.cyto.2004.10.003)
61. Cambien B, Karimjee BF, Richard-Fiardo P, Bziouech H, Barthel R, Millet MA, Martini V, Birnbaum D, Scoazec JY, Abello J, Al Saati T, Johnson MG, Sullivan TJ, Medina JC, Collins TL, Schmid-Alliana A, Schmid-Antomarchi H (2009) Organ-specific inhibition of metastatic colon carcinoma by CXCR3 antagonism. *Br J Cancer* 100(11):1755–1764. doi:[10.1038/sj.bjc.6605078](https://doi.org/10.1038/sj.bjc.6605078)
62. Winkler AE, Brotman JJ, Pittman ME, Judd NP, Lewis JS Jr, Schreiber RD, Uppaluri R (2011) CXCR3 enhances a T-cell-dependent epidermal proliferative response and promotes skin tumorigenesis. *Cancer Res* 71(17):5707–5716. doi:[10.1158/0008-5472.CAN-11-0907](https://doi.org/10.1158/0008-5472.CAN-11-0907)
63. Giuliani N, Bonomini S, Romagnani P, Lazzaretti M, Morandi F, Colla S, Tagliaferri S, Lasagni L, Annunziato F, Crugnola M, Rizzoli V (2006) CXCR3 and its binding chemokines in myeloma cells: expression of isoforms and potential relationships with myeloma cell proliferation and survival. *Haematologica* 91(11):1489–1497
64. Wu Q, Dhir R, Wells A (2012) Altered CXCR3 isoform expression regulates prostate cancer cell migration and invasion. *Mol Cancer* 11:3. doi:[10.1186/1476-4598-11-3](https://doi.org/10.1186/1476-4598-11-3)
65. Walser TC, Ma X, Kundu N, Dorsey R, Goloubeva O, Fulton AM (2007) Immune-mediated modulation of breast cancer growth and metastasis by the chemokine Mig (CXCL9) in a murine model. *J Immunother* 30(5):490–498. doi:[10.1097/CJI.0b013e318031b551](https://doi.org/10.1097/CJI.0b013e318031b551)
66. Andersson A, Yang SC, Huang M, Zhu L, Kar UK, Batra RK, Elashoff D, Strieter RM, Dubinett SM, Sharma S (2009) IL-7 promotes CXCR3 ligand-dependent T cell antitumor reactivity in lung cancer. *J Immunol* 182(11):6951–6958. doi:[10.4049/jimmunol.0803340](https://doi.org/10.4049/jimmunol.0803340)
67. Wendel M, Galani IE, Suri-Payer E, Cerwenka A (2008) Natural killer cell accumulation in tumors is dependent on IFN-gamma and CXCR3 ligands. *Cancer Res* 68(20):8437–8445. doi:[10.1158/0008-5472.CAN-08-1440](https://doi.org/10.1158/0008-5472.CAN-08-1440)
68. Ehler JE, Addison CA, Burdick MD, Kunkel SL, Strieter RM (2004) Identification and partial characterization of a variant of human CXCR3 generated by posttranscriptional exon skipping. *J Immunol* 173(10):6234–6240. doi:[10.4049/jimmunol.173.10.6234](https://doi.org/10.4049/jimmunol.173.10.6234)
69. Yates-Binder CC, Rodgers M, Jaynes J, Wells A, Bodnar RJ, Turner T (2012) An IP-10 (CXCL10)-derived peptide inhibits angiogenesis. *PLoS One* 7(7):e40812. doi:[10.1371/journal.pone.0040812](https://doi.org/10.1371/journal.pone.0040812)
70. Datta D, Banerjee P, Gasser M, Waaga-Gasser AM, Pal S (2010) CXCR3-B can mediate growth-inhibitory signals in human renal cancer cells by down-regulating the expression of heme oxygenase-1. *J Biol Chem* 285(47):36842–36848. doi:[10.1074/jbc.M110.170324](https://doi.org/10.1074/jbc.M110.170324)
71. Lo BK, Yu M, Zloty D, Cowan B, Shapiro J, McElwee KJ (2010) CXCR3/ligands are significantly involved in the tumorigenesis of basal cell carcinomas. *Am J Pathol* 176(5): 2435–2446. doi:[10.2353/ajpath.2010.081059](https://doi.org/10.2353/ajpath.2010.081059)

72. Yates CC, Krishna P, Whaley D, Bodnar R, Turner T, Wells A (2010) Lack of CXC chemokine receptor 3 signaling leads to hypertrophic and hypercellular scarring. *Am J Pathol* 176(4):1743–1755. doi:[10.2353/ajpath.2010.090564](https://doi.org/10.2353/ajpath.2010.090564)
73. Yates CC, Whaley D, Kulasekeran P, Hancock WW, Lu B, Bodnar R, Newsome J, Hebda PA, Wells A (2007) Delayed and deficient dermal maturation in mice lacking the CXCR3 ELR-negative CXC chemokine receptor. *Am J Pathol* 171(2):484–495. doi: [10.2353/ajpath.2007.061092](https://doi.org/10.2353/ajpath.2007.061092)
74. Yates CC, Whaley D, Wells A (2012) Transplanted fibroblasts prevents dysfunctional repair in a murine CXCR3-deficient scarring model. *Cell Transplant* 21(5):919–931. doi:[10.3727/096368911X623817](https://doi.org/10.3727/096368911X623817)
75. Yates CC, Whaley D, Y-Chen A, Kulesekaran P, Hebda PA, Wells A (2008) ELR-negative CXC chemokine CXCL11 (IP-9/I-TAC) facilitates dermal and epidermal maturation during wound repair. *Am J Pathol* 173(3):643–652. doi:[10.2353/ajpath.2008.070990](https://doi.org/10.2353/ajpath.2008.070990)
76. Collins TL, Johnson MG, Medina JC (2007) In: Neote K, Letts GL, Moser B (eds) *Chemokine biology-basic research and clinical application*, vol 2. Birkhauser Verlag, Basel, Switzerland p 79
77. Wijtmans M, Verzijl D, Leurs R, de Esch IJ, Smit MJ (2008) Towards small-molecule CXCR3 ligands with clinical potential. *ChemMedChem* 3(6):861–872. doi:[10.1002/cmde.200700365](https://doi.org/10.1002/cmde.200700365)
78. Wijtmans M, de Esch IJP, Leurs R (2011) In: Smit MJ, Lira SA, Leurs R (eds) *Chemokine receptors as drug targets*. Wiley-VCH, Weinheim, pp 301–315. doi:[10.1002/9783527631995.ch13](https://doi.org/10.1002/9783527631995.ch13)
79. Roumen L, Scholten DJ, de Kruijf P, de Esch IJP, Leurs R, de Graaf C (2012) C(X)CR in silico: Computer-aided prediction of chemokine receptor-ligand interactions. *Drug Discov Today Technol* 9(4):e281–e291. doi:[10.1016/j.ddtec.2012.05.002](https://doi.org/10.1016/j.ddtec.2012.05.002)
80. Scholten DJ, Roumen L, Wijtmans M, Verkade-Vreeker MC, Custers H, Lai M, de Hooge D, Canals M, de Esch IJ, Smit MJ, de Graaf C, Leurs R (2014) Identification of overlapping but differential binding sites for the high-affinity CXCR3 antagonists NBI-74330 and VUF11211. *Mol Pharmacol* 85(1):116–126. doi:[10.1124/mol.113.088633](https://doi.org/10.1124/mol.113.088633)
81. Katritch V, Cherezov V, Stevens RC (2013) Structure-function of the G protein-coupled receptor superfamily. *Annu Rev Pharmacol Toxicol* 53:531–556. doi:[10.1146/annurev-pharmtox-032112-135923](https://doi.org/10.1146/annurev-pharmtox-032112-135923)
82. Venkatakrishnan AJ, Deupi X, Lebon G, Tate CG, Schertler GF, Babu MM (2013) Molecular signatures of G-protein-coupled receptors. *Nature* 494(7436):185–194. doi:[10.1038/nature11896](https://doi.org/10.1038/nature11896)
83. Wu B, Chien EY, Mol CD, Fenalti G, Liu W, Katritch V, Abagyan R, Brooun A, Wells P, Bi FC, Hamel DJ, Kuhn P, Handel TM, Cherezov V, Stevens RC (2010) Structures of the CXCR4 chemokine GPCR with small-molecule and cyclic peptide antagonists. *Science* 330(6007):1066–1071. doi:[10.1126/science.1194396](https://doi.org/10.1126/science.1194396)
84. Tan Q, Zhu Y, Li J, Chen Z, Han GW, Kufareva I, Li T, Ma L, Fenalti G, Zhang W, Xie X, Yang H, Jiang H, Cherezov V, Liu H, Stevens RC, Zhao Q, Wu B (2013) Structure of the CCR5 chemokine receptor-HIV entry inhibitor maraviroc complex. *Science* 341(6152): 1387–1390. doi:[10.1126/science.1241475](https://doi.org/10.1126/science.1241475)
85. Ondeyka JG, Herath KB, Jayasuriya H, Polishook JD, Bills GF, Dombrowski AW, Mojena M, Koch G, DiSalvo J, DeMartino J, Guan Z, Nanakorn W, Morenberg CM, Balick MJ, Stevenson DW, Slattery M, Borris RP, Singh SB (2005) Discovery of structurally diverse natural product antagonists of chemokine receptor CXCR3. *Mol Diversity* 9:123–129. doi:[10.1007/s11030-005-1296-8](https://doi.org/10.1007/s11030-005-1296-8)
86. Schall TJ, Dairaghi DJ, McMaster BE (2001) Compounds and methods for modulating CXCR3 function. *WO0116114*
87. Johnson M, Li A-R, Liu J, Fu Z, Zhu L, Miao S, Wang X, Xu Q, Huang A, Marcus A, Xu F, Ebsworth K, Sablan E, Danao J, Kumer J, Dairaghi D, Lawrence C, Sullivan T, Tonn G, Schall T, Collins T, Medina J (2007) Discovery and optimization of a series of quinazolinone-

- derived antagonists of CXCR3. *Bioorg Med Chem Lett* 17(12):3339–3343. doi:[10.1016/j.bmcl.2007.03.106](https://doi.org/10.1016/j.bmcl.2007.03.106)
88. Storelli S, Verdijk P, Verzijl D, Timmerman H, van de Stolpe AC, Tensen CP, Smit MJ, De Esch IJP, Leurs R (2005) Synthesis and structure-activity relationship of 3-phenyl-3H-quinazolin-4-one derivatives as CXCR3 chemokine receptor antagonists. *Bioorg Med Chem Lett* 15(11):2910–2913. doi: [10.1016/j.bmcl.2005.03.070](https://doi.org/10.1016/j.bmcl.2005.03.070)
89. Heise CE, Pahuja A, Hudson SC, Mistry MS, Putnam AL, Gross MM, Gottlieb PA, Wade WS, Kiankarimi M, Schwarz D, Crowe P, Zlotnik A, Alleva DG (2005) Pharmacological characterization of CXC chemokine receptor 3 ligands and a small molecule antagonist. *J Pharmacol Exp Ther* 313(3):1263–1271. doi: [10.1124/jpet.105.083683](https://doi.org/10.1124/jpet.105.083683)
90. Medina JC, Johnson MG, Li A, Liu J, Huang AX, Zhu L, Marcus AP (2002) CXCR3 antagonists. WO02083143
91. Johnson MG (2006) Presented at the XIXth international symposium on medicinal chemistry, Istanbul, Turkey, Aug 29–Sep 2
92. Storelli S, Verzijl D, Al-Badie J, Elders N, Bosch L, Timmerman H, Smit MJ, De Esch IJP, Leurs R (2007) Synthesis and structure-activity relationships of 3H-quinazolin-4-ones and 3H-pyrido[2,3-d]pyrimidin-4-ones as CXCR3 receptor antagonists. *Arch Pharm* 340(6): 281–291. doi:[10.1002/ardp.200700037](https://doi.org/10.1002/ardp.200700037)
93. Floren LC (2003). Presented at inflammation 2003 – sixth world congress, Vancouver, Canada, Aug 2–6
94. Berry K, Friedrich M, Kersey K, Steimpel M, Wagner F, van Lier J, Sabat R, Wolk K (2004) Evaluation of T0906487, a CXCR3 antagonist, in a phase 2a psoriasis trial. *Inflammation Res Suppl* 53:pS222
95. Tonn GR, Wong SG, Wong SC, Johnson MG, Ma J, Cho R, Floren LC, Kersey K, Berry K, Marcus AP, Wang X, Van Lengerich B, Medina JC, Pearson PG, Wong BK (2009) An inhibitory metabolite leads to dose- and time-dependent pharmacokinetics of AMG 487 in human subjects following multiple dosing. *Drug Metab Disposit* 37:502–513. doi: [10.1124/dmd.108.021931](https://doi.org/10.1124/dmd.108.021931)
96. Henne KR, Tran TB, VandenBrink BM, Rock DA, Aidasani DK, Subramanian R, Mason AK, Stresser DM, Teffera Y, Wong SG, Johnson MG, Chen X, Tonn GR, Wong BK (2012) Sequential metabolism of AMG 487, a novel CXCR3 antagonist, results in formation of quinone reactive metabolites that covalently modify CYP3A4 Cys239 and cause time-dependent inhibition of the enzyme. *Drug Metab Disposit* 40(7):1429–1440. doi: [10.1124/dmd.112.045708](https://doi.org/10.1124/dmd.112.045708)
97. Li A-R, Johnson MG, Liu J, Chen X, Du X, Mihalic JT, Deignan J, Gustin DJ, Duquette J, Fu Z, Zhu L, Marcus AP, Bergeron P, McGee LR, Danao J, Sullivan T, Ma J, Tang L, Tonn G, Collins T, Medina JC (2008) Optimisation of the heterocyclic core of the quinazolinone-derived CXCR3 antagonists. *Bioorg Med Chem Lett* 18:688–693. doi: [10.1016/j.bmcl.2007.11.060](https://doi.org/10.1016/j.bmcl.2007.11.060)
98. Liu J, Fu Z, Li AR, Johnson M, Zhu L, Marcus A, Danao J, Sullivan T, Tonn G, Collins T, Medina J (2009) Optimization of a series of quinazolinone-derived antagonists of CXCR3. *Bioorg Med Chem Lett* 19(17):5114–5118. doi:[10.1016/j.bmcl.2009.07.032](https://doi.org/10.1016/j.bmcl.2009.07.032)
99. Bernat V, Heinrich MR, Baumeister P, Buschauer A, Tschauder N (2012) Synthesis and application of the first radioligand targeting the allosteric binding pocket of chemokine receptor CXCR3. *ChemMedChem* 7(8):1481–1489. doi: [10.1002/cmdc.201200184](https://doi.org/10.1002/cmdc.201200184)
100. Chen X, Mihalic J, Deignan J, Gustin DJ, Duquette J, Du X, Chan J, Fu Z, Johnson M, Li AR, Henne K, Sullivan T, Lemon B, Ma J, Miao S, Tonn G, Collins T, Medina JC (2012) Discovery of potent and specific CXCR3 antagonists. *Bioorg Med Chem Lett* 22(1): 357–362. doi:[10.1016/j.bmcl.2011.10.120](https://doi.org/10.1016/j.bmcl.2011.10.120)
101. Chan J, Burke BJ, Baucom K, Hansen K, Bio MM, DiVirgilio E, Faul M, Murry J (2011) Practical syntheses of a CXCR3 antagonist. *J Org Chem* 76(6):1767–1774. doi:[10.1021/jo102399a](https://doi.org/10.1021/jo102399a)
102. Du X, Chen X, Mihalic J, Deignan J, Duquette J, Li A-R, Lemon B, Ma J, Miao S, Ebsworth K, Sullivan TJ, Tonn G, Collins T, Medina J (2008) Design and optimisation of

- imidazole derivatives as potent CXCR3 antagonists. *Bioorg Med Chem Lett* 18:608–613. doi:[10.1016/j.bmcl.2007.11.072](https://doi.org/10.1016/j.bmcl.2007.11.072)
103. Du X, Gustin DJ, Chen X, Duquette J, McGee LR, Wang Z, Ebsworth K, Henne K, Lemon B, Ma J, Miao S, Sabalan E, Sullivan TJ, Tonn G, Collins TL, Medina JC (2009) Imidazo-pyrazine derivatives as potent CXCR3 antagonists. *Bioorg Med Chem Lett* 19(17): 5200–5204. doi:[10.1016/j.bmcl.2009.07.021](https://doi.org/10.1016/j.bmcl.2009.07.021)
104. Afantitis A, Melagraki G, Sarimveis H, Koutentis PA, Iglessi-Markopoulos O, Kollias G (2010) A combined LS-SVM & MLR QSAR workflow for predicting the inhibition of CXCR3 receptor by quinazolinone analogs. *Mol Divers* 14(2):225–235. doi:[10.1007/s11030-009-9163-7](https://doi.org/10.1007/s11030-009-9163-7)
105. Allen DR, Bolt A, Chapman GA, Knight RL, Meissner JWG, Owen DA, Watson RJ (2007) Identification and structure-activity relationships of 1-aryl-3-piperidin-4-yl-urea derivatives as CXCR3 receptor antagonists. *Bioorg Med Chem Lett* 17(3):697–701. doi:[10.1016/j.bmcl.2006.10.088](https://doi.org/10.1016/j.bmcl.2006.10.088)
106. Watson RJ, Allen DR, Birch HL, Chapman GA, Hannah DR, Knight RL, Meissner JWG, Owen DA, Thomas EJ (2007) Development of CXCR3 antagonists. Part 2: Identification of 2-amino(4-piperidinyl)azoles as potent CXCR3 antagonists. *Bioorg Med Chem Lett* 17: 6806–6810. doi:[10.1016/j.bmcl.2007.10.029](https://doi.org/10.1016/j.bmcl.2007.10.029)
107. Watson RJ, Allen DR, Birch HL, Chapman GA, Galvin FC, Jopling LA, Knight RL, Meier D, Oliver K, Meissner JW, Owen DA, Thomas EJ, Tremayne N, Williams SC (2008) Development of CXCR3 antagonists. Part 3: tropenyl and homotropenyl-piperidine urea derivatives. *Bioorg Med Chem Lett* 18:147–151. doi:[10.1016/j.bmcl.2007.10.109](https://doi.org/10.1016/j.bmcl.2007.10.109)
108. Knight RL, Allen DR, Birch HL, Chapman GA, Galvin FC, Jopling LA, Lock CJ, Meissner JWG, Owen DA, Raphy G, Watson RJ, Williams SC (2008) Development of CXCR3 antagonists, Part 4: discovery of 2-amino-(4-tropinyl) quinolines. *Bioorg Med Chem Lett* 18:629–633. doi:[10.1016/j.bmcl.2007.11.075](https://doi.org/10.1016/j.bmcl.2007.11.075)
109. McGuinness BF, Carroll CD, Zawacki LG, Dong G, Yang C, Hobbs DW, Jacob-Samuel B, Hall JW 3rd, Jenh CH, Kozlowski JA, Anilkumar GN, Rosenblum SB (2009) Novel CXCR3 antagonists with a piperazinyl-piperidine core. *Bioorg Med Chem Lett* 19(17):5205–5208. doi:[10.1016/j.bmcl.2009.07.020](https://doi.org/10.1016/j.bmcl.2009.07.020)
110. Bongartz JP, Buntinx M, Coesmans E, Hermans B, Lommen GV, Wauwe JV (2008) Synthesis and structure-activity relationship of benztetramide derivatives as human CXCR3 antagonists. *Bioorg Med Chem Lett* 18:5819–5823. doi:[10.1016/j.bmcl.2008.07.115](https://doi.org/10.1016/j.bmcl.2008.07.115)
111. Shao Y, Anilkumar GN, Carroll CD, Dong G, Hall JW 3rd, Hobbs DW, Jiang Y, Jenh CH, Kim SH, Kozlowski JA, McGuinness BF, Rosenblum SB, Schulman I, Shih NY, Shu Y, Wong MK, Yu W, Zawacki LG, Zeng Q (2011) II. SAR studies of pyridyl-piperazinyl-piperidine derivatives as CXCR3 chemokine antagonists. *Bioorg Med Chem Lett* 21(5): 1527–1531. doi:[10.1016/j.bmcl.2010.12.114](https://doi.org/10.1016/j.bmcl.2010.12.114)
112. McGuinness BF, Rosenblum SF, Kozlowski JA, Anilkumar GN, Kim SH, Shih N-Y, Jenh C-H, Zavodny PJ, Hobbs DW, Dong G, Shao Y, Zawacki LG, Yang C, Carroll CD (2006) Pyridyl and phenyl substituted piperazine-piperidines with CXCR3 antagonist activity. WO2006088919
113. Wijtmans M, Verzijl D, van Dam CM, Bosch L, Smit MJ, Leurs R, de Esch IJ (2009) Exploring a pocket for polycycloaliphatic groups in the CXCR3 receptor with the aid of a modular synthetic strategy. *Bioorg Med Chem Lett* 19(8):2252–2257. doi:[10.1016/j.bmcl.2009.02.093](https://doi.org/10.1016/j.bmcl.2009.02.093)
114. Kim SH, Anilkumar GN, Zawacki LG, Zeng Q, Yang DY, Shao Y, Dong G, Xu X, Yu W, Jiang Y, Jenh CH, Hall JW 3rd, Carroll CD, Hobbs DW, Baldwin JJ, McGuinness BF, Rosenblum SB, Kozlowski JA, Shankar BB, Shih NY (2011) III. Identification of novel CXCR3 chemokine receptor antagonists with a pyrazinyl-piperazinyl-piperidine scaffold. *Bioorg Med Chem Lett* 21(23):6982–6986. doi:[10.1016/j.bmcl.2011.09.120](https://doi.org/10.1016/j.bmcl.2011.09.120)
115. Nair AG, Wong MKC, Shu Y, Jiang Y, Jenh C-H, Kim SH, Yang D-Y, Zeng Q, Shao Y, Zawacki LG, Duo J, McGuinness BF, Carroll CD, Hobbs DW, Shih N-Y, Rosenblum SB,

- Kozlowski JA (2014) IV. Discovery of CXCR3 antagonists substituted with heterocycles as amide surrogates: Improved PK, hERG and metabolic profiles. *Bioorg Med Chem Lett* 24(4): 1085–1088. doi:[10.1016/j.bmcl.2014.01.009](https://doi.org/10.1016/j.bmcl.2014.01.009)
116. Thoma G, Baenteli R, Lewis I, Wagner T, Oberer L, Blum W, Glickman F, Streiff MB, Zerwes HG (2009) Special ergolines are highly selective, potent antagonists of the chemokine receptor CXCR3: discovery, characterization and preliminary SAR of a promising lead. *Bioorg Med Chem Lett* 19(21):6185–6188. doi:[10.1016/j.bmcl.2009.09.002](https://doi.org/10.1016/j.bmcl.2009.09.002)
117. Thoma G, Baenteli R, Lewis I, Jones D, Kovarik J, Streiff MB, Zerwes HG (2011) Special ergolines efficiently inhibit the chemokine receptor CXCR3 in blood. *Bioorg Med Chem Lett* 21(16):4745–4749. doi:[10.1016/j.bmcl.2011.06.070](https://doi.org/10.1016/j.bmcl.2011.06.070)
118. Christen S, Holdener M, Beerli C, Thoma G, Bayer M, Pfeilschifter JM, Hintermann E, Zerwes HG, Christen U (2011) Small molecule CXCR3 antagonist NIBR2130 has only a limited impact on type 1 diabetes in a virus-induced mouse model. *Clin Exp Immunol* 165(3): 318–328. doi:[10.1111/j.1365-2249.2011.04426.x](https://doi.org/10.1111/j.1365-2249.2011.04426.x)
119. Hayes ME, Wallace GA, Grongsaard P, Bischoff A, George DM, Miao W, McPherson MJ, Stoffel RH, Green DW, Roth GP (2008) Discovery of small molecule benzimidazole antagonists of the chemokine receptor CXCR3. *Bioorg Med Chem Lett* 18(5):1573–1576. doi:[10.1016/j.bmcl.2008.01.074](https://doi.org/10.1016/j.bmcl.2008.01.074)
120. Hayes ME, Breinlinger EC, Wallace GA, Grongsaard P, Miao W, McPherson MJ, Stoffel RH, Green DW, Roth GP (2008) Lead identification of 2-iminobenzimidazole antagonists of the chemokine receptor CXCR3. *Bioorg Med Chem Lett* 18(7):2414–2419. doi:[10.1016/j.bmcl.2008.02.049](https://doi.org/10.1016/j.bmcl.2008.02.049)
121. Wang Y, Busch-Petersen J, Wang F, Kiesow TJ, Graybill TL, Jin J, Yang Z, Foley JJ, Hunsberger GE, Schmidt DB, Sarau HM, Capper-Spudich EA, Wu Z, Fisher LS, McQueney MS, Rivero RA, Widdowson KL (2009) Camphor sulfonamide derivatives as novel, potent and selective CXCR3 antagonists. *Bioorg Med Chem Lett* 19:114–118. doi:[10.1016/j.bmcl.2008.11.008](https://doi.org/10.1016/j.bmcl.2008.11.008)
122. Wijtmans M, Verzijl D, Bergmans S, Lai M, Bosch L, Smit MJ, de Esch IJ, Leurs R (2011) CXCR3 antagonists: quaternary ammonium salts equipped with biphenyl- and polycycloaliphatic-anchors. *Bioorg Med Chem* 19(11):3384–3393. doi:[10.1016/j.bmc.2011.04.035](https://doi.org/10.1016/j.bmc.2011.04.035)
123. Crosignani S, Missotten M, Cleva C, Dondi R, Ratinaud Y, Humbert Y, Mandal AB, Bombrun A, Power C, Chollet A, Proudfoot A (2010) Discovery of a novel series of CXCR3 antagonists. *Bioorg Med Chem Lett* 20(12):3614–3617. doi:[10.1016/j.bmcl.2010.04.113](https://doi.org/10.1016/j.bmcl.2010.04.113)
124. Cole AG, Stroke IL, Brescia MR, Simhadri S, Zhang JJ, Hussain Z, Snider M, Haskell C, Ribeiro S, Appell KC, Henderson I, Webb ML (2006) Identification and initial evaluation of 4-N-aryl-[1,4]diazepane ureas as potent CXCR3 antagonists. *Bioorg Med Chem Lett* 16(1): 200–203. doi:[10.1016/j.bmcl.2005.09.020](https://doi.org/10.1016/j.bmcl.2005.09.020)
125. Stroke IL, Cole AG, Simhadri S, Brescia MR, Desai M, Zhang JJ, Merritt JR, Appell KC, Henderson I, Webb ML (2006) Identification of CXCR3 receptor agonists in combinatorial small-molecule libraries. *Biochem Biophys Res Commun* 349(1):221–228. doi:[10.1016/j.bbrc.2006.08.019](https://doi.org/10.1016/j.bbrc.2006.08.019)
126. Afantitis A, Melagraki G, Sarimveis H, Iglessi-Markopoulos O, Kollias G (2009) A novel QSAR model for predicting the inhibition of CXCR3 receptor by 4-N-aryl-[1,4] diazepane ureas. *Eur J Med Chem* 44(2):877–884. doi:[10.1016/j.ejmech.2008.05.028](https://doi.org/10.1016/j.ejmech.2008.05.028)
127. Vummidi BR, Noreen F, Alzeer J, Moelling K, Luedtke NW (2013) Photodynamic agents with anti-metastatic activities. *ACS Chem Biol* 8(8):1737–1746. doi:[10.1021/cb400008t](https://doi.org/10.1021/cb400008t)
128. Wise E, Pease JE (2007) Unravelling the mechanisms underpinning chemokine receptor activation and blockade by small molecules: a fine line between agonism and antagonism? *Biochem Soc Trans* 35:755–759. doi:[10.1042/BST0350755](https://doi.org/10.1042/BST0350755)
129. Nedjai B, Li H, Stroke IL, Wise EL, Webb ML, Merritt JR, Henderson I, Klon AE, Cole AG, Horuk R, Vaidehi N, Pease JE (2012) Small molecule chemokine mimetics suggest a molecular basis for the observation that CXCL10 and CXCL11 are allosteric ligands of CXCR3. *Br J Pharmacol* 166(3):912–923. doi:[10.1111/j.1476-5381.2011.01660.x](https://doi.org/10.1111/j.1476-5381.2011.01660.x)

130. O'Boyle G, Fox CR, Walden HR, Willet JD, Mavin ER, Hine DW, Palmer JM, Barker CE, Lamb CA, Ali S, Kirby JA (2012) Chemokine receptor CXCR3 agonist prevents human T-cell migration in a humanized model of arthritic inflammation. *Proc Natl Acad Sci U S A* 109(12):4598–4603. doi:[10.1073/pnas.1118104109](https://doi.org/10.1073/pnas.1118104109)
131. O'Boyle G, Mellor P, Kirby JA, Ali S (2009) Anti-inflammatory therapy by intravenous delivery of non-heparan sulfate-binding CXCL12. *FASEB J* 23(11):3906–3916. doi:[10.1096/fj.09-134643](https://doi.org/10.1096/fj.09-134643)
132. Wijtmans M, Scholten DJ, Roumen L, Canals M, Custers H, Glas M, Vreeker MC, de Kanter FJ, de Graaf C, Smit MJ, de Esch IJ, Leurs R (2012) Chemical subtleties in small-molecule modulation of peptide receptor function: the case of CXCR3 biaryl-type ligands. *J Med Chem* 55(23):10572–10583. doi:[10.1021/jm301240t](https://doi.org/10.1021/jm301240t)
133. Ballesteros JA, Weinstein H (1995) Integrated methods for the construction of three dimensional models and computational probing of structure-function relations in G-protein coupled receptors. *Methods Neurosci* 25:366–428. doi:[10.1016/S1043-9471\(05\)80049-7](https://doi.org/10.1016/S1043-9471(05)80049-7)
134. Hollenstein K, de Graaf C, Bortolato A, Wang MW, Marshall FH, Stevens RC (2014) Insights into the structure of class B GPCRs. *Trends Pharmacol Sci* 35(1):12–22. doi:[10.1016/j.tips.2013.11.001](https://doi.org/10.1016/j.tips.2013.11.001)
135. Wu H, Wang C, Gregory KJ, Han GW, Cho HP, Xia Y, Niswender CM, Katritch V, Meiler J, Cherezov V, Conn PJ, Stevens RC (2014) Structure of a class C GPCR metabotropic glutamate receptor 1 bound to an allosteric modulator. *Science* 344(6179):58–64. doi:[10.1126/science.1249489](https://doi.org/10.1126/science.1249489)
136. Wang C, Wu H, Katritch V, Han GW, Huang XP, Liu W, Siu FY, Roth BL, Cherezov V, Stevens RC (2013) Structure of the human smoothened receptor bound to an antitumour agent. *Nature* 497(7449):338–343. doi:[10.1038/nature12167](https://doi.org/10.1038/nature12167)
137. Kooistra AJ, Roumen L, Leurs R, de Esch IJ, de Graaf C (2013) From heptahelical bundle to hits from the Haystack: structure-based virtual screening for GPCR ligands. *Methods Enzymol* 522:279–336. doi:[10.1016/B978-0-12-407865-9.00015-7](https://doi.org/10.1016/B978-0-12-407865-9.00015-7)
138. Michino M, Abola E, participants GD, Brooks CL 3rd, Dixon JS, Moult J, Stevens RC (2009) Community-wide assessment of GPCR structure modelling and ligand docking: GPCR Dock 2008. *Nat Rev Drug Discov* 8(6):455–463. doi:[10.1038/nrd2877](https://doi.org/10.1038/nrd2877)
139. Kufareva I, Rueda M, Katritch V, Stevens RC, Abagyan R, participants GD (2011) Status of GPCR modeling and docking as reflected by community-wide GPCR Dock 2010 assessment. *Structure* 19(8):1108–1126. doi:[10.1016/j.str.2011.05.012](https://doi.org/10.1016/j.str.2011.05.012)
140. Manglik A, Kruse AC, Kobilka TS, Thian FS, Mathiesen JM, Sunahara RK, Pardo L, Weis WI, Kobilka BK, Granier S (2012) Crystal structure of the micro-opioid receptor bound to a morphinan antagonist. *Nature* 485(7398):321–326. doi:[10.1038/nature10954](https://doi.org/10.1038/nature10954)
141. Roumen L, Sanders MP, Vroeling B, de Esch IJ, de Vlieg J, Leurs R, Klomp JP, Nabuurs SB, de Graaf C (2011) In Silico Veritas: the pitfalls and challenges of predicting GPCR-ligand interactions. *Pharmaceuticals* 4(9):1196–1215. doi:[10.1021/ci200088d](https://doi.org/10.1021/ci200088d)
142. Brelo A, Heveker N, Montes M, Alizon M (2000) Identification of residues of CXCR4 critical for human immunodeficiency virus coreceptor and chemokine receptor activities. *J Biol Chem* 275(31):23736–23744. doi:[10.1074/jbc.M000776200](https://doi.org/10.1074/jbc.M000776200)
143. Kofuku Y, Yoshiura C, Ueda T, Terasawa H, Hirai T, Tominaga S, Hirose M, Maeda Y, Takahashi H, Terashima Y, Matsushima K, Shimada I (2009) Structural basis of the interaction between chemokine stromal cell-derived factor-1/CXCL12 and its G-protein-coupled receptor CXCR4. *J Biol Chem* 284(50):35240–35250. doi:[10.1074/jbc.M109.024851](https://doi.org/10.1074/jbc.M109.024851)
144. Colvin RA, Campanella GS, Manice LA, Luster AD (2006) CXCR3 requires tyrosine sulfation for ligand binding and a second extracellular loop arginine residue for ligand-induced chemotaxis. *Mol Cell Biol* 26(15):5838–5849. doi:[10.1128/MCB.00556-06](https://doi.org/10.1128/MCB.00556-06)
145. Anghescu AV, DeLisle RK, Lowrie JF, Klon AE, Xie X, Diller DJ (2008) Technique for generating three-dimensional alignments of multiple ligands from one-dimensional alignments. *J Chem Inform Model* 48(5):1041–1054. doi:[10.1021/ci700395f](https://doi.org/10.1021/ci700395f)

146. Rosenkilde MM, Andersen MB, Nygaard R, Frimurer TM, Schwartz TW (2007) Activation of the CXCR3 chemokine receptor through anchoring of a small molecule chelator ligand between TM-III, -IV, and -VI. *Mol Pharmacol* 71(3):930–941. doi: [10.1124/mol.106.030031](https://doi.org/10.1124/mol.106.030031)
147. Scholten DJ (2012) Chemokine receptors CXCR3 and CXCR7: allosteric ligand binding, biased signaling, and receptor regulation. VU University Amsterdam, Amsterdam
148. Zhang J, Chen P, Yuan B, Ji W, Cheng Z, Qiu X (2013) Real-space identification of intermolecular bonding with atomic force microscopy. *Science* 342(6158):611–614. doi:[10.1126/science.1242603](https://doi.org/10.1126/science.1242603)
149. Pierce AC, Sandretto KL, Bemis GW (2002) Kinase inhibitors and the case for CH...O hydrogen bonds in protein-ligand binding. *Proteins* 49(4):567–576. doi:[10.1002/prot.10259](https://doi.org/10.1002/prot.10259)
150. van Linden OP, Kooistra AJ, Leurs R, de Esch IJ, de Graaf C (2014) KLIFS: a knowledge-based structural database to navigate kinase-ligand interaction space. *J Med Chem* 57(2): 249–277. doi:[10.1021/jm400378w](https://doi.org/10.1021/jm400378w)
151. Becker OM, Marantz Y, Shacham S, Inbal B, Heifetz A, Kalid O, Bar-Haim S, Warshaviak D, Fichman M, Noiman S (2004) G protein-coupled receptors: in silico drug discovery in 3D. *Proc Natl Acad Sci USA* 101(31):11304–11309. doi:[10.1073/pnas.0401862101](https://doi.org/10.1073/pnas.0401862101)
152. Bayry J, Tchilian EZ, Davies MN, Forbes EK, Draper SJ, Kaveri SV, Hill AV, Kazatchkine MD, Beverley PC, Flower DR, Tough DF (2008) In silico identified CCR4 antagonists target regulatory T cells and exert adjuvant activity in vaccination. *Proc Natl Acad Sci USA* 105(29):10221–10226. doi:[10.1073/pnas.0803453105](https://doi.org/10.1073/pnas.0803453105)
153. Kellenberger E, Springael JY, Parmentier M, Hachet-Haas M, Galzi JL, Rognan D (2007) Identification of nonpeptide CCR5 receptor agonists by structure-based virtual screening. *J Med Chem* 50(6):1294–1303. doi:[10.1021/jm061389p](https://doi.org/10.1021/jm061389p)
154. Kim J, Yip ML, Shen X, Li H, Hsin LY, Labarge S, Heinrich EL, Lee W, Lu J, Vaidehi N (2012) Identification of anti-malarial compounds as novel antagonists to chemokine receptor CXCR4 in pancreatic cancer cells. *PLoS One* 7(2):e31004. doi:[10.1371/journal.pone.0031004](https://doi.org/10.1371/journal.pone.0031004)
155. Huang D, Gu Q, Ge H, Ye J, Salam NK, Hagler A, Chen H, Xu J (2012) On the value of homology models for virtual screening: discovering hCXCR3 antagonists by pharmacophore-based and structure-based approaches. *J Chem Inform Model* 52(5): 1356–1366. doi:[10.1021/ci300067q](https://doi.org/10.1021/ci300067q)
156. Mysinger MM, Weiss DR, Ziarek JJ, Gravel S, Doak AK, Karpik J, Heveker N, Shoichet BK, Volkman BF (2012) Structure-based ligand discovery for the protein-protein interface of chemokine receptor CXCR4. *Proc Natl Acad Sci USA* 109(14):5517–5522. doi:[10.1073/pnas.1120431109](https://doi.org/10.1073/pnas.1120431109)
157. Vitale RM, Gatti M, Carbone M, Barbieri F, Felicita V, Gavagnin M, Florio T, Amodeo P (2013) Minimalist hybrid ligand/receptor-based pharmacophore model for CXCR4 applied to a small-library of marine natural products led to the identification of phidianidine a as a new CXCR4 ligand exhibiting antagonist activity. *ACS Chem Biol* 8(12):2762–2770. doi:[10.1021/cb400521b](https://doi.org/10.1021/cb400521b)
158. Yoshikawa Y, Oishi S, Kubo T, Tanahara N, Fujii N, Furuya T (2013) Optimized method of G-protein-coupled receptor homology modeling: its application to the discovery of novel CXCR7 ligands. *J Med Chem* 56(11):4236–4251. doi:[10.1021/jm400307y](https://doi.org/10.1021/jm400307y)
159. Evers A, Klabunde T (2005) Structure-based drug discovery using GPCR homology modeling: successful virtual screening for antagonists of the alpha1A adrenergic receptor. *J Med Chem* 48(4):1088–1097. doi:[10.1021/jm0491804](https://doi.org/10.1021/jm0491804)
160. Kolb P, Rosenbaum DM, Irwin JJ, Fung JJ, Kobilka BK, Shoichet BK (2009) Structure-based discovery of beta2-adrenergic receptor ligands. *Proc Natl Acad Sci USA* 106(16):6843–6848. doi:[10.1073/pnas.0812657106](https://doi.org/10.1073/pnas.0812657106)
161. Varady J, Wu X, Fang X, Min J, Hu Z, Levant B, Wang S (2003) Molecular modeling of the three-dimensional structure of dopamine 3 (D3) subtype receptor: discovery of novel and

- potent D3 ligands through a hybrid pharmacophore- and structure-based database searching approach. *J Med Chem* 46(21):4377–4392. doi:[10.1021/jm030085p](https://doi.org/10.1021/jm030085p)
162. Carlsson J, Coleman RG, Setola V, Irwin JJ, Fan H, Schlessinger A, Sali A, Roth BL, Shiochet BK (2011) Ligand discovery from a dopamine D3 receptor homology model and crystal structure. *Nat Chem Biol* 7(11):769–778. doi:[10.1038/nchembio.662](https://doi.org/10.1038/nchembio.662)
163. de Graaf C, Kooistra AJ, Vischer HF, Katritch V, Kuijer M, Shiroishi M, Iwata S, Shimamura T, Stevens RC, de Esch IJ, Leurs R (2011) Crystal structure-based virtual screening for fragment-like ligands of the human histamine H(1) receptor. *J Med Chem* 54(23):8195–8206. doi:[10.1021/jm2011589](https://doi.org/10.1021/jm2011589)
164. Kooistra AJ, Kuhne S, de Esch IJ, Leurs R, de Graaf C (2013) A structural chemogenomics analysis of aminergic GPCRs: lessons for histamine receptor ligand design. *Br J Pharmacol* 170(1):101–126. doi:[10.1111/bph.12248](https://doi.org/10.1111/bph.12248)
165. Mason JS, Bortolato A, Congreve M, Marshall FH (2012) New insights from structural biology into the druggability of G protein-coupled receptors. *Trends Pharmacol Sci* 33(5):249–260. doi:[10.1016/j.tips.2012.02.005](https://doi.org/10.1016/j.tips.2012.02.005)
166. Nicholls DJ, Tomkinson NP, Wiley KE, Brammall A, Bowers L, Grahames C, Gaw A, Meghani P, Shelton P, Wright TJ, Mallinder PR (2008) Identification of a putative intracellular allosteric antagonist binding-site in the CXC chemokine receptors 1 and 2. *Mol Pharmacol* 74(5):1193–1202. doi:[10.1124/mol.107.044610](https://doi.org/10.1124/mol.107.044610)
167. Salchow K, Bond ME, Evans SC, Press NJ, Charlton SJ, Hunt PA, Bradley ME (2010) A common intracellular allosteric binding site for antagonists of the CXCR2 receptor. *Br J Pharmacol* 159(7):1429–1439. doi:[10.1111/j.1476-5381.2009.00623.x](https://doi.org/10.1111/j.1476-5381.2009.00623.x)
168. de Kruijf P, Lim HD, Roumen L, Renjaan VA, Zhao J, Webb ML, Auld DS, Wijkmans JC, Zaman GJ, Smit MJ, de Graaf C, Leurs R (2011) Identification of a novel allosteric binding site in the CXCR2 chemokine receptor. *Mol Pharmacol* 80(6):1108–1118. doi:[10.1124/mol.111.073825](https://doi.org/10.1124/mol.111.073825)